Studies on Hydraulic Gates

- Relating to Increase in Their Sizes and Operating Head-

March, 1996

Hiroshi Terata

Studies on Hydraulic Gates

- Relating to Increase in Their Sizes and Operating Head-

March, 1996

Hiroshi Terata

Contents

3.1

Structural analysis of torsion type gates

Contents

Page

Abstract

Section 3.1 is "Structural analysis of torsion type gates". It shows contents of various analytical methods in detail and makes clear their relationships. Difficulty in structural analysis of the torsion type structure impedes its wider application. In Article 3.1.2, characteristics of the torsion type structure are made clear and it is shown that the number of applicable cases of this structure is greater than our expectations. In Article 3.1.3, detailed explanation is given on the elastic equation assembly made of the simple torsion theory and it is shown that the torsion type structures can also be analyzed by the space frame theory. In Article 3.1.4, explanation is given on the elastic equation assembly made of the bending- torsion theory. Characteristics of deformation due to the bending- torsion are made clear and it is shown that effect of the bending- torsion appears in the stress distribution of the section much more than the internal forces of the section. It is shown furthermore that analytical results obtained through the finite element method could reflect the bending- torsion phenomena well. Eventually it is bound to lead to the conclusion that super- large structures of the torsion type have to be analyzed by the finite element method. In Annex 3.1- 2, the basic theory of torsion is given in an organized form.

3．1 Structural analysis of torsion type gates

3．1．1 Introduction

External forces acting on structures are grouped into loads and their reaction forces, and the loads are transmitted from loading points to reaction points through rigidity of the structure. The structural rigidity[*1] sometimes refers to a shearing rigidity, a bending rigidity, a torsional rigidity, an axial rigidity and so on, but a structure generally provides all these rigidities together and a major rigidity among them depends upon not only their relative magnitudes but also distribution of external forces. Suppose bending deformation and shearing deformation causes a certain amount of displacement in structure, the bigger rigidity between bending and shearing will be dominant in load transmittal in the structure whereas only axial rigidity is good for the load transmittals in case that all loading points and reaction points exist in a load vector line. Although hydraulic gates are classified into many structural types, most of radial gates is a compression type, roller gates of dam crests and river weirs is a bending type and high pressure roller gates is a shearing type. Shearing type, bending type and compression type are most general type of hydraulic gates as the above examples show but the gate would become torsion type if its torsion rigidity was increased or other rigidity was decreased as long as the external forces on the gate can compose twisting moments. A structure most of whose external forces compose couples and whose torsion rigidity is comparatively big is characterized by its torsion rigidity and is defined as a torsion type structure in this thesis and gates of torsion type structure are defined as torsion type gates. Hydraulic gates which provide external force condition of torsion type structure are much more than our expectation .

[*1] The rigidity referred to here is conceptually different from rigidity which is defined for each direction of a nodal point in matrix analyses of structure .

A flap gate of the torsion type structure is called a fish belly flap in Europe and a fabrication record shows this type was in operation at 1931 already. The first application of this type in Japan was in 1963 at Matsukawa diversion works[*1]. Since then this gate type had quickly spread all over Japan. Different kinds of application appeared such as double gates or multiple step fish- ladder gates. Furthermore, it was applied for shipyard repair dock gates[*2], one of which is 100m in width and more than one thousand tons of steel in weight. A superiority of torsion type structure is (1) small steel weight when it is applied to a low height long span gate and (2) advantage in fatigue strength because of almost pure shearing status of stress distribution, and this type have been proposed for gate plans in the study of alternatives for the Panama canal[*3]. The result of this study suggests that torsion type gates could become larger in scale and replace slide gates, roller gates, miter gates or other gate types.

Structural analysis of torsion type structure is very complicated and it is impossible to carry out the analysis efficiently without supports by computers. Reason of delay in construction of this type in Japan is a difference of river circumstance but a difficulty in structural analysis seems to be another reason[*4]. Option for method of structural analysis has been increased according to rapid development of a computer and its soft. Late 1960 was ages of a large computer which used to install a pile of integrated circuits. A computer employed at daily technical calculation used to occupy one floor of a big business building. A computer whose performance is much more than a several hundred times of the large computer is put on each engineer's desk today. FEM soft wear is always available besides tridimensional frame softs. The purpose of this study is to clarify the contents of analytical methods used in the past and to define their relations.

[*1] Bibliography (1) and (3).
[*2] Bibliography (6) and (7).
[*3] Bibliography (8) and (9).
[*4] Bibliography (1) and (3).

The essential part of the analysis is to obtain many statically indeterminate values and this process is extremely complicated. Although torsion in a structure is a combination of simple torsion and bending- torsion, the latter is not considered in usual structural analysis because a handling of bending- torsion is very complicated. But torsion type structures cannot be described without bending- torsion. Especially sound designs would not be obtained for super large scale gates of torsion type without considering stress distribution due to bending- torsion as well as simple torsion. Eventually, whole structural analysis by FEM is inevitable.

The above is a conclusion of this study and the process to get there will be explained according to following items.

（1）Characteristics of torsion type structure and examples of application

（2）Analysis of simple torsion theory

（3）Analysis of bending- torsion theory

In this study, the simple torsion theory means analytical theory in which bending- torsion is neglected and the bending- torsion theory means analytical theory which includes bending- torsion. Although the first half part of the thesis was supposed to be a basic theory of torsion structure due to technical content contained by the study theme, they are shown in appendix 3．1－2 "Stress distribution of closed thin shell being subjected to torsion" and 3．1－3 "Stress distribution of closed thin shell being subjected to bending" owing to avoid the thesis goes off its track.

3．1．2 Characteristics of torsion type structure and examples of application

（1） History of torsion type gates[*1]

A fabrication record shows this a flap gate of torsion type structure was in operation at 1931 already in Europe[*2]. The reference[*3] describes in detail how and why the torsion type structure was accepted. Followings are its partial translation. A flap gate at its initial stage was very simple structure, and a bending type main girder is provided to top of a skin plate stiffened by angles and floor plates and the floor plate bottoms are supported by hinge metals installed on a riverbed at an appropriate intervals (Fig. 3．1－1). The main girder is supported at its both terminals by hoisting tools such as racks, chains or something else. It was found later that the initial flap gate did not use essential advantage of its structure. Although the gate bottom was supported by the hinge metals, its main girder was subjected to a big bending due to a free support at weir width terminals. Accordingly it was

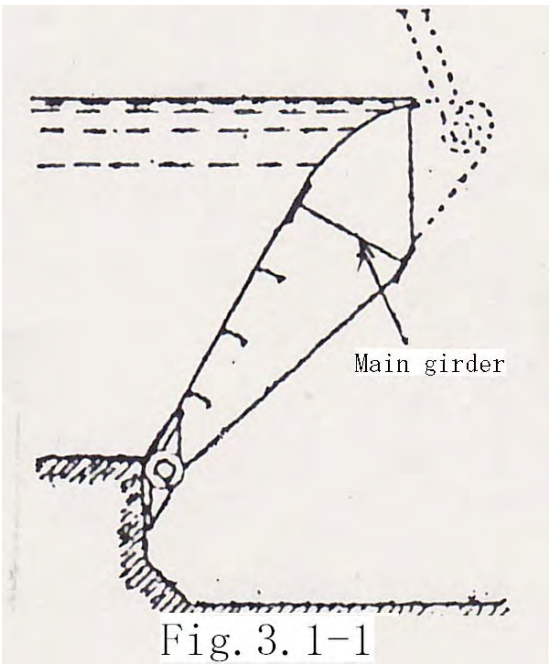

Fig. 3. 1-1

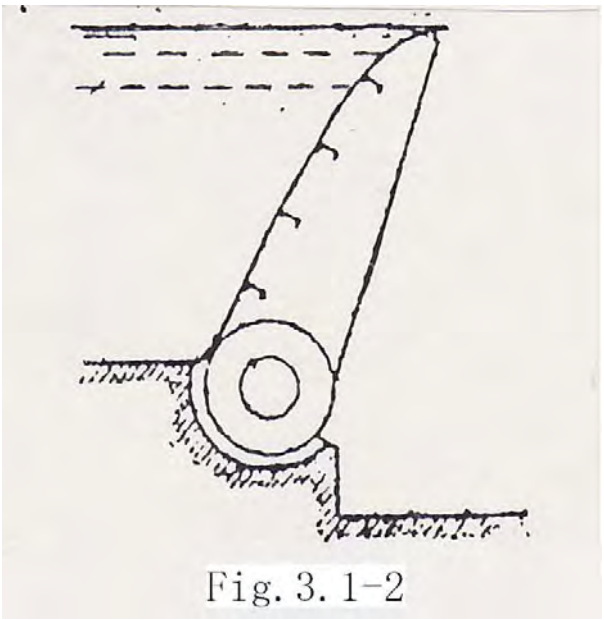
Fig. 3. 1-2

[*1] Bibliography (12)
[*2] Bibliography (12)
[*3] Bibliography (11)

improved and structure which could resist torsion moment started to be used. In stead of a skin plate top girder which resists bending moment, a bottom tube which resist torsion moment is provided and the gate rotates around the tube axis (Fig. 3. 1－2). The improvement was bound to bring out longer spanned flap gate due to resistibility to twisting and continuity of bottom support. But new structure had a difficulty in keeping seal function along the bottom tube. It was a big structural progress that the bottom tube was removed from the rotation axis to the skin plate top. Water sealing at gate bottom could be realized by a flexible sealing band covering the gap between riverbed and the skin plate bottom (Fig. 3. 1－3). Range of flap gate application was expanded by this new improvement but still there was a limit to the application. The structurally most difficult part of the gate is a tube which resists rotation moment and the cause of application limit was increase in diameter and plate thickness of the torque tube due to increase in gate span. This demerit was excluded by the invention of fish belly flap which was disclosed in 1930. The fish belly flap has a uniform hollow body which resists torsion moment. A torque tube and a skin plate of previous flap were integrated and replaced by a uniform hollow body composing of a cylindrical skin plate which is convex toward upstream and a cylindrical back plate which is convex toward downstream (Fig. 3. 1－4).

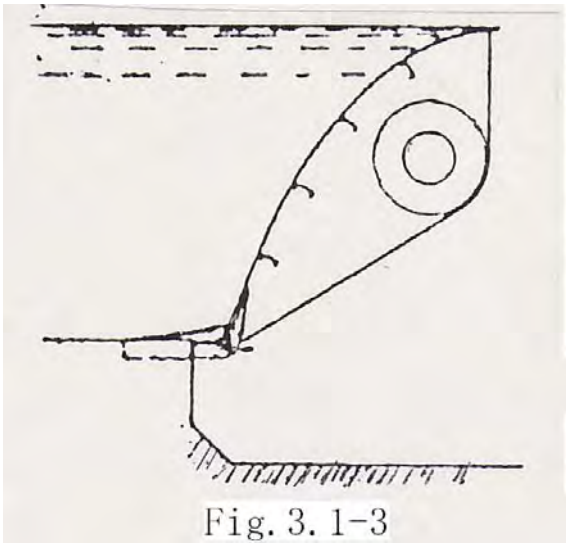

Fig. 3. 1-3

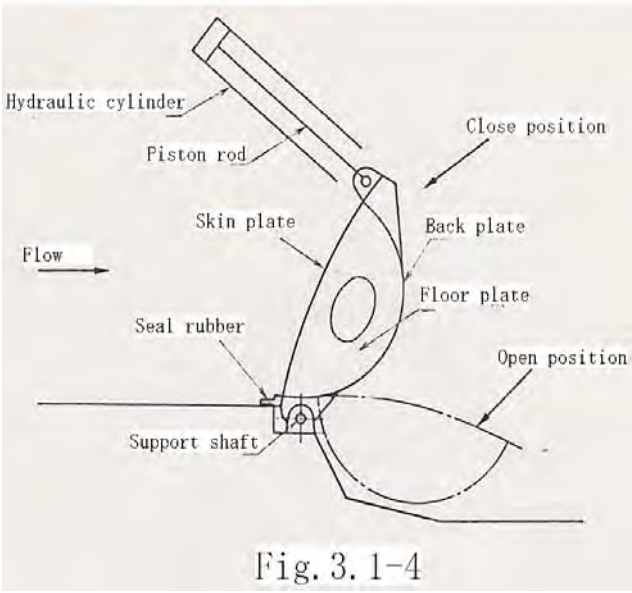

Fig. 3. 1-4

The hollow body has a lens section which is similar to a fish belly and whose closed area is so large that its resistibility may be as several times as the torque tube composed of the same weight of steel. At identical time, its bending rigidity is far bigger than that of a torque tube type structure.

Fish belly flap gates have been widely employed since then in Europe. But their need is mainly for riverin use and seems to have had no big difference since its birth. The first application of fish belly flap in Japan was 1963 as previously mentioned and this gate type has quickly spread since then. But its development in Japan seems to be in a somewhat different direction. Its application is beyond a flap gate of riverin use and its gate shape sometimes differs from fish belly shape because much effort was made to increase torsion rigidity while to decrease bending rigidity of the gate section and it is often inappropriate to call them "fish belly type." This is the reason why the expression "torsion type structure" or "torsion type gate" was introduced in this thesis.

（2） Characteristics of torsion type structure

In the preceding section（3．1．1）, it was described that structure usually provides multiple kinds of rigidity, that the rigidity which plays a major role in load carriage in the structure will become obvious according to external force condition and comparative intensity of rigidities and that the condition of torsion type structure is ① external force condition which can compose twisting moments and ② comparatively big torsion rigidity. And also it was pointed out that a superiority of torsion type structure is ③ small steel weight and ④ advantage in fatigue strength. These four points are major characters of torsion type structure and they are drilled down in this article so that the characteristics of torsion type structure may be grasped more concretely.

① External force satisfies a condition of composing twisting moments.

As the torsion type structure intends to carry majority of its loads to reaction points by its torsion rigidity, the structure does not work effectively even if its torsion rigidity is particularly big unless external forces satisfy a condition of composing twisting moments. The external force means forces acting on the structure from outside of it and consists of loads and their reaction forces. A long span roller gate does not work as a torsion type structure even if twisting moment is built due to a difference between a loading point and a sectional shear center, because the twisting moment consists of the load and shearing force on the section and the shearing force is a kind of internal force and not external force. Definition of external force condition which can compose twisting moments is that external forces can form couples and furthermore another external couple which is in equilibrium with the couples exists. The most simple example is a flap gate. Hydraulic water pressure and gravity force acting on the gate body and their reaction forces acting at the gate bottom hinge supports compose couples and they can be in equilibrium with a reaction moment acting at the gate body terminal. The reaction moment is moment of a couple which is composed of supporting force of the gate terminal and its reaction force, and dose not need to exist on both terminals of the gate body. A sector gate and a drum gate provide same condition as a flap gate. A dry dock gate of ship building yards is often a pontoon type or flap type and, if their terminal support is such type as a reaction moment is composed there, their external forces can compose couples since there is a support line along their bottom. A rolling gate which removes in horizontal direction can establish this condition. An upper leaf of double leaf roller gate which is often applied to a tall dam crest discharge exit provides this condition. In stead of a double leaf roller gate, the discharge exit is divided vertically at its center line into two compartments and two vertical type flap gates are installed to cover the whole exit. This arrangement can provide the condition also if the flap rotation is prevented at its top or bottom. As the above examples show, number of case in which a condition of composing twisting moments is satisfied is much more than our expectation.

② Torsion rigidity is comparatively big

The comparatively big means torsion rigidity is much more than bending rigidity and also means bending rigidity is comparatively small. As deformation is mainly controlled by torsion rigidity, bending stress will become small in case that bending rigidity is small. Under the deformation control by torsion rigidity, the same result can be sometimes obtained by direct reduction of bending deformation [*1]. In case that the y axis of a rectangular coordinate (x, y) coincides with a direction of water pressure, the original point of it coincides with shearing center of a structural section and a hinge support of the section is put on the x axis, there will be no displacement of the shear center since the section rotates around the support and a bending deformation in x direction, i.e. bending moment equals zero accordingly. Furthermore, the curvature in the x direction will be much mitigated and corresponding to bending moment will decrease even if the support stay at any point as long as the section can remove in the x direction at will and a restrictions to bending deformation in the x direction disappear. Above- mentioned facts will be shown in the examples of analysis by the simple torsion theory later. Bending stress in the y direction can not be decreased by same procedure because the bottom support of section can not be put on the y axis and also the restriction in the y direction can not be released since a big bending moment occurs due to water pressure. But it is a big advantage in selecting a section shape that bending stress in the x direction can be decreased without decreasing bending rigidity. The description above leads to following conclusion. The torsion rigidity in torsion type structure is comparatively big. Although the bending rigidity in right angle to the direction of water pressure sometimes very big, there is a possibility of reducing its impact by another procedure.

[*1] Curvature deformation = curvature. It is in linear to bending moment.

③ Small steel weight

Steel weight of a gate made of bending type structure mostly reduces when torsion type structure is adopted in stead but it does not happen always. A study was made on an impact factor to unit weight of a gate (weight ÷ width ÷ height) under the below assumption.

A similarity exists between sectional shape and hydraulic water heads of all gates.

Conditions of constrain are allowable stress and allowable displacement ratio (displacement ÷ gate width), only a simple torsion deformation of the torsion type structure and a bending deformation of the bending type structure are considered for the allowable displacement condition and a load carried by the structures is hydraulic water only. Table 3. 1－1 shows result of the study[*1]. The unit weight of a gate made of rotation type structure increases in linear to (gate width × gate height) and that of a gate made of bending type structure increases in linear to (gate width)^2 for the allowable stress condition but to (gate width^3 ÷ gate height) for the allowable displacement condition. Accordingly it is concluded that gate weight of the torsion type structure will be smaller than gate weight of the bending type structure in case of a smaller height and larger width gate, in short, a horizontally long gate. A bifurcation point of the unit weight shall be found out on record base.

Constrain condition	Allowable stress	Allowable displacement
Torsion type structure	Gate height x gate width	Gate height x gate width
Bending type structure	Gate width^2	Gate width^3 ÷ gate height

Table 3. 1－1 Impact factor of unit weight

[*1]Unit weight and the impact factor on a graph shows approximately an linear relation but the strait line dose not run the original point of the graph.

④ Advantage in fatigue strength

Canal gates whose operation frequency is very high have a possibility of fatigue failure. A fatigue failure is very sensitive to a magnitude of tensile stress[*1]. Whole major part of torsion type structure is almost in pure shearing state. There are a several theories about a yield condition of materials. Application of shear strain energy theory of Huber- Mises is the most common in design of steel structures at this moment and maximum shearing stress is limited up to $1/\sqrt{3}$ of allowable tensile stress. Tensile stress in pure shearing state is equal to shearing stress and accordingly tensile stress keeps its magnitude at lower level so that the torsion type structure has an essential advantage against its fatigue failure. Start of fatigue failure is microscopic defect in material and compression stress in the pure shearing state equals the tensile stress in its magnitude and increases stress concentration rate around the defect. Stress concentration ratio around a circular hole in pure tension and in pure shearing state is 3:4. Tensile stress including this ratio will become $4/3/\sqrt{3} = 0.77$ of allowable tensile stress that still proves a merit of the torsion type structure against fatigue failure.

[*1] Page 12 of Bibliography (37) and page 207 of Bibliography (34)

（３） Examples of application

A brief explanation was given on application of the torsion type structure at preceding section（３．１．１）and concrete examples will be shown in this section.

Fig. ３．１－５ shows the first application of this type in Japan, a gate for Matsukawa diversion works[*1].

The gate is flap type of 1.7m height and 9.0m width and supported by a drive shaft provided to a gate span end.

The section shape is fish belly composing of a cylindrical skin plate which is convex toward upstream and a cylindrical back plate which is convex toward downstream. Floor plates in the gate body are arranged at a constant pitch and support hinges are provided to each of their bottoms. Fig. ３．１－６ shows the inside of model gate used at the experiment carried out in advance of constructing the Matsukawa. The torsion

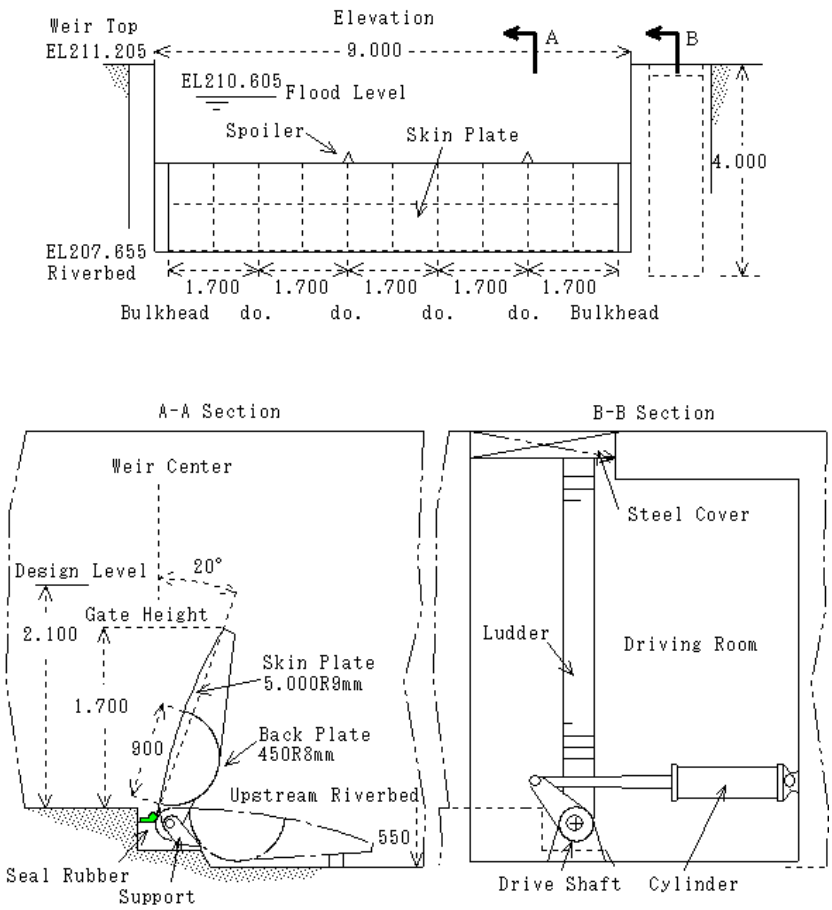

Fig. ３．１－５

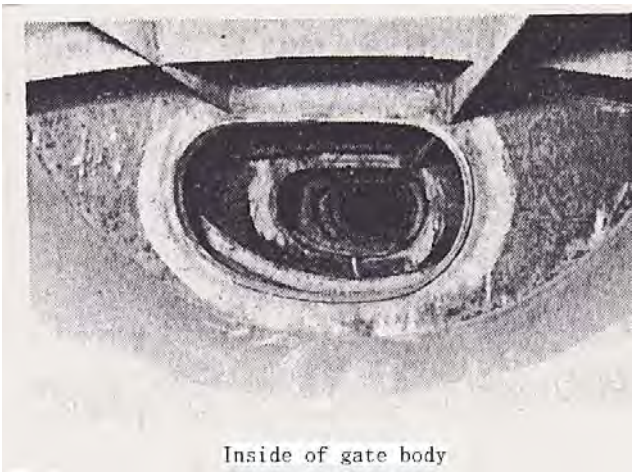

Fig. ３．１－６ r

[*1] Bibliography (1)。

member of the model is stiffened by reinforcing angles to increase its resistibility against shear buckling and rigidity against water pressure. The reinforcing angles are supported by the floor plates. Fig. 3. 1－7 shows a double gate. This idea was proposed by a manager of Agricultural Engineering Consultants Co., Ltd in 1964 and a fish belly flap on a long span shell gate has become a very important

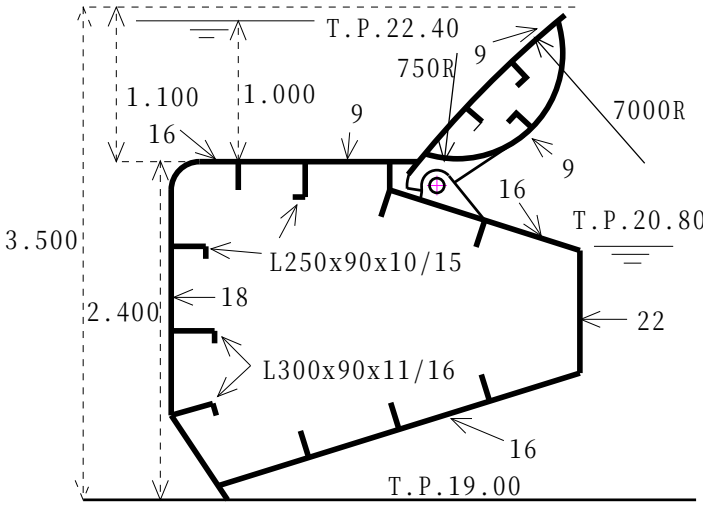

Fig. 3. 1－7

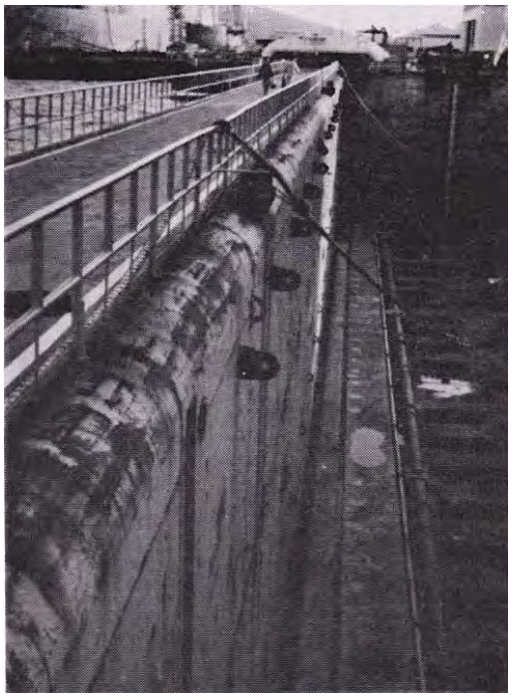

Fig. 3. 1－8

gate type. Author was engaged in technically supporting him to realize his idea. The most big problem to be analyzed is a operability of the top gate during the bottom gate is in deforming that will be described in detail later. Fig. 3. 1－8 thru 10 show examples of applying the torsion type structure for shipyard repair dock gates[*1] and a gate on Fig. 8 is 13.5m height x 100m width x 1270ton weight, and a gate on Fig. 9 is 12m height x 80m width x 780ton weight. In case of Fig. 8, the

Fig. 3. 1－9

[*1] Bibliography (6)。

gate weight of bending type structure was 1900ton which means that the weight reduction rate by torsion type structure is no less than 33%. The top edge line of the gate body on Fig. 8 is a cylindrical section while that of Fig. 9 is right angle section. Although this is a result of improvement aiming at cost cut, shearing stress concentration must occur at the right angle section. This point will be described later. Fig. 10 is the gate of Fig. 8 during its maintenance and shows the bottom metal which enables to generate a reaction moment to support the gate terminals. The direction of water pressure working on the gate in service is upward. The gate terminal wall is a very heavy structure whose top in a service condition is supported by a gate frame embedded in dock side concrete wall and whose bottom in a service condition intends to remove from the dock side concrete wall and the bottom metal shown on Fig. 10 tries to prevent the bottom remove. The metal has a widely opened mouth which enables a quick removal of the gate leaf out of place for its maintenance. The hinge supports are installed on the sea bed just below the terminals and center of the gate leaf and their hinge pins mate very loose fitting hub metals set on the gate leaf. A Long wood seat is provided along the gate leaf bottom edge and the seat in service moves toward the dock bottom concrete wall and is supported by the gate frame embedded in the concrete. Eventually the water load on the gate leaf and the gate weight are supported respectively by the wood seat and by the hub metals. The gate leaf sections have become almost a rectangular shape as a result of pursuing a section shape which has big torsion rigidity and less bending rigidity in the water load direction and "fish belly" is already not a right name of them. The bending rigidity in the gate height direction

Fig. 3. 1－10

is remarkably big but its impact has been mitigated by a restriction release of gate bottom movement in the gate height direction. Fig. 3. 1－11 shows an example of torsion type plans which were proposed as alternatives to the future Panama canal gates[*1]. It is a rolling type gate of 27.5m height x 200m width x 5950 ton weight and is divided at its span center into two blocks one of which is shown on the figure. The purpose of this gate is to separate tide level of Pacific ocean and Atlantic ocean, and water pressure acts on the gate leaf alternatively from both ocean sides and the gate is operated with a quantity of water load acting on the gate leaf. A roller tread of the gate is semi circular in section shape and run on a circular section rail transforming the operation water load of the roller to the rail. The roller center coincides with a vertical line which passes through a shearing center of the gate leaf section. Each gate block is supported by one side of it. Support points of the block during operation are horizontal rollers set at the top and the bottom of the block terminal and a huge quantity of water load on the gate leaf of totally closed position is supported directly by the concrete structure at the top and the bottom of the gate leaf terminal. The figure shown is a tentative plan and just to show idea of the gate and shape and dimension of the members are just for a reference.

[*1] Page 14- 73 of Bibliography (8) and page App 3- 5 of Bibliography (9)。

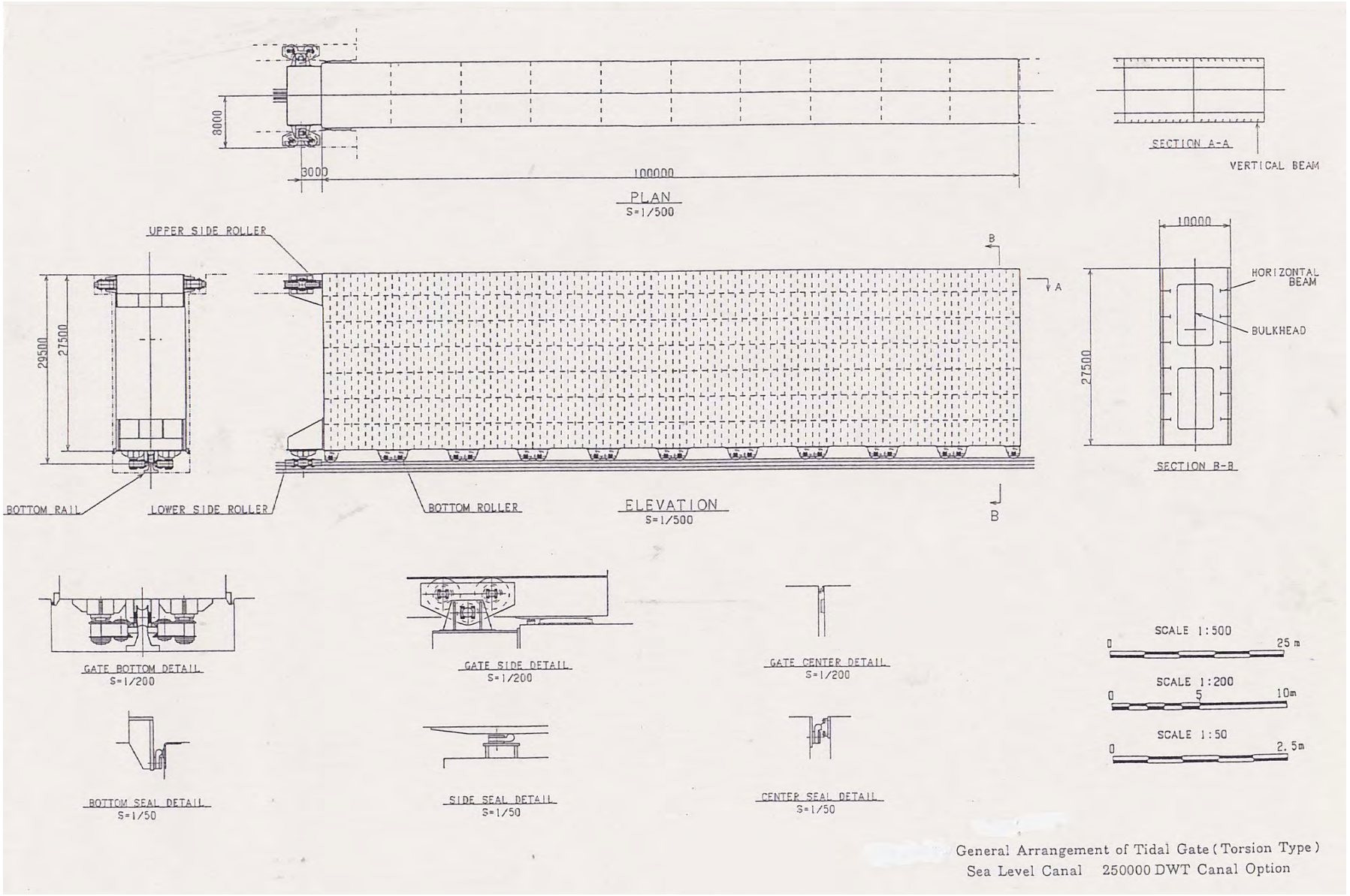

General Arrangement of Tidal Gate (Torsion Type)
Sea Level Canal 250000 DWT Canal Option

Fig. 3. 1－11

3．1．3 Analysis based upon the simple torsion theory

Torsion in a structure is a combination of simple torsion and bending- torsion and method of structural analysis where bending- torsion is neglected is described in this section. Method of simple torsion theory is in general at a structural analysis. Basic theory of torsion in a closed thin shell section is shown at Appendix 3．1－2 and 3．1－3 and application results on the two kinds of section of the basic theory are shown at Appendix 3．1－4 and 3．1－5. The description in this section will start based upon these appendices. The formula which has an alphabetical number is a formula drawn from the appendix. Definition of terms in the drawn formula is shown in Appendix 3．1－1.

3．1．3．1 Stress distribution on gate sections

At the starting point of the structural analysis, specific features in stress distribution on a closed thin shell are given. Let axis of rectangular coordinate (x, y) coincide principal axis of a gate section. Section forces are simple torsion moment T_s, bending moment m_y and m_x around the y- axis and x- axis m_y and m_x and shearing force Q_x and Q_y in the x- direction and y- direction. Sectional stress corresponding to each sectional force is calculated according to following formulae.

［Shearing center］

$$\left.\begin{aligned} y_s &= \oint r_0 \left(\int_0^s x\,t\,ds + c_x\right) ds \div I_y = \left(J_{11} + 2A_s c_x\right) \div I_y \\ x_s &= -\oint r_0 \left(\int_0^s y\,t\,ds + c_y\right) ds \div I_x = -\left(J_{12} + 2A_s c_y\right) \div I_x \end{aligned}\right\} \quad \cdots\cdots (bj)$$

［Shear flow constant due to bending］

$$\left.\begin{aligned} c_x &= -\oint \frac{1}{t}\left(\int_0^s x\,t\,ds\right) ds \div \oint \frac{1}{t} ds = -J_9 \div I_0 \\ c_y &= -\oint \frac{1}{t}\left(\int_0^s y\,t\,ds\right) ds \div \oint \frac{1}{t} ds = -J_{10} \div I_0 \end{aligned}\right\} \quad \cdots\cdots (bh)$$

[Shear flow due to bending]

$$\left.\begin{aligned} q_{bx} &= M_y + c_x \quad (\text{corresponding to } Q_x) \\ q_{by} &= M_x + c_y \quad (\text{corresponding to } Q_y) \end{aligned}\right\} \qquad \cdots\cdots(bf)$$

[Shearing stress due to bending]

$$\left.\begin{aligned} \tau_{bx} &= -\frac{Q_x}{I_y}\cdot\frac{q_{bx}}{t} = -E\frac{q_{bx}}{t}\cdot\frac{d^3\xi}{dz^3} \\ \tau_{by} &= -\frac{Q_y}{I_x}\cdot\frac{q_{by}}{t} = -E\frac{q_{by}}{t}\cdot\frac{d^3\eta}{dz^3} \end{aligned}\right\} \qquad \cdots\cdots(bf)$$

[Bending stress]

$$\sigma_b = \sigma_{bx} + \sigma_{by} = \frac{m_y}{I_y}x + \frac{m_x}{I_x}y \qquad \cdots\cdots(ba)$$

[Shear flow due to simple torsion]

$$q_s = \frac{2A_s}{I_0} \qquad \cdots\cdots(aj)$$

[Shearing stress due to simple torsion]

$$\tau_s = \frac{1}{2A_s t}T_s = \frac{q_s}{t}\cdot\frac{T_s}{J_t} = \frac{q_s}{t}G\frac{d\Theta}{dz} \qquad \cdots\cdots(aj)$$

[Stress distribution on a section]

Distribution of shearing stress is governed by shear flow on the section. Shear flow of simple torsion is constant throughout a section. Shear flows due to bending are shown on Fig. 3. 1－14 and 15 which give the results of calculation on sections shown in Fig. 3. 1－12 (fish belly section) and 13 (rectangular section). All formulae used in the calculation are shown at Appendix 3.1- 4 (fish belly section) and 3.1- 5 (rectangular section). These are results of applying the above general formulae to the specified section. G, S, and to and ti in Fig.- 12 are center of gravity, shearing center and thickness of the shell section respectively. Although the original point of rectangular coordinate on Fig. 3. 1－12 and 13 has been set according to a convenience of structural analysis carried out later, the point has to be removed to the gravity center for a calculation of above

formulae. The center of r_0 (zero) is gravity center of the section and x_s and y_s are given as a distance from the gravity center. The x- axis on Fig.- 12 is set vertically for the sake of convenience in a comparison of analytical results to a reference later. The above formulae correspond to a rectangular coordinate whose x axis is horizontal (like Fig－13) and x and y are supposed to be switched when they are applied to Fig.- 12. As the x axis on Fig.- 14 is horizontal, this figure corresponds to a reverse paper side view of Fig.- 12 after rotated by 90 degrees anticlockwise. The coordinate axis in Fig.－13 and 15 coincides with the formulae. The shear flow due to bending shown on Fig.－14 and 15 corresponds to the section and its scantlings shown on the same figure and equals the length of the normal vector set on the section divided by the figure shown at the graph bottom. Vertical and horizontal component of a vector are obtained according to the axis scales. Inside of the section is minus and outside is plus and the clockwise shear flow is plus. Shearing stress on a section equals the quantity of shear flow multiplied by the shearing force on each section. Distribution of bending stress on a section follow a ordinary beam theory.

Structural analysis of whole gate is necessary to get section internal forces used in stress calculation.

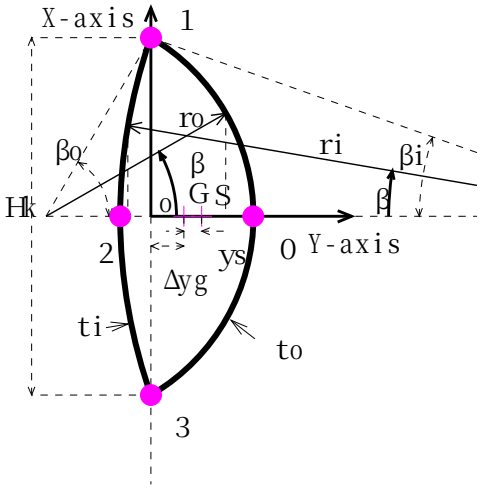

Fig. 3. 1－12

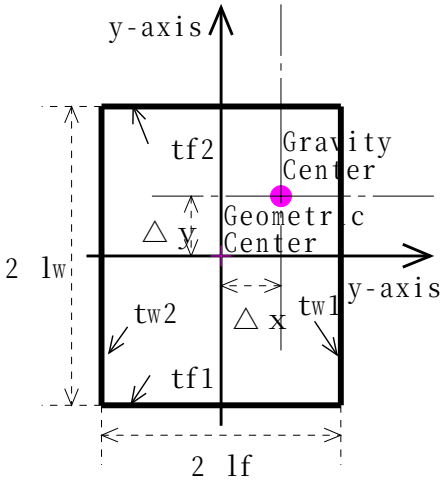

Fig. 3. 1－13

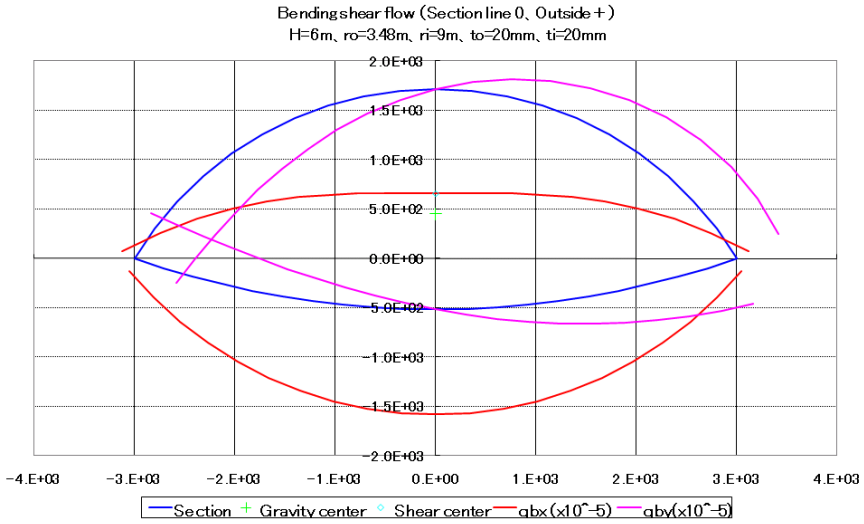

Fig. 3. 1－14

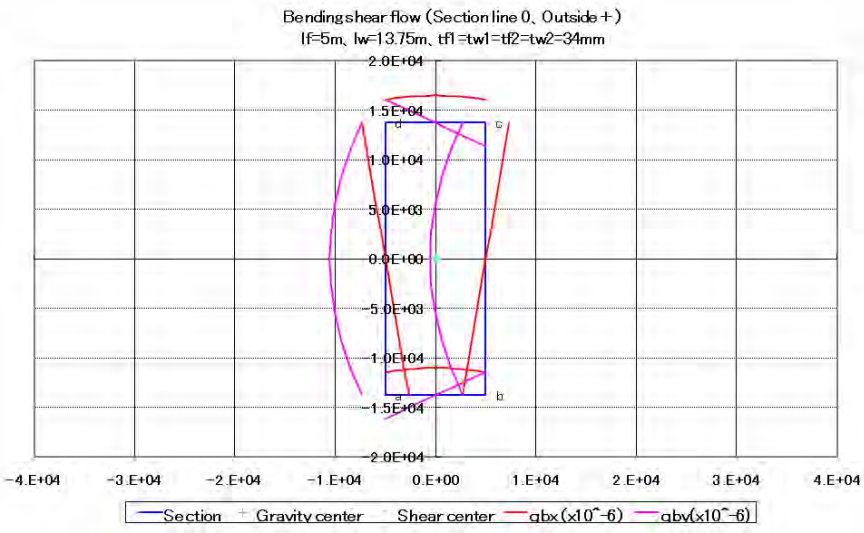

Fig. 3. 1－15

3．1．3．2 Analysis by elastic equation

This is a fundamental analytical method of torsion type structure. Elastic displacement at supports of a gate is given in the form of elastic equations and internal forces are determined so that all support conditions may be satisfied. The main flow in the analysis follows the paper[*1] presented by Paul Cicin in 1958. The equations generated are erected to a matrix equation whose solutions are obtained by a computer.

（1） Analytical model

As a gate leaf section rotates around its shear center, the gate to be analyzed is replaced by a shear centerline of the gate and it is assumed that bending rigidity is also concentrated along this line. Bending rigidity in the case of simple beam theory is supposed to be concentrated along the gravity center line, but no difference would occur even if the line moves to the shear center line. Load for bending deformation has to be located on the shear center line.

（2） External loads in analysis

The external force applied to the gate body is load and its reaction force and the load is water pressure force, earth pressure force, gravity force etc. that widely distribute the outside and inside of gate body. As the load will be transmitted by local rigidity to the web plates located in the gate body at a constant pitch, it can be replaced by concentrated loads on each web plate. As there is no adverse effect of an assumption that the distribute uniformly over the gate width, the magnitude of concentrated loads is equal except at both ends where the loads are half of the others. These loads are reacted at bottom supports of the web plates and at the

[*1] Bibliography (11)

drive ends of gate body. Reaction forces at the gate end creates a reaction moment M_o by which the gate end is supported. Let us consider one end drive because both ends drive can be deemed to be special cases of one end drive. Reaction forces at bottom supports are divided into (W_x', W_y') which are equal to loads (W_x, W_y) on the web plates in magnitude and (X, Y) which are remainder portions of reaction forces and their + directions are defined as in Fig. 3.1－16. We call the former statically determinate values and the latter statically indeterminate values. (W_x, W_y) and (W_x', W_y') equal in magnitude but are opposite in direction and compose couples, which we call statically determinate torsion moments represented by m_s for all sections except at both ends where their value is a half. Total of m_s equals M_0. We now think about the remainder (X, Y). As indicated in Fig. 3.1－17, let us imagine that (X, Y) and (X', Y') which are equal to (X, Y) in magnitude but have opposite directions act at shear centers on the gate sections. The remainder (X, Y) and imagined (X', Y') create couples which we call imagined statically indeterminate torsion moments or m_{fi} where i denotes sectional number. Magnitude of m_{fi} varies according to a section and its summation over the gate body equals 0 in case gate section is uniform all over the width.[*1] The imagined (X, Y) acting on the shear centers cause bending deformation in the gate body. A sum of X or Y over the gate is zero. The external force on the gate body is divided into

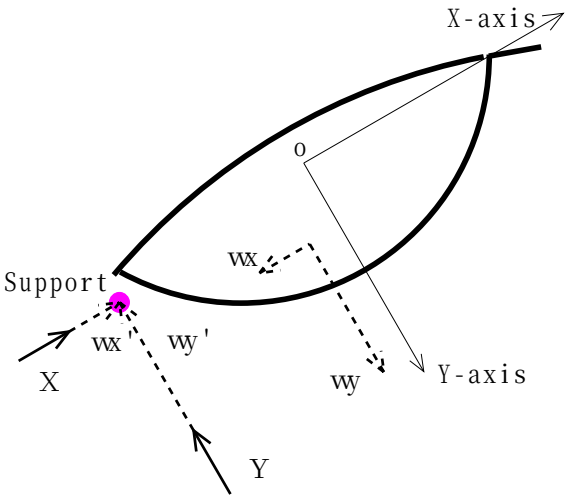

Fig. 3.1－16

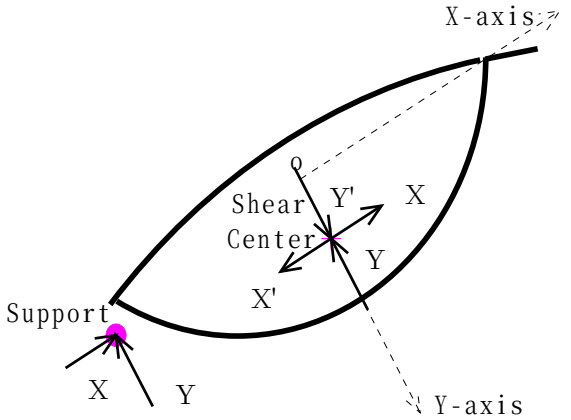

Fig. 3.1－17

[*1] In case of variable section, the sumation including torsion moments given by formula (9) equals 0.

statically determinate torsion moment group, assumed statically indeterminate torsion moment group and assumed statically indeterminate force group in the end and the first two groups cause a twisting and the last group causes a bending of the gate body. Sum of each group is given by following formulae where n is number of web frame spaces and sum is a summation of value on section 0 thru n.

(1) Statically determinate torsion moment m_s:

$$m_s \times n = M_0 \qquad \cdots\cdots(1)$$

(2) Assumed statically indeterminate torsion moment m_{fi}:

$$\sum m_{fi} = 0 \text{ (uniform section)} \qquad \cdots\cdots(2)$$

(3) Assumed statically indeterminate force X_i and Y_i:

$$\sum X_i = 0、\ \sum Y_i = 0 \qquad \cdots\cdots(3)$$

（３） Deformation formulae

The elastic equation consists of elastic deformation of support points on the gate body and formulae to calculate displacement at the support points are required. As it is described in the preceding clause, the gate body is twisted by statically determinate torsion moment and statically indeterminate torsion moment and is bent by statically indeterminate force acting on a shearing center of section. Accordingly formulae of (a) twisting deformation and (b) bending deformation due to external force shall be provided. There will be no internal torsion moment if the shear center line of all sections is straight but as each section is supposed to have structural members different from other sections, the shear center line would be a curve and bending deformation due to imagined (X, Y) would be followed by deformation due to internal torsion moment. Accordingly formulae of (c) twisting deformation due to internal torsion moment shall be provided.

Torsion and bending deformation will occur in the gate body due to external loads mentioned in the preceding article. As each section is supposed to have structural members different from other sections, the shear center line would be a curve and bending deformation due to imagined (X, Y) would be followed by internal torsion deformation whose estimation procedure is necessary besides for torsion and bending deformation due to external load. The support point of the gate during bending deformation makes a movement amount of which will be obtained in the resolution of the elastic equation. Followings are calculation formulae of gate support point displacement due to various deformation.

(a) Deformation due to concentrated torsion moment

Fig. ３．１－１８ shows boundary conditions to be considered. End a is fixed for rotation and end b is free for rotation and displacement. Let the x, y and z axes of a rectangular coordinate (x, y, z) set as shown on the figure and the original point of coordinate in the section including End a. Let the directions of axis in the

rectangular coordinate (x, y, z) set as shown on the figure and let the original point of the coordinate fix on the section including End a. 0 ～ n denotes support numbers and l_s x n equals the gate width. In short, the gate body is divided by the bottom support and the web frame into n compartments at interval of l_s. The line which represents the gate is a curve which consists of straight lines parallel to z- axis between bottom supports. Concentrated torsion moment m_i acting on i section creates internal torsion moment shown in Fig. 3. 1－18. A section rotates due to the internal moment and the rotation angle on a section will be a sum of the torsion angles along the gate body of the left hand side to the section since the gate boundary condition is fixed at End a and free at end b. Suppose the distance between a shearing center and a bottom support of gate section are l_{px} and l_{py} in the x and the y directions as shown on Fig. 3. 1－19, and state of a section which rotates by θ due to twisting of the left hand side gate body to the section is shown on Fig. 3. 1－20. Suppose the x and the y axes rotate by θ and move to the location of the x' and the y' axes, l_{px} and l_{py} indicate distance in the x' and the y' directions respectively and distance i the x and the y directions, l_{px}' and l_{py}', will be given by following formulae since the rotation is always very small.

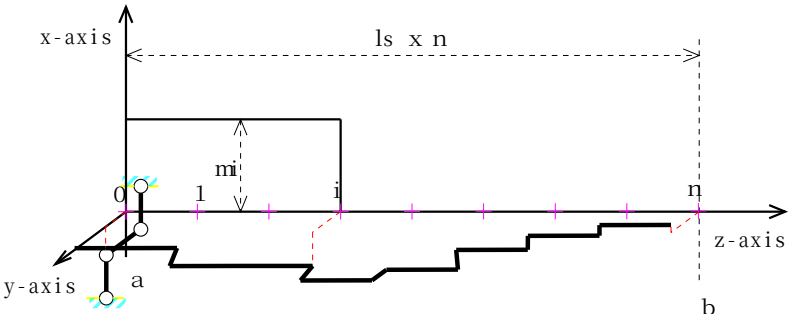

Fig. 3. 1－18

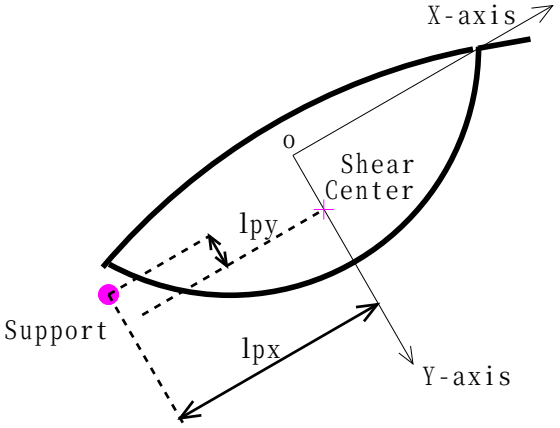

Fig. 3. 1－19

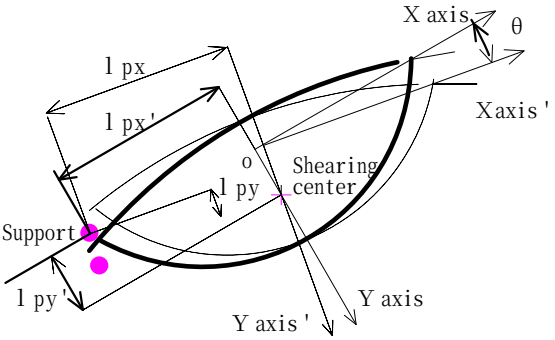

Fig. 3. 1－20

$$\left.\begin{aligned} l_{px}' &= l_{px} - l_{py}\theta \\ l_{py}' &= l_{py} + l_{px}\theta \end{aligned}\right\} \qquad \cdots\cdots(4)$$

Suppose variables in formulae (4) corresponding to k section is symbolized by additional suffix k, the support displacement of k section due to additional torsion moment on the section equals additional rotation angle due to twisting of the gate body left hand to k section multiplied by l_{pxk}' or l_{pyk}' and the elastic equation becomes a nonlinear type. Accordingly a shearing center movement due to twisting deformation is deemed to be negligible with a condition that the twisting angle of gate body is very small. Bottom support displacement, ξ_{tij} in the x direction and η_{tij} in the y direction, of j section due to simple torsion by a concentrated torsion moment acting on i section is calculated according to following procedure under this assumption.

[Section modulus of simple torsion]

$$J_t = \frac{4A_s^2}{I_0} \qquad \cdots\cdots(y)$$

[Displacement at support j due to m_i on i section]

$$\left.\begin{aligned} \xi_{tij} &= \sum_{k=1}^{j} \frac{m_i l_s}{GJ_{tk}} l_{pyk} \quad \text{in case of } J > i \qquad \sum_{k=1}^{i} \frac{m_i l_s}{GJ_{tk}} l_{pyk} \\ \eta_{tij} &= -\sum_{k=1}^{j} \frac{m_i l_s}{GJ_{tk}} l_{pxk} \quad \text{in case of } J > i \qquad -\sum_{k=1}^{i} \frac{m_i l_s}{GJ_{tk}} l_{pxk} \end{aligned}\right\} \qquad \cdots\cdots(5)$$

Formulae (5) become as folloings in case that gate body sections are uniform.

[Displacement at support j due to m_i on i section : for uniform section]

$$\left.\begin{aligned} \xi_{tij} &= \frac{m_i l_{sj}}{GJ_t} l_{py} \quad \text{in case of } J > i \qquad \frac{m_i l_{si}}{GJ_t} l_{py} \\ \eta_{tij} &= -\frac{m_i l_{sj}}{GJ_t} l_{px} \quad \text{in case of } J > i \qquad -\frac{m_i l_{si}}{GJ_t} l_{px} \end{aligned}\right\} \qquad \cdots\cdots(6)$$

(b) Bending deformation due to concentrated load

Fig. 3. 1－21 shows boundary conditions to be considered in calculation of bending deformation due to concentrated load. This is a simple support beam as a bending moment diaphragm shows. The contents common with Fig. 3. 1- 18 are of same definition. Amount of deflection is obtained by integrating bending moment two times but the integration can be done just a bit easily by applying the relation between bending moment and deflection to the relation between load and bending moment as shown on the figure. Deflection at j support, ξ_{wij} in the x direction and η_{wij} in the y direction, due to concentrated load w_i on i section is given by following formulae.

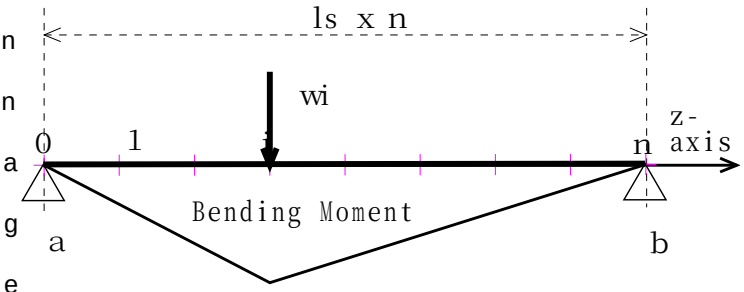

Fig. 3. 1－21

$$\left.\begin{aligned}\xi_{wij} &= X_i \sum_{k=1}^{n} \frac{l_s^3}{E I_{yk}} A_{ijk} \\ \eta_{wij} &= -Y_i \sum_{k=1}^{n} \frac{l_s^3}{E I_{xk}} A_{ijk}\end{aligned}\right\} \quad \cdots\cdots(7)$$

where $A_{ijk}=$

$(n-j)(n-i)\{k^3-(k-1)^3\}\div(3n^2)$ (in case of $k \leqq i, k \leqq j$)

$(n-i)j\{3k^2-3n(k-1)^2-2k^3+2(k-1)^3\}\div(6n^2)$ (in case of $k \leqq i, k > j$)

$(n-j)i\{3k^2-3n(k-1)^2-2k^3+2(k-1)^3\}\div(6n^2)$ (in case of $k > i, k \leqq j$)

$ji\{(n-k+1)^3-(n-k)^3\}\div(3n^2)$ (in case of $k > i, k > j$)

I_x and I_y denote geometrical moment of inertia around x and y axis which coincide with the major axes of the gate section. The load w_i has been replaced by assumed statically indeterminate force. Displacement at End a on the actual gate is restrained. End b is movable keeping equilibrium between reaction force and load.

Compatibility between the End b boundary conditions of term (a) and (b) is maintained by this procedure and a big amount of the n support displacement which is calculated according to the statically determinate torsion moment is adjusted to meet its real state (the real displacement of the bottom supports are zero.). Let this point be described in more detail. The support displacement occurs due to statically determinate moment, assumed statically indeterminate moment and assumed statically indeterminate force and the n support movements which occur due to the statically indeterminate moment and force have a tendency of going back to zero since the sum over the gate body of these load factors equals zero respectively as shown by formula (2) and (3). Eventually the n support which moved by a big amount due to the statically determinate moment can recover its original position because of the End b's free removal. Amount of End b displacement is a unknown value and it is given as a solution of the elastic equation. This value is added, in the elastic equation, to all support displacement which is calculated by formula (7) of bending.

(c) Deformation due to internal torsion

As the internal torsion moment concerned is caused by the load of previous clause (b) since the shearing center line is not straight, let the moment distribution be calculated first and then deformation due to the moment be obtained.

(c- 1) Internal torsion moment

The internal torsion moment due to a load acting on shearing center is calculated with a boundary condition shown on Fig. 3. 1－22. The condition equals to the one in preceding clause (a) and rotation is fixed at End and both rotation and displacement are free

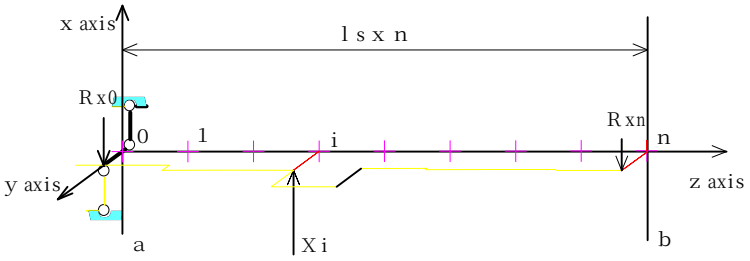

Fig. 3. 1－22

at End b. This figure shows a projection view of y- z plane in the Fig. 3. 1－18 for simplification of the figure and indicates only assumed statically indeterminate force and its support reaction force as external forces which cause torsion. The support reaction force is calculated with the boundary condition of Fig. 3. 1－21. Fig. 3. 1－23 shows l_{sx} and l_{sy} which denote distances of shear center from z- axis in x and y direction on the section. The internal torsion moment is given by the following formulae which are obtained through equilibrium condition of moments around the z- axis.

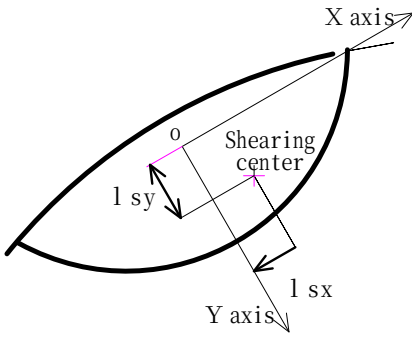

Fig. 3. 1－23

［Reaction forces at 0 and n section due to load at i section］

$$\left.\begin{aligned} R_{x0i} &= X_i \cdot (n-i) \div n \\ R_{y0i} &= Y_i \cdot (n-i) \div n \\ R_{xni} &= X_i \cdot i \div n \\ R_{yni} &= Y_i \cdot i \div n \end{aligned}\right\} \quad \cdots\cdots(8)$$

［Reaction moment at 0 section due to load at i section］

$$\left.\begin{aligned} m_{xi} &= X_i l_{syi} - R_{x0i} l_{sy0} - R_{xni} l_{syn} \\ m_{yi} &= Y_i l_{sxi} - R_{y0i} l_{sx0} - R_{yni} l_{sxn} \end{aligned}\right\} \quad \cdots\cdots(9)$$

［Torsion moment between j- 1 and j section due to load at i section］

$$\left.\begin{aligned} m_{xij} &= m_{xi} - R_{x0i}(l_{syj} - l_{sy0}) \\ &= X_i l_{syi} - R_{x0i} l_{syj} - R_{xni} l_{syn} \quad (\text{in case of } j \leqq i) \\ &= R_{xni}(l_{syj} - l_{syn}) \quad (\text{in case of } j > i) \\ m_{yij} &= m_{yi} - R_{y0i}(l_{sxj} - l_{sx0}) \\ &= Y_i l_{sxi} - R_{y0i} l_{sxj} - R_{yni} l_{sxn} \quad (\text{in case of } j \leqq i) \\ &= R_{yni}(l_{sxj} - l_{sxn}) \quad (\text{in case of } j > i) \end{aligned}\right\} \quad \cdots\cdots(10)$$

Distribution pattern of the internal torsion moment differs much according to the shearing center line form and the loading point. Fig. 3. 1－24 shows the patterns corresponding to 3 kinds of the line form (straight, parabolic and 3/4 sin) and 3 loading points (1, 5 and 9). The magnitude of load at point 5 is 20 % of other case for the sake of graph display. The clock wise moment around the z axis of End a side view is plus and the corresponding reaction moment at End a is minus.

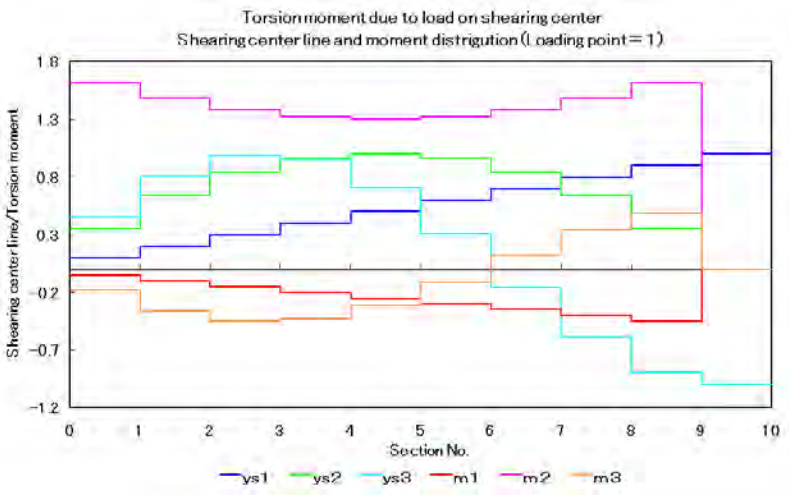

Fig. 3. 1－24 (1／3)

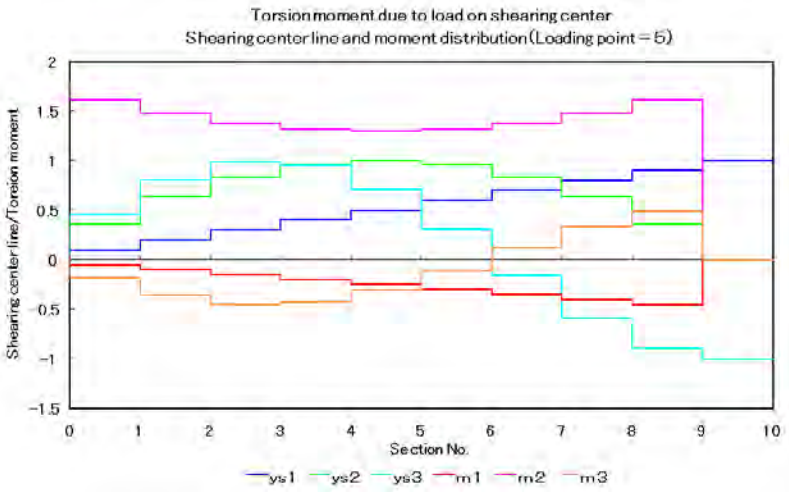

Fig. 3. 1－24 (2／3)

(c-2) Torsion deformation

Deformation due to m_{xij} and m_{yij} will be given by formula (5) after m_i in the formula is replaced by them. Let displacement of the bottom support in the x direction and the y direction due to assumed statically indeterminate force X and Y be (ξ_x, ξ_y) and (η_x, η_y) respectively. They are given

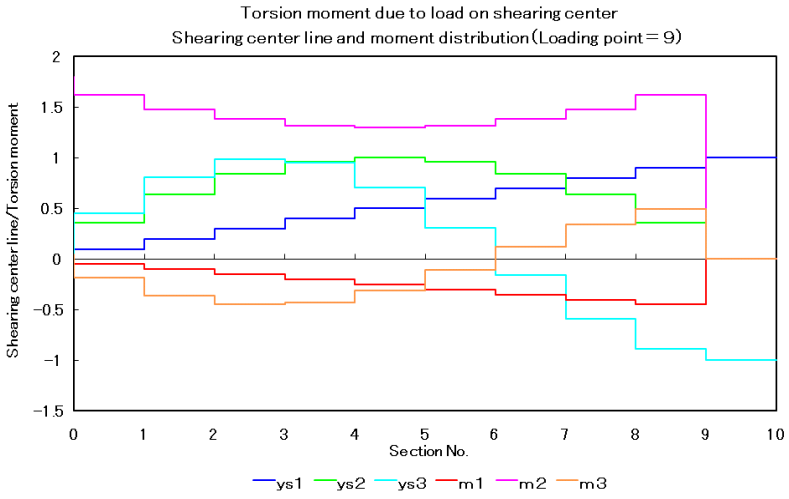

Fig. 3. 1－24 (3／3)

by following formulas.

［Displacement at j support due to (X_i, Y_i) on i section］

$$\left.\begin{aligned}
\xi_{Xij} &= \sum_{k=1}^{j} \frac{m_{xik}\, l_s}{G J_{tk}}\, l_{pyk} \\
\eta_{Xij} &= -\sum_{k=1}^{j} \frac{m_{xik}\, l_s}{G J_{tk}}\, l_{pxk} \\
\xi_{Yij} &= \sum_{k=1}^{j} \frac{m_{yik}\, l_s}{G J_{tk}}\, l_{pyk} \\
\eta_{Yij} &= -\sum_{k=1}^{j} \frac{m_{yik}\, l_s}{G J_{tk}}\, l_{pxk}
\end{aligned}\right\} \quad \cdots\cdots(11)$$

Calculation of the deformation was described according to three parts in the above explanation but eventually the calculation method is grouped into two parts one of which is of torsion deformation and other is of bending deformation since the deformation of clause (c) can be obtained by replacement of the load moment in clause (a).

(4) Elastic equation

Conditions which the elastic equation shall satisfyes are ① bottom support displacement = 0 and ② support reaction force at End b (shearing center line terminal) = 0.

【Bottom support displacement】

Displacement factors of the bottom supports are as follows.

(1) Statically indeterminate reaction force acting on the supports

(2) Rigid displacement of End b

(3) Statically determinate torsion moment

The condition of bottom support displacement = 0 in a matrix form is given by formula (12a).

$$\left[\text{Displacement coefficient of statically indeterminant force}\right]\left[\begin{matrix}\text{Statically}\\ \text{indeterminant force}\end{matrix}\right]+\left[\text{Displacement coefficient of End b}\right]\left[\begin{matrix}\text{End b}\\ \text{move}\end{matrix}\right]+\left[\begin{matrix}\text{Support displacement due to}\\ \text{statically determinant moment}\end{matrix}\right]=\left[\begin{matrix}0\\ \vdots\\ 0\end{matrix}\right] \quad \cdots(12a)$$

This formula is transformed to formula (12b).

$$\left[\text{Displacement coefficient of statically indeterminant force}\right]\left[\begin{matrix}\text{Statically}\\ \text{indeterminant force}\end{matrix}\right]+\left[\text{Displacement coefficient of End b}\right]\left[\begin{matrix}\text{End b}\\ \text{move}\end{matrix}\right]=-\left[\begin{matrix}\text{Support displacement due to}\\ \text{statically determinant moment}\end{matrix}\right] \quad \cdots\cdots\cdots(12b)$$

【Reaction force at End b】

The reaction force of End b is deemed to be a reaction force of the assumed statically indeterminate force acting on the shearing center of vertical sections including bottom supports, and this condition is given by formula (12c) in matrix expression.

$$\left[\text{Reaction force coefficient at End b}\right]\left[\begin{matrix}\text{Statically}\\ \text{indeterminant force}\end{matrix}\right]=\left[0\right] \quad \cdots\cdots\cdots(12c)$$

This formula is transformed by a null matrix and formula (12d) is obtained.

$$\left[\text{Reaction force coefficient at End b}\right]\left[\begin{matrix}\text{Statically}\\ \text{indeterminant force}\end{matrix}\right]+\left[\begin{matrix}0\\ \vdots\\ 0\end{matrix}\right]\left[\begin{matrix}\text{End b}\\ \text{move}\end{matrix}\right]=\left[0\right] \quad \cdots\cdots\cdots(12d)$$

Let the left hand sides of formula (12b) and formula (12d) be incorporated and product of a square matrix and a column vector is obtained, and let the right hand sides of both formulae be incorporated and a column vector is obtained, then the condition which the elastic equation satisfies is written in the form of formula (12).

$$\underset{(2n+2)\times(2n+2)}{\begin{bmatrix} F \end{bmatrix}} \quad \underset{(2n+20)\times 1}{\begin{bmatrix} \chi \end{bmatrix}} = \underset{(2n+2)\times 1}{\begin{bmatrix} S \end{bmatrix}} \qquad \text{(size of matrix)} \qquad \cdots\cdots(12)$$

or, $F \quad \chi \quad = S$

Matrix F is a square matrix which has $2n+2$ rows and $2n+2$ columns and contains support displacement coefficients of statically indeterminate reaction force, rigid displacement of supports due to End b movement and reaction force conditions of End b. Vector χ is a column vector which has $2n+2$ unknown elements. Vector S is also a column vector which has $2n+2$ rows and corresponds to constants which are -1 multiplied by support displacement due to statically determinate torsion moments and reaction force condition values of End b.

Fig. 3．1－25 shows detailed contents of each matrix.

［Matrix F］: The lateral axis is unknowns of $2n+2$ columns which are statically indeterminate reaction force X_j and Y_j, and End b displacement ξ_b and η_b, and the vertical axis is support numbers of $2n+2$ rows which are bottom supports in the x and the y direction and End b in the x and the y direction. Sub matrixes A thru D are displacement coefficients which are sums of support displacement coefficient calculated by the method of (3) for the described external force. Each of them is a square symmetrical matrix and matrix B equals matrix C. The right side down line mask area of ξ_b and η_b column is a displacement matrix of End b and contains rigid displacement of each support due to End b movement. The magnitude of rigid displacement is determined according to an assumption that the

End b movement is caused by a rigid rotation of the gate body around End a and is added to the support displacement due to statically indeterminate reaction force. The element which has no impact on any other element is set as 0. The left side down line mask area of End b row is a reaction force matrix which specifies the reaction force condition of End b movement. End b can move without any restriction except that its reaction force has to be in equilibrium with load. The value of reaction force matrix element can be easily determined since dynamical condition of End a and End b is a simple support and load between End a and End b is transmitted to End b according to ratio of the distance between the loading point and End a over the distance between both Ends. The element which has no impact on any other element is set as 0. The load is statically indeterminate force, X_j and Y_j, acting on shearing center of sections. This new definition is necessary as long as the reaction force matrix is concerned although X_j and Y_j were previously defined as statically indeterminate reaction force. Product sum of the load and the distribution rate equals 0. This is a value of End b reaction force condition mentioned before. The reaction force matrix is a transposed matrix of

Matrix name $\begin{pmatrix} F \end{pmatrix}$ $\begin{pmatrix} \chi \end{pmatrix}$ $\begin{pmatrix} S \end{pmatrix}$

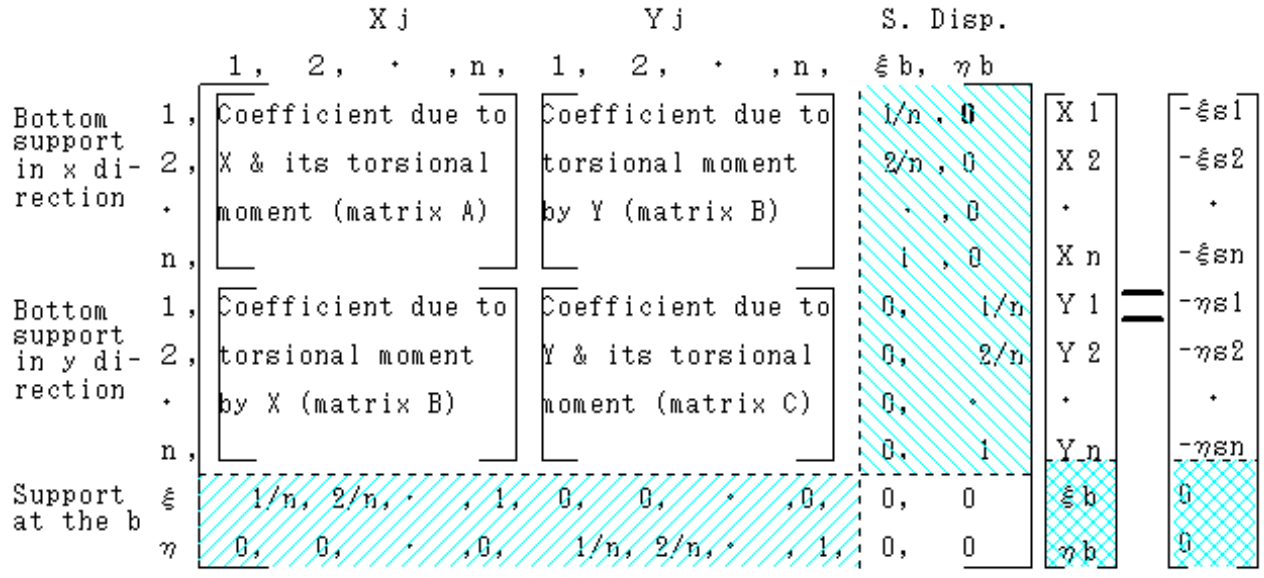

Fig. 3. 1－25

the displacement matrix and both matrix stay at symmetrical positions. The four elements of right bottom area which is left by the two matrixes are filled with 0. It is quite apparent according to above explanation that the matrix F is a symmetrical matrix as a whole as it is ordinary seen in this kind of structure.

[Vector χ] : The is a column matrix of unknowns whose masked portion is displacement of End b and other is statically indeterminant reaction force.

[Vector S] : The masked portion is filled with the reaction force condition and other portion is filled with product of - 1 and support displacement calculated by the method in (a) of (3) against statically determinate torsion moment.

Solutions of formula (12) are given by formula (13) where F^{-1} is an inverted matrix of F. Matrix operation required to obtain χ can be carried out quite easily with the assistance of a computer.

$$\chi = F^{-1} S \qquad \cdots\cdots(13)$$

So far the gate body which is driven only by one end is considered. In short, one end of the gate body is fixed for rotation and other end is free. For both end drives or, in other words, both ends fixed for rotation, the theory described in this section can be applied in its entirety except that half of statically determinate torsion moment M_0 which is sum of the torsion moment given by formula (1) of clause (2) is applied at n section. The difference will exist only in column vector S of formula (13) and (X, Y) of both end drives would agree with the results of one end drive if the gate section is uniform throughout. Statically determinate torsion moment which acts on n section in both cases are given by formula (14) and (15).

For one end drive, $m_{sn} = m_s \div 2 \qquad \cdots\cdots(14)$

For both end drives, $m_{sn} = m_s \div 2 - M_0 \div 2 \qquad \cdots\cdots(15)$

Formula (13) can be transformed to formula (16) for the sake of the both end drives

analysis since statically determinate torsion moment acting on other than n section is equal in the both cases where S_b is a matrix S whose support displacement element is replaced by the displacement due to additional torsion moment acting

$$\chi = F^{-1}(S - S_b) = F^{-1}S - F^{-1}S_b \quad \cdots\cdots(16)$$

on n section. Solution of the first term in right side of the formula (16) is for one end drive and that of the second term corresponds to the same structure except that only reaction torsion moment acts on End b and its statically indeterminate reaction force equals 0 since the support displacement is in a straight line and no bending occurs in the gate body as long as the body section is uniform over its width. Statically indeterminate reaction force of the both end drives in this case equals the one ene drive according y. It can be confirmed referring to this result that End b movement goes back to 0.

(5) Results of analysis

Statically indeterminate reaction force obtained by the elastic equation is inserted to the following formulae to get internal force and structural deformation and then the internal force is inserted to formulae explained at clause 3. 1. 3. 1 to get stress distribution.

[Statically indeterminate reaction force at 0 section]

$$\left.\begin{aligned} X_0 &= -\sum_{k=1}^{n} X_k \\ Y_0 &= -\sum_{k=1}^{n} Y_k \end{aligned}\right\} \quad \cdots\cdots(17)$$

[Support reaction force at j section]

$$\left.\begin{aligned} R_{xj} &= w_x c + X_j \\ R_{yj} &= w_y c + Y_j \end{aligned}\right\} \quad \cdots\cdots(18)$$

where c is 0.5 for $j = 0$ and n and 1 for other section, and subscript x and y indicates force direction.

[Shearing force at j section]

$$\left.\begin{aligned} Q_{xj} &= \sum_{k=0}^{j-1} X_k \\ Q_{yj} &= \sum_{k=0}^{j-1} Y_k \end{aligned}\right\} \quad \cdots\cdots(19)$$

where subscript x and y indicates force direction.

[Bending moment at j section]

$$\left.\begin{aligned} M_{yj} &= l_s \sum_{k=1}^{j} Q_{xk} \\ M_{xj} &= l_s \sum_{k=1}^{j} Q_{yk} \end{aligned}\right\} \quad \cdots\cdots(20)$$

where M_y and M_x is bending moment around the y and the x axis.

[Internal torsion moment at j section]

$$T_j = \sum_{k=j}^{n} m_{sk} + Q_{xj} l_{pyj} + Q_{yj} l_{pxj} \quad \cdots\cdots(21)$$

[Torsion angle at j section]

$$\theta_j = \sum_{k=1}^{j} \frac{T_k l_s}{G J_{tj}} \quad \cdots\cdots(22)$$

Five kinds of typical examples analyzed by the elastic equation are shown below.

［Example 1］

This is an ordinary case whose gate body has a uniform fish belly section and is driven at one end. This case will be compared with the results of bending-torsion theory later. Fig. 3.1－26 shows the gate section at its installed position. Conditions for the calculation are as follows.

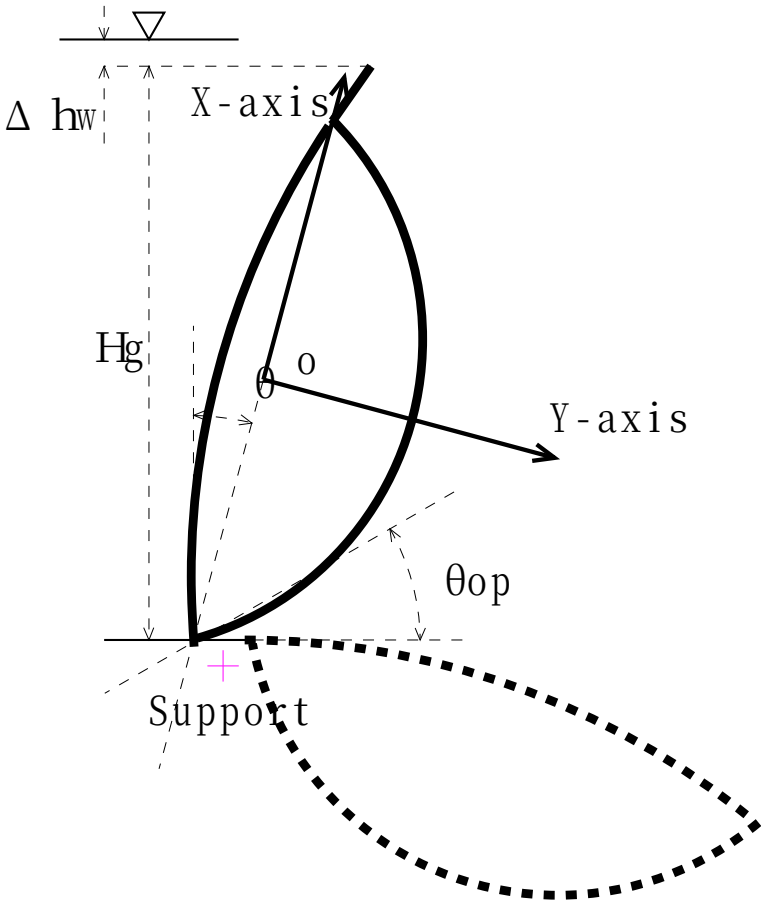

Fig. 3.1－26

A. Principal data

Height : H_g = 6400 mm

Width : L_g = 25000 mm

Section : H_k = 6000 mm

r_o = 3480 mm

r_i = 9000 mm

t_o = 20 mm

t_i = 20 mm

Inclination : θ = 15 °

Support : L_{py} = 391 mm

L_{px} = 3206 mm

Support space : n = 8

Over flow : Δh_w = 300 mm

Calculation : θ_c = 30 °

Young m. : E = 21000kgf/mm2

Poisson ratio : ν = 0.3

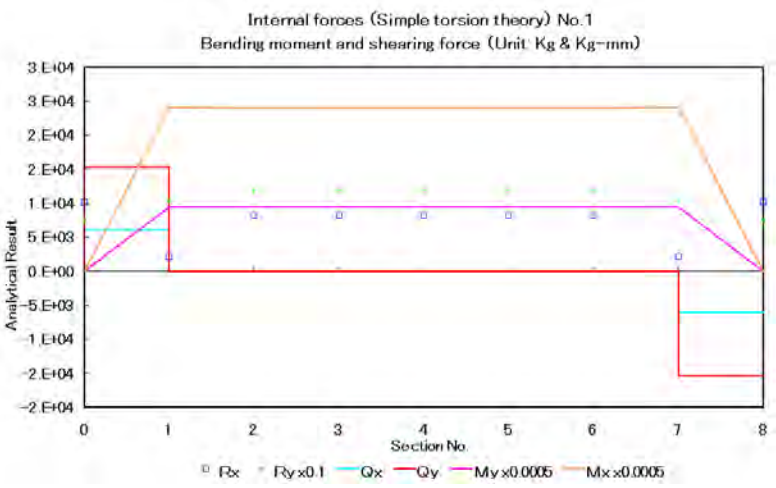

Fig. 3.1－27

Shear m.: G = 8077 kgf/mm2

B. Sectional data

M. area: J_0 = 267017 mm2

S. area: A_s = 9366848 mm2

G. center: Δ_{xg} = 0 mm

Δ_{yg} = 451 mm

S. mod: $I_y = 8.81 \times 10^{11}$ mm4

$I_x = 1.84 \times 10^{11}$ mm4

Bend. s.: c_x = 14097265 mm3

c_y = -48565429 mm3

Shear center: x_s = 0 mm

y_s = 204 mm

Simple t.: $J_t = 5.26 \times 10^{11}$ mm4

C. Load: w_y = 118749 Kg/n

w_x = 8188 Kg/n

m_s = 3.08E+8 Kg·mm/n

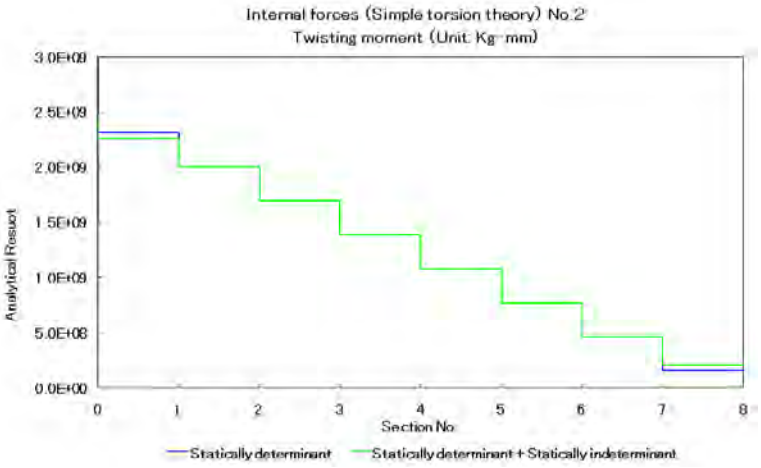

Fig. 3.1-28

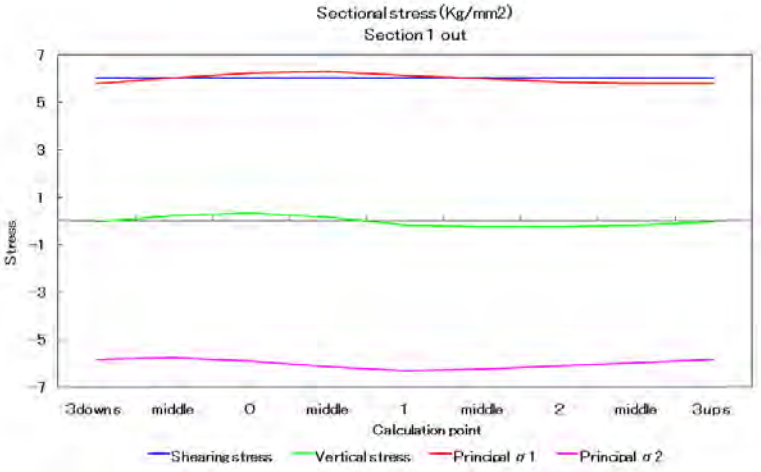

Fig. 3.1-29

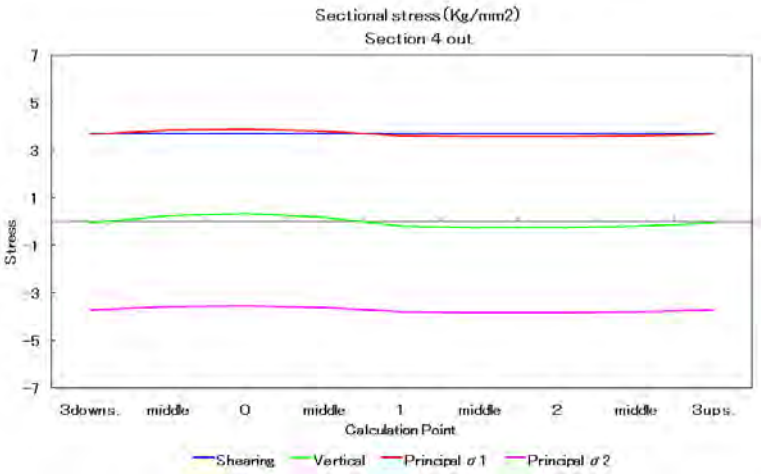

Fig. 3.1-30

Symbols other than specified in Fig. 3.1-26 follow Fig. 3.1-12. Bending shear flow of this section is shown on Fig. 3.1-14. Figs. 3.1-27 thru 31 show results of the analysis where X and Y axis correspond to those defined in Fig. 3.1-26 and symbols are common to those appearing at other places in section 3.1.3. Fig. 3.1-

２７ and ２８ show sectional internal force and Fig.- ２７ shows support reaction force, shearing force and bending moment and Fig- ２８ shows two kinds of internal torsion moment, the one including statically determinate torsion moment alone and the other including statically indeterminate

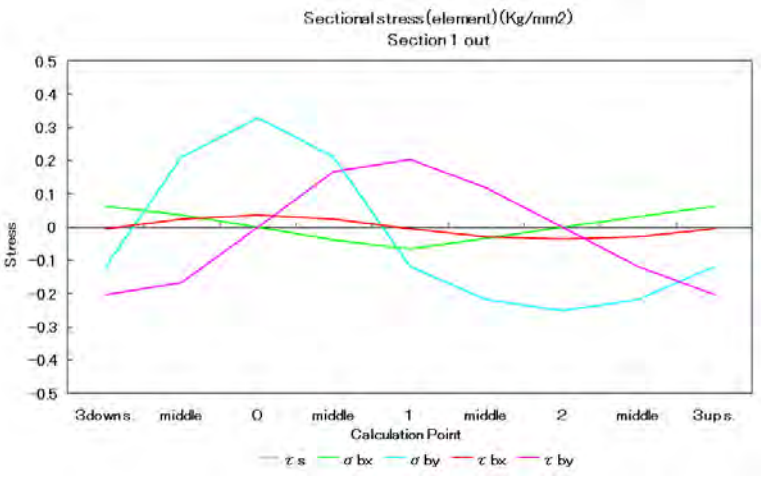

f

Fig. ３. １－３１

torsion moment in addition to statically determinate torsion moment. The + direction of the internal force coincides with the definition of formulae. The lateral axes in these figures represent section numbers and the vertical axes represent analytical results after multiplying by rates shown in thefigures. Unit used is as shown in the figures. As the statically indeterminate reaction force of a sectionally homogeneous case is very small, the corresponding shearing force and bending moment are also very small and, eventually, torsion moment almost equals to the statically determinate torsion moment anddecreases almost lineally toward the unsupported gate end. Fig. ３. １－２９ thru ３１ shows stress distribution. Fig. ３. １－２９ and ３０ shows shearing stress, normal stress and principal stress on sections, and Fig. ３. １－３１ shows shearing stress due to torsion and bending stress and shearing stress due to bending, and the Fig.- ２９ and ３１ correspond to section 1 (near the gate terminal) and Fig ３０ corresponds to section 4 (the gate midst). The lateral axis represents locations on the section and numbers on the axis agree with those in Fig. ３. １－１２ and the middle means middle point between adjacent numbers. Shearing stress is dominant on both sections, which are almost in pure shearing state. Fig. ３. １－３１ has been zoomed up to show all stress except torsion shearing stress which is out of the sight .

［Example 2］

This an example to show difference between the one end drive and the both end drives and its model equals Example 1. Fig. 3. 1－32 and 33 show results of internal force analysis. Fig. -32 shows support reaction force, shearing force and bending moment and statically indeterminate reaction force on the bottom support exactly equals that of Example 1 the figure coincides with Fig. 3. 1－27 accordingly since the gate section is uniform over the gate width. Fig. -33 shows internal torsion moment which equals Fig. 3. 1－28 after shifted by $M_0 \div 2$ upward because of same reason as above.

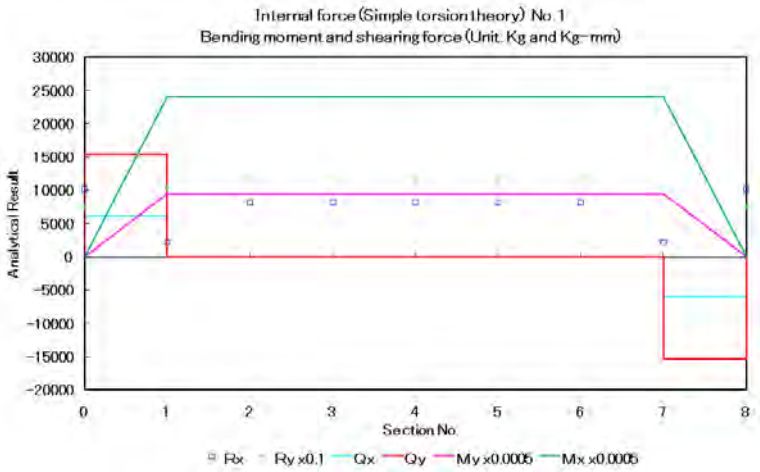

Fig. 3. 1－32

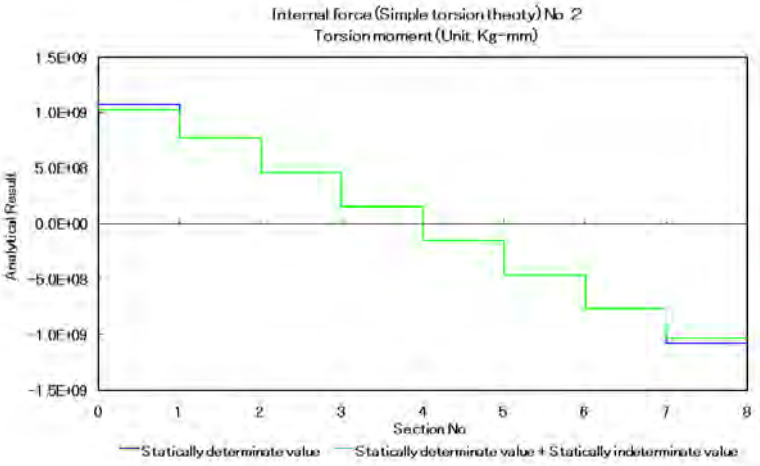

Fig. 3. 1－33

［Example 3］

This case intends to show the difference in internal force of sectionally non uniform structure which was taken from reference[*1]. Fig. 3. 1－34 shows the gate section at its installed position. This gate is 50 m width with both ends supported but structurally separated at its center. Eventually each half of the gate is independent and its length is 25 m which is divided into 8 spaces by 9 bottom

[*1] Bibliography (12)

supports. Sectional rigidity at section 0 ～ 2 is maximum, then section 2 ～ 4, and section 4 ～ 8 is minimum. Example 1 conforms to this case as far as the gate length and number of bottom supports are concerned, and the both sectional shapes are almost same. Fig. 3. 1－35 and －36 show analytical results of internal force. Direction of internal force in all examples shown in this thesis coincides with the both figures. Fig. -35 shows bottom support reaction, shearing force and bending moment. They exactly correspond to the original figures except that their + directions agree with the definitions made in this section. Note that the scale on the vertical axis and the figures to be multiplied to the analytical results do not agree with Fig. 3. 1－27. Sectionally non uniform structure result in a wide increase of sectional forces and

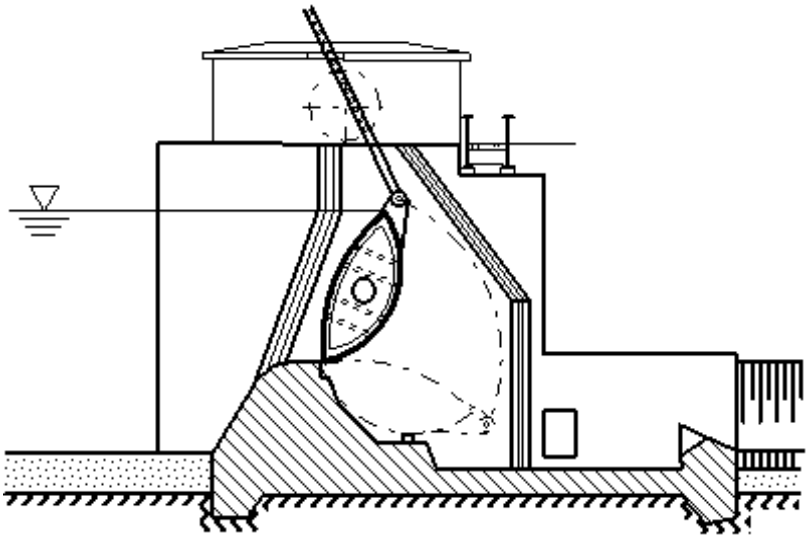

Fig. 3. 1－34

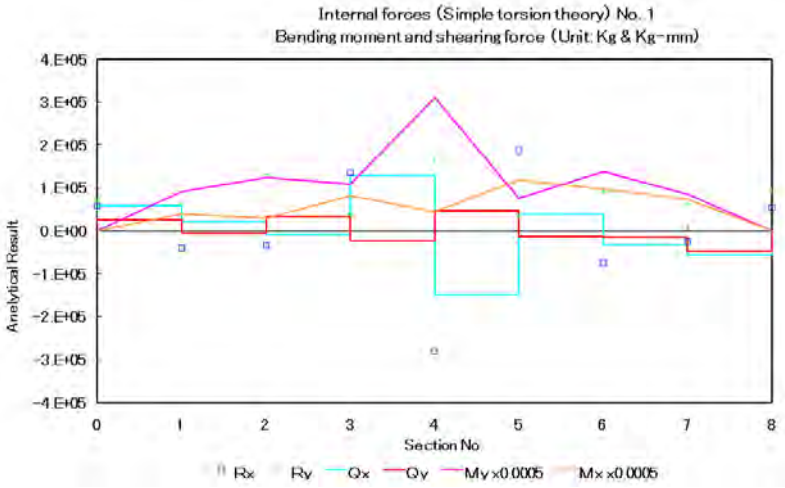

Fig. 3. 1－35

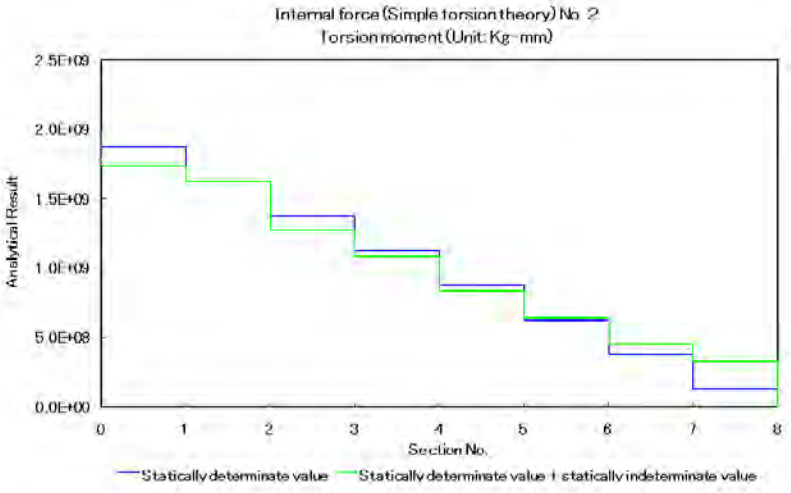

Fig. 3. 1－36

disturbance in their distribution. All of them show the impact of a remarkable increase in statically indeterminate reaction forces that agrees with the results obtained by the author in his own projects. Fig. 3. 1－36 shows internal torsion moment. Although remarkable difference is there in the internal force shown on Fig. 3. 1－35 and the statically indeterminate reaction force, it is confirmed that there is no big variation in internal torsion moment and the overall tendency is similar to internal force shown on Fig. 3. 1－28.

［Example 4］

The purpose of this example is to show one of two methods to mitigate impact of a big I_y described in section (2) of 3. 1. 2 and this it corresponds to the Example 3 except that the restraint in the x direction on the bottom supports is released[*1]. In other words, all bottom supports except two outside supports can move in the x direction without restriction. Fig. 3. 1－37 and 38 show analytical results. Fig. -37 shows bottom support reaction, shearing force and bending moment. In case of the Example 3 bending moment M_y on Fig. 3. 1－35 indicates a big amount since statically indeterminate reaction force X_j is very large due to the big I_y and on the other hand M_y of Fig. -37 has remarkably decreased. The cause of this improvement is mitigated slope change rate of gate deformation because statically indeterminate reaction force in the x direction does not occur at the bottom

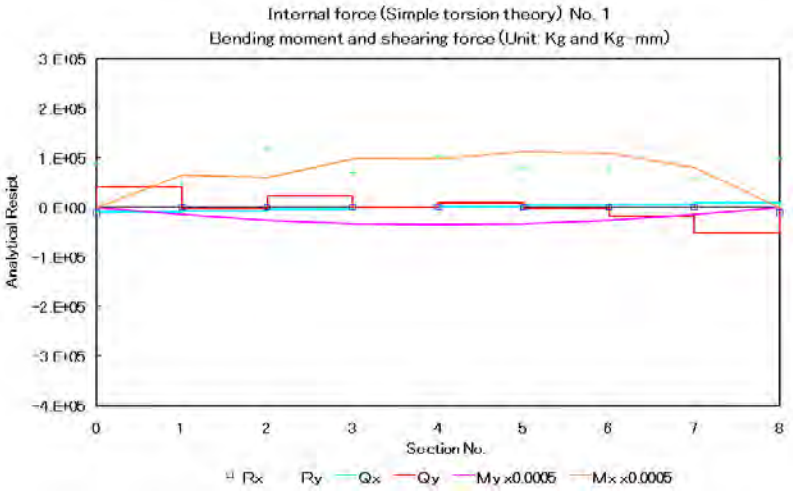

Fig. 3. 1－37

[*1] Bibliography (12)

supports but at same time statically determinate reaction force w_x' shown on Fig. 3. 1 - 16 dose not occur so that another bending moment due to w_x which used to be a partner of w_x' to make a couple appears. Fortunately load in the x direction is generally not so much and eventually M_y is much mitigated. Although a couple of w_x disappeared, another rotation moment also occurs and has to be counted in Vector S shown on Fig.- 25 since the loading point of w_x does not coincide with sectional shearing centers and also the shearing center line is not straight. But fortunately again this matter does not make any big difference of major trend. For a reference, the rows and columns relating to the x direction of Fig.- 25 are excluded from the matrix. Fig.- 38 shows internal torsion moment which does not differ much from Fig. 3. 1－36.

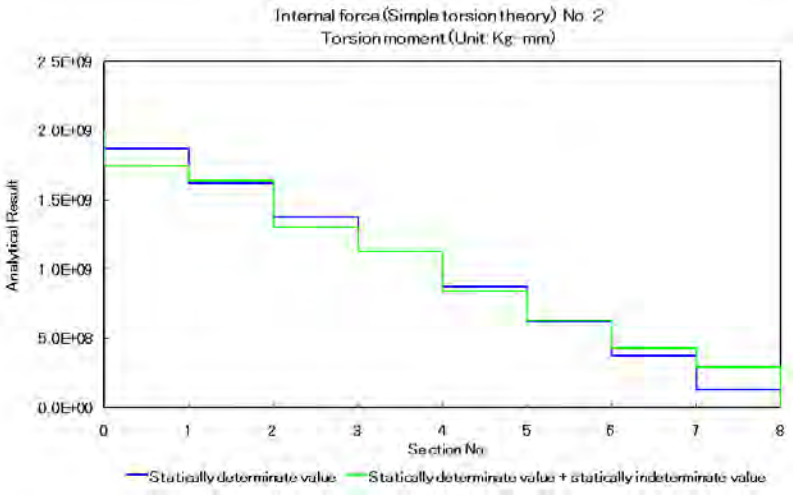

Fig. 3. 1－38

［Example 5］

The purpose of this example is to show another method to mitigate impact of a big I_y than one explained at Example 4. And it will be compared with bending- torsion theory later. This case is of a sectionally uniform rectangular gate driven at one end. Fig. 3. 1－39 shows the gate section at installed position. A rectangular coordinate is so set that the x axis is in gate height direction and the y axis is at right angle to the gate height. X- axis passes through shear center and a bottom support. Bending moment around y- axis would

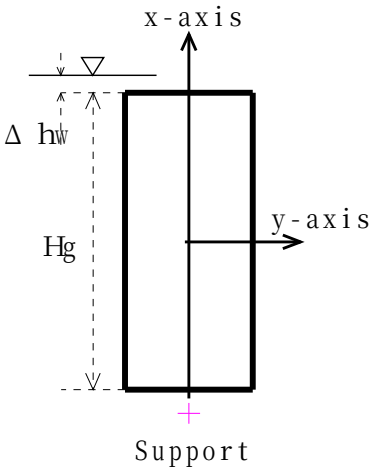

Fig. 3. 1－39

not be created in this arrangement even if the section rotates around the support since the shearing center does not move toward the x direction. Conditions for analysis are as follows.

A. Principal data

Height : H_g = 27500 mm

Width : L_g = 100000 mm

Section : L_f = 5000 mm

L_w = 13750 mm

$t f_1$ = 34 mm

$t w_1$ = 34 mm

$t f_2$ = 34 mm

$t w_2$ = 34 mm

Inclination : θ = 0 °

Support : L_{py} = 0 mm

L_{px} = 15750 mm

Support space : n = 8

Over flow : Δh_w = 0 mm

Calculation : θ_c = 90 °

Young m. : E = 21000kgf/mm2

Poisson ratio : ν = 0.3

Shear m. : G = 8077 kgf/mm2

B. Section data

M. area : J_0 = 2550000 mm2

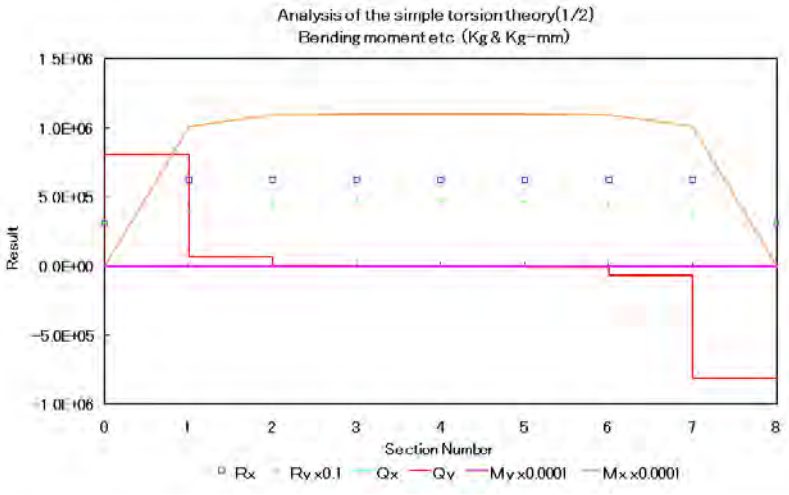

Fig. 3. 1－40

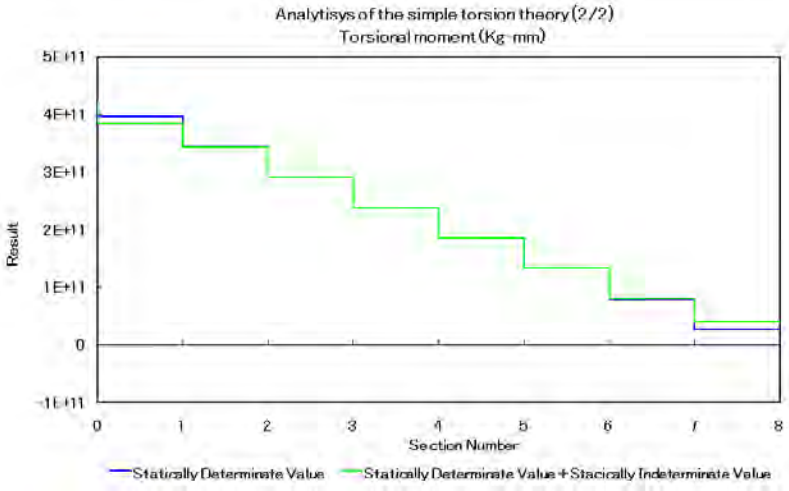

Fig. 3. 1－41

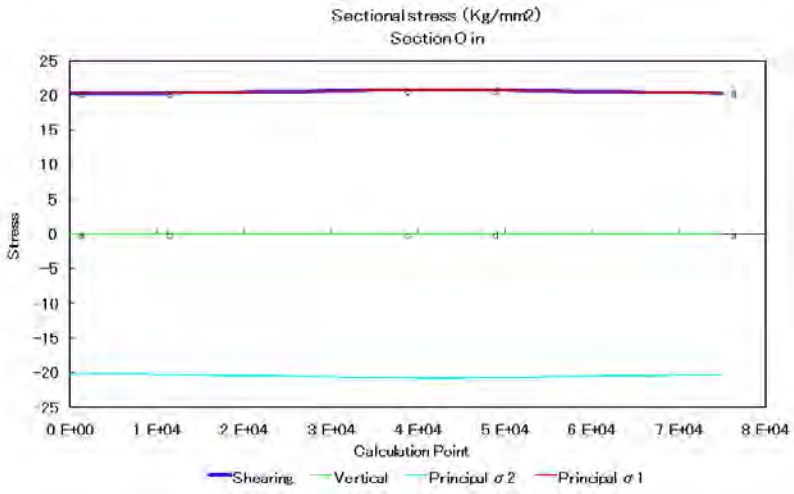

Fig. 3. 1－42

S. area : $A_s = 275000000$ mm2

Gravity c. : $\Delta_{xg} = 0$ mm

$\Delta_{yg} = 0$ mm

S. mod. : $I_y = 5.24E+13$mm4

$I_x = 2.46E+14$mm4

Bend. s.: $c_x = -2.34E+09$mm3

$c_y = 2.34E+09$ mm3

Shear center : $x_s = 0$ mm

$y_s = 0$ mm

Simple t.: $J_t = 1.37E+14$ mm4

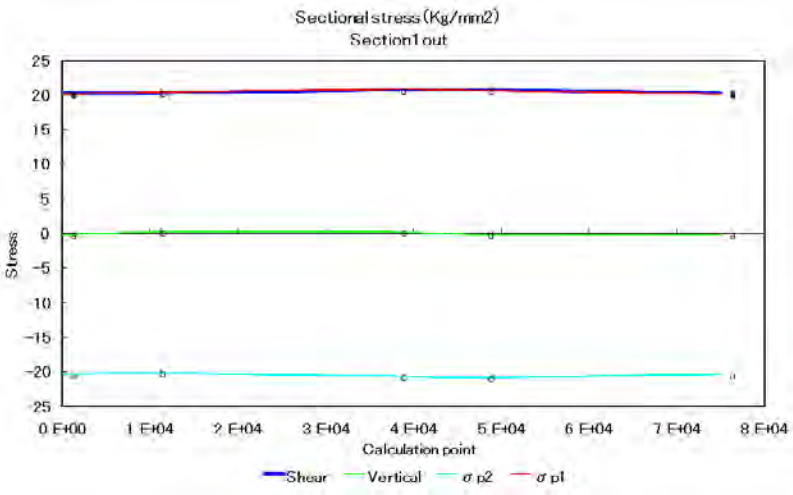

Fig. 3. 1－43

C. Load : $w_y = 4726563$Kg/n

$w_x = 625547$ Kg/n

$m_s = 5.28E+10$Kgmm/n

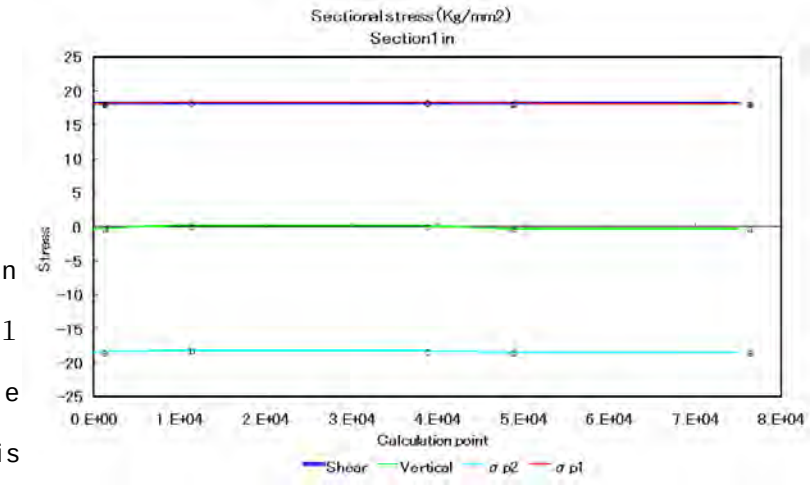

Fig. 3. 1－44

Symbol other than defined in the Fig.- 39 follows Fig. 3. 1 - 12 and Fig. 3. 1 - 13. The coordinate in the Fig. - 13 is set with its x axis in the gate height direction and y axis in right angle to the height. The calculation conditions are shown according to the coordinate of the Fig. - 13 and others are the Fig.- 39. The bending shear flow of this section is shown on Fig. 3. 1－15. Fig. 3. 1－40 thru 44 is the results of analysis. The Fig. －40 and 41 show internal force. The Fig. －40 is support reaction force, shearing force and bending moment and the Fig.－41 is internal torsion moment. The internal force is shown according to the coordinate of the Fig. －39 and its plus direction coincides with the definition made in the description of formulae. Magnitude of Q_x and M_y in the Fig. －40 is 0 that shows the impact of large I_x has been completely eliminated. As the sectional shearing center and the bottom support stay on the x axis, all the

elements in the x direction of matrix B and C and vector S shown in Fig. 3. 1 −25 equals 0 and accordingly Q_x and M_y can not be created since statically indeterminate reaction force X_j becomes 0. All shearing center of the gate section which is unsymmetrical with respect to the vertical axis and non-uniform over the gate width such as the Example 3 and 4 can not be set on the x axis but the impact of large I_x can be decreased by setting all the shearing centers close to the x axis as long as possible. The Fig. −42 thru 44 show sectional distribution of shearing stress, vertical stress and principal stress. The Fig. -42 is section 0, the Fig. -43 is section 1 out (opposite to the gate leaf center side) and the Fig. -44 is section 1 in (the gate leaf center side). The stress is shown according to the coordinate on the Fig. -13. The lateral axis is a gauss length along the gate section. The alphabets shown on the figure coincide with the alphabets along the section shown on Fig. 3. 1−13. The magnitude of the stress is very big because the assumed load level is much higher than an ordinary level.

(6) Model test

Fig. 3. 1−45 thru 47 show the results of large scale model shop experiment which was carried out to verify the validity of analytical result of the elastic equations. The contents of experiment is shown on Appendix 3. 1−6. The model used is a fish belly flap of 17m width x 1m height supported by one end and it was loaded so that all statically determinate torsion moments are constant. The measured stress and analyzed stress corresponding to maximum load is shown together. The fig. −45 shows sectional distribution of the principal stress. The measuring points are at middle of section 0 and 1. The analytical results of the simple torsion theory (simple σ2) and bending-torsion theory (bending σ2) which will be described later are shown together. Sectional shape, gravity center and shearing center are also shown in mm scale on the figure and the stress is shown after multiplied by 20 for the sake of display on the common axes. There is not big difference between results of the bending-torsion theory and the simple

torsion theory that is an accidental agreement and its detail will be discussed later in the section of the bending- torsion theory. The Fig.－４６ shows longitudinal distribution of principal stress. The measuring point is center of the back plate (at 12 o'clock on Fig. －４５). The Fig.－４７ shows gate leaf displacement along the upper edge of the gate body. Although there is a certain deviation of experimental points, the tendency of analytical result shows good agreement with the experiment in general.

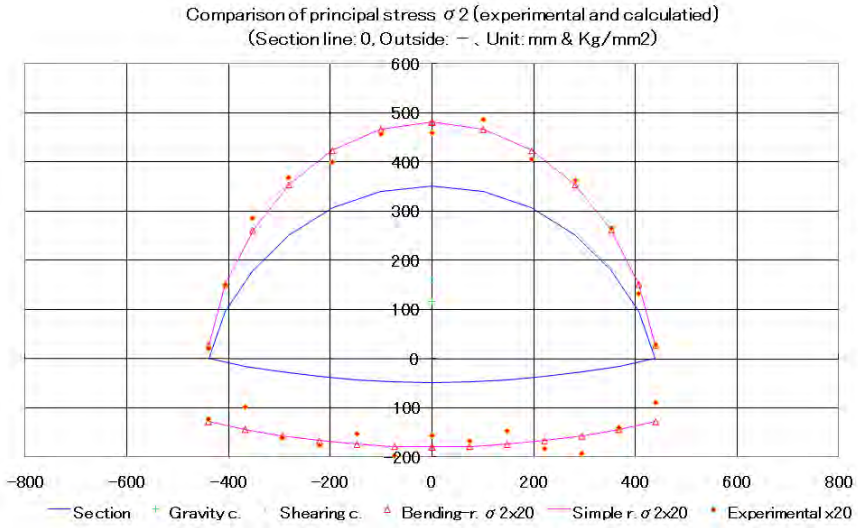

Fig. ３. １－４５

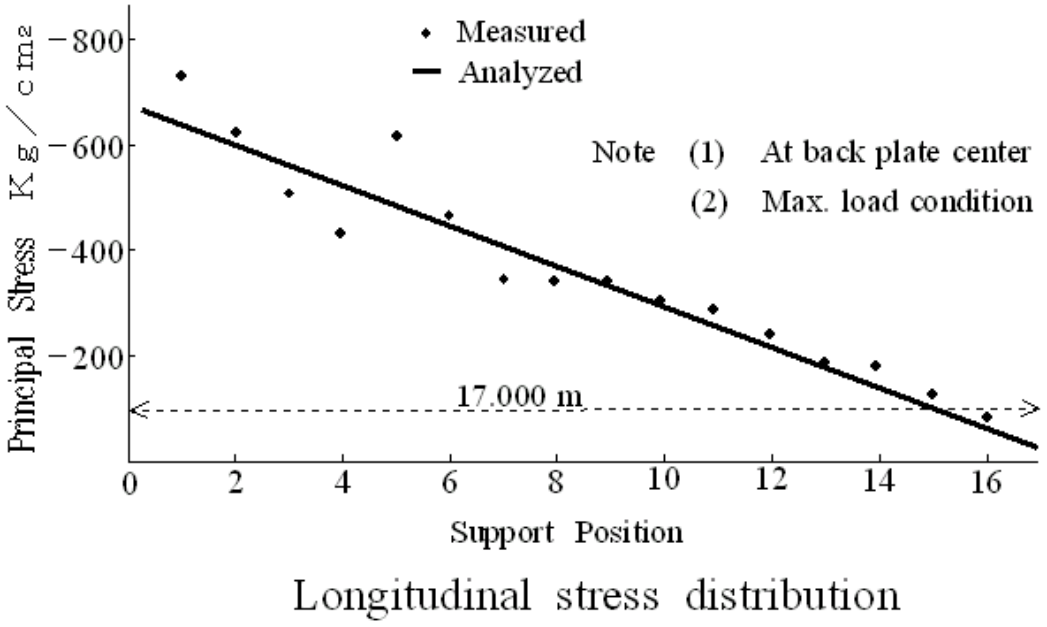

Fig. ３. １－４６

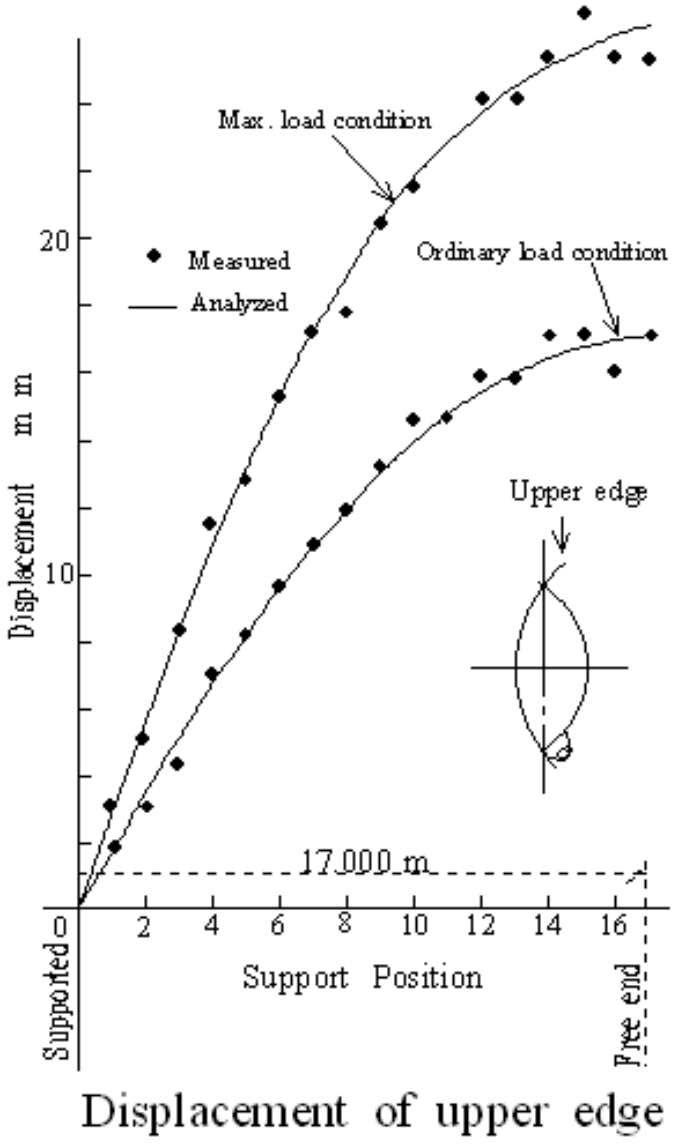

Fig. 3. 1－47

（7） Effect of bottom support move

As an example of application of the elastic equation, the operation load analysis of a flap gate on main gate shown in Fig. 3. 1－7 (double gate) when the main gate deflects due to water load is shown. It was technically critical subject during development stage of a double gate to estimate effect of the main gate deflection on operation function of the flap gate since hinge support centers of the flap gate move due to the main gate deformation. It was possible to estimate the effect of

center movement with help of the elastic equation and it was found out that magnitude of the effect is not so important except that a partial stress on the gate body extremely increases which needs a proper remedial homology. Operational load due to the gate rotation around the hinge supports is torsion moment caused by water pressure, earth pressure, gravity force, seal rubber friction and hinge axle friction acting on the flap gate and difference in the operational load due to the hinge center movement can be handled separately from the torsion moment without big error. Suppose θ denotes rotation angle in the clockwise direction of the gate body operation, U_0 denotes strain energy when $\theta = 0$ and U denotes strain energy, M_f denotes torsion moment due to friction and M_d denotes the difference of operation moment due to the support center move when $\theta = \theta$, then following relation holds according to the energy conservation law.

$$\int_0^{\theta} M_d \, d\theta + U_0 = \int_0^{\theta} M_f \, d\theta + U \qquad \cdots\cdots(23)$$

Following formula which gives M_e is obtained by differentiating the formula (23)

$$M_d = M_f + \frac{dU}{d\theta} \qquad \cdots\cdots(24)$$

by θ. Let a change in the left- hand of the formula (24) due to the support center move be found out. Let the impact to the main gate deformation of the flap gate deformation be negligible since the main gate rigidity is usually much bigger than the flap gate rigidity. As it is acceptable that the deformation pattern of main gate at its totally closed position does not change even if the magnitude of the load on the gate body varies, the over all gate deformation can be defined by displacement δ of the representative point on the gate. Suppose u_x and u_y denote total strain energy of the gate body due to the point movement by a unit distance in the x and the y direction respectively, then the strain energy corresponding to

displacement δ is given by following formula. The x and y axes and the direction

$$U = u_x (\delta \cos^2(\theta_d + \theta))^2 + u_y (\delta \sin^2(\theta_d + \theta))^2 \quad \cdots\cdots(25)$$

where θ_d is angle between the x axis and δ when $\theta = 0$ (refer to right figure).

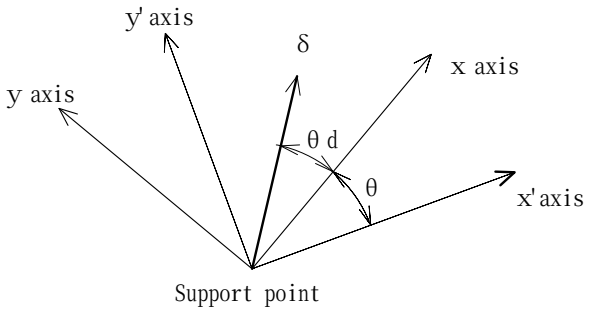

of δ and θ are defined as right figure.

The second term at the right-hand of formula (24) is obtained by differentiating the formula (25). It is found out by this

$$\frac{dU}{d\theta} = \delta (u_x - u_y) \sin 2(\theta_d + \theta) \quad \cdots\cdots(26)$$

formula that the support movements will not give any difference when u_x equals u_y since the strain energy is constant. To relate u_x and u_y to the result of elastic equation, they have to be divided into portions corresponding to the composition of the equation. Firstly the elements are divided into bending portion and torsion portion which are identified by suffix b and t respectively and let them be expressed as following.

$$\left.\begin{aligned} u_x &= u_{xb} + u_{xt} \\ u_y &= u_{yb} + u_{yt} \end{aligned}\right\} \quad \cdots\cdots(27)$$

Then the bending portion are divided into portions of statically indeterminate reaction force X and Y which are identified by suffix X and Y respectively and let them be expressed as following.

$$\left.\begin{aligned} u_{xb} &= u_{xbX} + u_{xbY} \\ u_{yb} &= u_{ybX} + u_{ybY} \end{aligned}\right\} \quad \cdots\cdots(28)$$

The strain energy u_b and u_t due to bending and torsion are related to bending moment M_b and internal torsion moment T which are obtained from solutions of the elastic equation by following formulae. Formula (27) and (28) can be

$$\left.\begin{aligned} u_b &= -\frac{1}{2}\int_0^l \frac{M_b^2}{EI}\,dz \\ u_t &= -\frac{1}{2}\int_0^l \frac{T^2}{GJ_t}\,dz \end{aligned}\right\} \qquad \cdots\cdots(29)$$

calculated by the values of formula (29) whose M_b and T correspond to unit displacement in the x and the y direction respectively and then the value of formula (26) is determined. The x and y axes shall coincide with the main axes of the flap gate. In preparation of the elastic equation on the Fig. 3. 1－25, an S Vector element which corresponds to a support of the representative point is filled with unit displacement in the x and y direction respectively and other elements in S Vector are filled with values corresponding to a deformation pattern of the main gate since no statically determinate torsion moment exists. The first term M_f at the right- hand of formula (24) is hinge axle friction load due to support reaction force and its value is determined in following way just like the second term of the formula. Suppose the friction load of support axle due to unit displacement in the x and y direction of the representative point are w_{xp} and w_{yp} respectively, M_f is given by following formulae. r_p denotes radius of support axle and c_{pf} denotes its

$$M_f = r_p c_{pf} \delta \left(w_{xp} \cos(\theta_d + \theta) + w_{yp} \sin(\theta_d + \theta)\right) \qquad \cdots\cdots(30)$$

frictional coefficient. w_p is approximately calculated from statically indeterminate reaction force X and Y which are solution of the elastic equation according to following formulae.

$$w_p = (w_{pX}^2 + w_{pY}^2)^{1/2} \qquad \cdots\cdots(31)$$

where $w_{pX} = \sum_{k=0}^{n} | X_k |$

$$w_{pY} = \sum_{k=0}^{n} | Y_k |$$

As it is explained above, operational load of torsion moment at any gate opening can be calculated by formulae (26) and (30) against arbitrary direction of δ if u_x, u_y, w_{px} and w_{py} which correspond to unit support movement in the x and y direction is calculated before hand with help of the elastic equation. The $x-y$ axis shall coincide with sectional principal axes of the flap gate.

[Calculation example and measured result]

Calculation condition and results of the double gate on Fig. 3. 1－7 are

Main gate			Flap gate		Calculation/ (Max.)	
Width		40.000	Width	40.000	dU／dθ	0.1 t－m
Heigth		2.400	Height	1.100	M_f	0.007 t－m
Design depth		3.500	N.space	13	S.r.f.	0.5 t
Operate depth	Up	3.400	S.interval	3.333		
	Dw	1.800	N.support	14		
Earth height		1.500	Design d.	1.000		
Lifting height		10.500	Inc.angle	45°		
Hoist type		2M2D	Limit disp	1/800		
Limit disp.	Hol	1/800	Leaf block	1		
	Var	1/600	Drive	B.end		
Operation method (1) Main operation with flap totally opened (2) Flap operation with main totally closed						

Table 3. 1－2

shown. Scantling is in m. dU/d θ trys to prevent the flap opening but its magnitude is about 1% of the moment due to gate weight and about 0.5% of the total moment including water pressure and M_f is about 0.5% of the moment due to seal rubber friction although it works in same direction as the seal rubber friction. As a consequence these increase are practically negligible. To verify the result, a operation test was carried out by the large scale model described at section (6). The content of test is shown in Appendix 3. 1－6. Operation load was measured with the supports in a straight line and with the supports after moved and no meaningful difference was found between both cases. It can be concluded that difference of operation load due to the support movement is negligible since design specification and dimensional scale of the intended gate is a general class but the increase in support reactions is about 10% which has to be taken into account for gate leaf design.

3. 1. 3. 3 Analysis by space frame theory

The time came when a space frame program was daily available for structural analysis since computers and their soft had developed rapidly and a new choice as an analytical procedure of the torsion type structure was added. As it is quite clear in the explanation of analysis by the elastic equation at preceding section that the torsion type gate is a structure of in- plane displacement in the x and y directions as well as out- of- plane displacement in right direction to it and is deemed to be a space frame. In this section, analytical method of the torsion type gate by the space frame theory will be described on an example of the gates for ship yard dry docks which are shown on Fig. 3. 1－8 thru 10. The content of space frame theory will not be referred to since it has been already well- known.

(1) Analytical model

Table 3. 1－3 shows Principal items of the two gates to be analyzed and Fig.

Design criteria for the repair dock gates		
Item	Koyagi	MSHI
Scale of dock	500 000 DWT	400 000DWT
Dock sill dimension	100mx13.5m	80mx12m
Design criteria	Specification for highway bridges	DIN
Allowable stress (JIS SS41 yield point 25 kgf/mm2)		
Tensile strength	14 kgf/mm2	14.5 kgf/mm2
Shearing stress	8 kgf/mm2	8.4 kgf/mm2
Compined stress	21 kgf/mm2	18.75 kgf/mm2
Gate weight	1270 ton	780 ton
Material of main parts		
Outer plate	SS41, SM50	SS41, SMA41
Hinge bracket	SC49	SC49
End bearing plate	S35C	Kempus
Wooden plank	Tub	Kempus
Seal rubber	Neoprene	Neoprene
Anticorrosive plate	Alnode P.05	Alnode P.10S

Table 3．1－3

3．1－48 shows the general structural construction of MSHI repair dock gate which is one of the two gates and Fig. 3．1－49 shows the bottom metal of the same gate. Structure of both gates is a kind of torsion type gate with a closed thin shell having web frames arranged at a constant interval and a heavy terminal wall which can resists great terminal reaction force and deference from the ordinary type is ① the gate section is

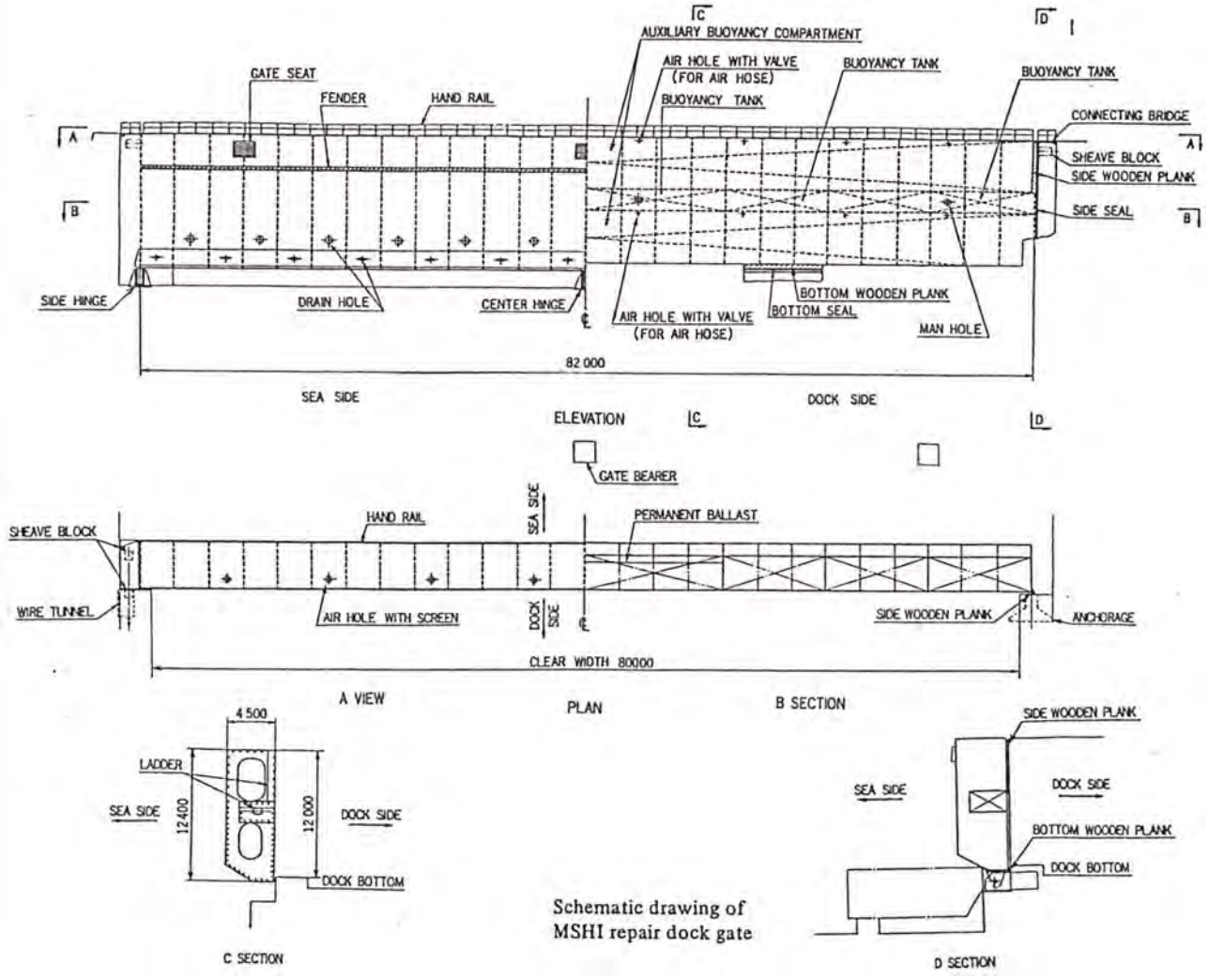

Fig. 3．1－48

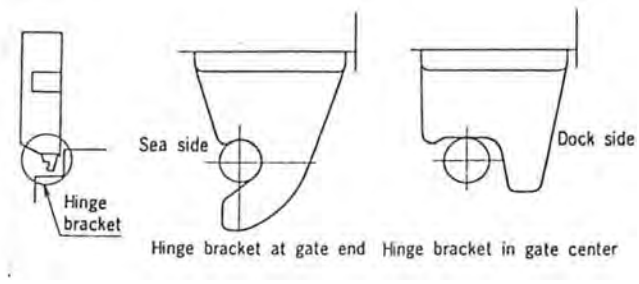

Fig. 3. 1－49

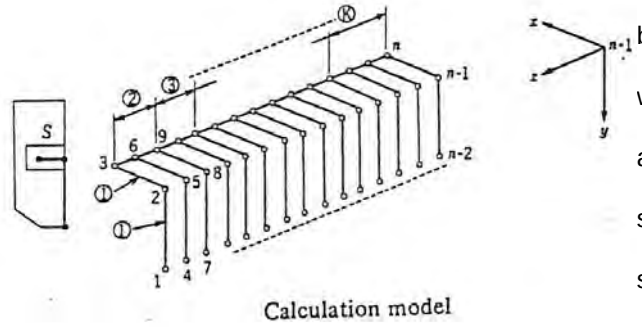

Fig. 3. 1－50

divided into a several closed compartments of buoyancy, ② there are no supports along the gate bottom except a vertical dock bottom concrete sill wall against which the gate bottom with its wooden bearing seats is pressed by water pressure on the gate (see SECTION D of the Fig.－48) and ③ the bottom metal (the Fig.－49) and the wooden bearing seat (Fig. 3. 1－54) are provided to the gate leaf ends to be subject to coupled reaction force. The shear flow on the section of ① includes a several loop flows so that formula (bf) and (aj) need small modification and calculation method of corresponding shearing center and sectional torsion rigidity become a little bit different, but this thesis does not go into their contents. For a reference a computer soft which is applicable to calculation of shear flow on arbitrary section is available without any difficulty. Fig. 3. 1－50 shows the analytical model which consists of the closed thin shell replaced by 3 ～ 6, 6 ～ 9 etc. passing through sectional shear center and the web frame members replaced by 1 ～ 2, 2 ～ 3 etc. An analytical model of space frame structure is usually built on the assumption that rigidities in each structural member are concentrated along at the sectional center of gravity because the bending moments and axial forces play main roles in the structural deformation. Even in the case where torsion rigidity is not negligible, problems seldom arise because the sectional shear center of members in most space frames coincides with the sectional center of gravity. In the case of torsion type structures, both centers usually do not coincide with and if it is assumed that bending rigidity of a torsion member is concentrated along its shear center, the joint interval of the member next to the torsion member would change.

The interval change is bound to bring about the same result as rigidity change of the next member, and the rigidity has to be adjusted according to the interval change so that proper internal forces may be obtained through computer analysis. Rigidities of the web frame members in the Fig.- 5 0 are supposed to be adjusted in taking into account the disagreement between sheer and gravity centers of the gate body but this model could be justified by giving so larger rigidity to the web members that their deformations are deemed to be zero, that has been a tacitly accepted premise in the analysis by the elastic equations. Concerning the boundary condition of the model, the node 1, 4, 7, ···· and n－2 which correspond to lower end of the web frames and the node 2 which corresponds to the top of gate leaf terminal is fixed against their displacement in the dock longitudinal direction (the x axis direction)[*1] and the node 3 which corresponds to the shearing center of the gate leaf terminal section is fixed against rotation around the axis in dock width direction (the z axis) and displacement in the dock longitudinal direction (the x axis direction). As the gate is bilaterally symmetric with respect to the gate width center line and the analytical model covers left side half of the gate body, the node n- 2 is fixed against displacement in the three direction and rotation around the longitudinal axis (the x axis) and vertical axis (the y axis) and the node n- 1 and n are fixed against displacement in the width direction (the z axis direction) and rotation around the longitudinal axis (the x axis) and vertical axis (the y axis). Although the gate leaf bottom is supported by the linear wooden seat as explained in the item ② and the model boundary condition differs a little bit from it, this condition is unavoidable compromise since this modelization started from replacement of space members by lines.

（2） Calculation load

Although the acting point of load in the analysis of elastic equation is a load

[*1] The fix of node 2 is originally not required.

center point of the section including web frame, the load in the space frame theory is load acting at the node of sectional shearing center and torsion moment to compensate difference between the load center point and the loading node since loading point in the space frame theory is only a node.

(3) Analytical results

Fig. 3. 1－51 shows internal torsion moment and bending moment which are the output from a computer. They show similar tendency to the results of elastic equation. Bending moment only around the vertical axis (the y axis) is shown on the figure since the bending moment around the anteroposterior direction axis (the x axis direction) is remarkably small because the wooden seat is not fixed against displacement in the vertical direction (in the y axis direction). Although the torsion moment shows a linear distribution as a whole, difference exists between the step heights on the curve. This is caused by extreme plate thickness change of the closed section according to the distribution of torsion moment. Fig. 3. 1－52 and 53 show the measured data versus the analyzed values during the loading test. The

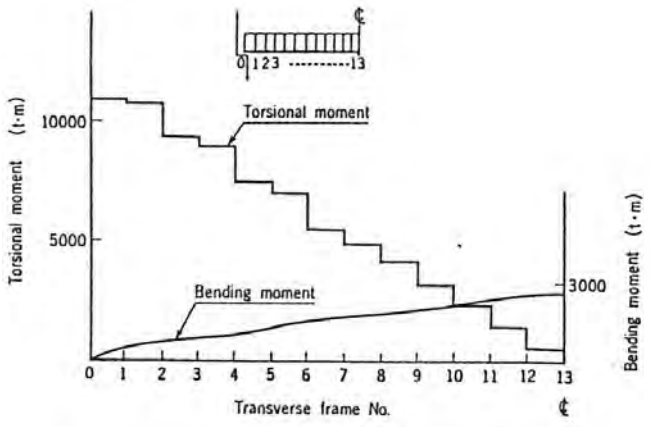

Fig. 3. 1－51

Fig. －52 shows stress and hydraulic condition during the test and the measured points Strain gauges used are 45°&3- directions and two gauges were used

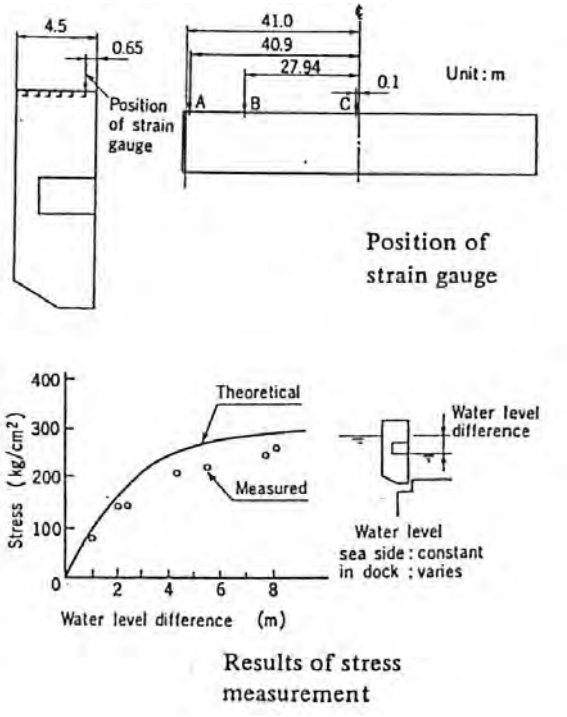

Fig. 3. 1－52

for a point for the sake of accuracy. The Fig. －５３ shows displacement of the gate top and its loading condition. The measured displacement showed a big value at the start of loading and increased rapidly until the water head difference became around 70 cm, and then began to increase in so stable as the water head difference growth. It is understood that the first rapid increase was caused by uneven contact of the wooden seat with the gate frame embedded in dock concrete and the stable increase is a real displacement

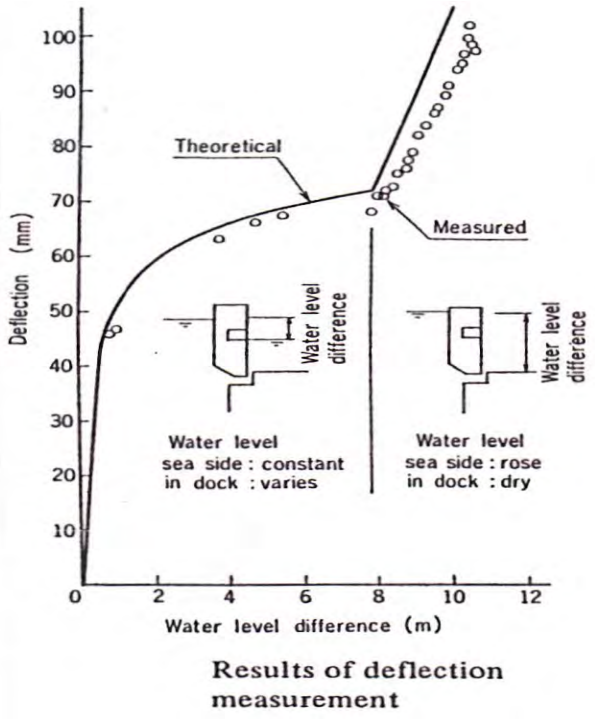

Results of deflection measurement

Fig. 3. 1－５３

corresponding to elastic deformation of the gate leaf and the measured value was compared with the analyzed value after added by the difference between the measured value and the analyzed value at the beginning of stable increase. Analyzed results of stress and displacement replicate the tendency of measured results and their magnitude indicate fairly good agreement. Analytical result of the space frame theory is supposed to be same as those obtained from the analysis by elastic equation. The major purpose of this section is to show that the torsion type gate can be analyzed as a space frame structure.

（４） Lateral strength

Although analysis by space frame theory was shown with the assumption that no deformation arises on vertical gate sections including web frames, actual gate section deforms to some extent and separate analysis is necessary to clarify the effect of these deformation on the gate strength. As the magnitude of deformation in the lateral section of the gate differs according to the position of section in

longitudinal direction (the z axis direction) and type of deformation at terminal, intermediate and center sections are different, examples of sectional analysis on the three locations are shown.

［Terminal section］

External load elements on the section including a heavy terminal wall are bending and torsion shearing stresses working through the closed thin shell section, a terminal load which is transmitted through stiffeners on shell plate of the water sealing side (skin plate), terminal couple which is reaction force to support the gate terminal, and, statically determinate and indeterminate reaction forces (w and X) acting on the terminal support. These elements are in equilibrium within each combination shown on following table. M_0 is a sum of statically determinate torsion moment given by formula (1). Fig. 3.1－54 shows working points of the terminal couple. The couple consists of the reaction force R_H which acts from sea side to the bottom metal on the gate terminal and the reaction force R_T which acts from the dock side to the wooden bearing seat on the gate terminal top. R_T is obtained through following formula since the couple equals a half of M_0.

Number	Conbination Elements
①	Statically indeterminate reaction force & Integrated Bending shearing stress
②	Statically determinate reaction force & Terminal load
③	Reaction moment & Coupling of Torsional shearing stress ,Combination ① and Combination ②

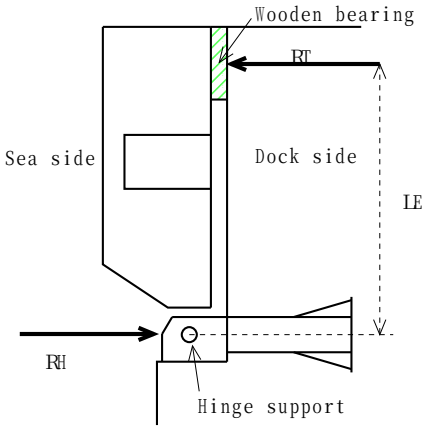

Fig. 3.1－54

$$R_T = M_0 \div 2 \div L_E \quad \cdots\cdots (31)$$

L_E is arm length as shown on the Fig. －54. R_T is uniformly distributed load along the wooden bearing seat. Let R_H include statically determinate and indeterminate reaction force acting on the bottom metal and be expressed by

following formula although the original R_H equals R_T. Subscripts x denotes x direction and the figure 1 denotes node number.

$$R_H = R_T - ((SDRF)_x + (SIRF)_{x1}) \quad \cdots\cdots(32)$$

where SDRF is abbreviation of statically determinate reaction force and SIRF is that of statically indeterminate reaction force.

The $(SIRF)_{x1} < 0$ in general and if the $((SDRF)_x + (SIRF)_{x1}) < 0$, then $R_H > R_T$. R_H is reaction force in x direction of the bottom metal and the gate weight multiplied by (3/16) has to be considered as a reaction force in y direction of the bottom metal in this case. Concerning the terminal load, the gate weight acts at gravity center and water pressure force acts at pressure center and they are shared by the stiffeners. Stress distribution in the section can be analyzed by two dimensional finite element method or by manual calculation after the section is replaced by a box section, the terminal load is neglected and the whole section is replaced by a statically determinate structure. Fig. 3.1－55 explains the manual calculation. Rectangular b b'c'c b shows the closed section where L_W and L_H are the section width and height respectively and L_h and L_E are the load acting positions of R_H and R_T respectively. The closed section is replaced by beam a c and the x axis is set with its original point at the a and its direction as shown on the figure. The load acting on the beam are concentrated load R_H, distributed load r t corresponding to R_T, concentrated load w b corresponding to a sum of shearing stress on the shell b b', concentrated load w c corresponding to a sum of shearing stress on the shell c c' and distributed

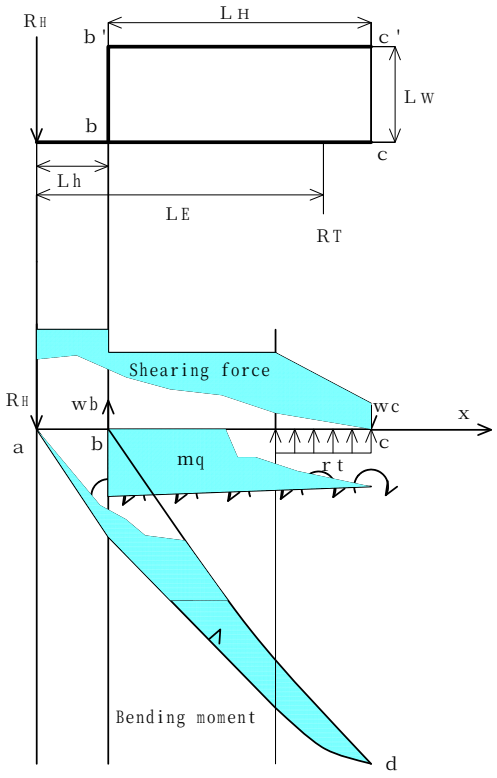

Fig. 3.1－55

bending moment m_q corresponding to couple composed of shearing stress on shell b c and shell b'c'. The shearing force on the figure is obtained by integration of the loads on beam, the bending moment curve a d on the figure is obtained by integration of the shearing force, the bending moment curve b d on the figure is obtained by integration of the bending moment m_q and the difference between the curve a d and b d shows bending moment of the beam. Although this figure shows only concept of bending moment distribution of the beam, it is found out that the maximum values of the shearing force and bending moment in the beam occur at the b and they can be calculated easily according to the figure. Furthermore, suppose statically indeterminate reaction force is negligible and concentrated load R_T acts at the c, the shearing force Q_b and the bending moment M_b are given by following formulae as a function of torsion shear flow q_t. The terminal wall will become to be in a pure shearing status since $M_b = 0$ when $L_h = 0$, in short, $L_H = L_E$.

$$
\begin{aligned}
&R_H = R_T \quad 2 q_t L_W L_H \div L_E \\
&w_b = w_c = m_q \quad q_t L_W \\
&Q_b \propto -2 q_t L_W L_H \div L_E \qquad (x \leqq L_h) \\
&\quad \propto -q_t L_W (2 L_H \div L_E - 1) \qquad (x > L_h) \\
&M_b \propto -2 q_t L_W L_H \div L_E \, x \qquad (x \leqq L_h) \\
&\quad \propto -2 q_t L_W ((L_H \div L_E - 1) x + L_h) \qquad (x > L_h)
\end{aligned}
\qquad \cdots\cdots (33)
$$

[Intermediate section]

Deformation of the intermediate section can be grasped by analysis of a plane frame model which corresponds to one compartment of the gate body including a web frame. Fig. 3. 1－56 shows the analytical model and bending moment distribution. The load for calculation is hydraulic pressure only and displacement restriction is two points of vertical directions and one point of dock longitudinal direction. The minimum 3 restrictions are required to let displacement in two directions and rotation in one direction remain finite and the given conditions

satisfy them. Actual state of restriction is only the longitudinal displacement restriction at the bottom wooden seat and other two restrictions are replaced by shearing rigidity of members composing the closed section. The method to replace the two restrictions of displacement and rotation by the shearing rigidity is shown on the figure

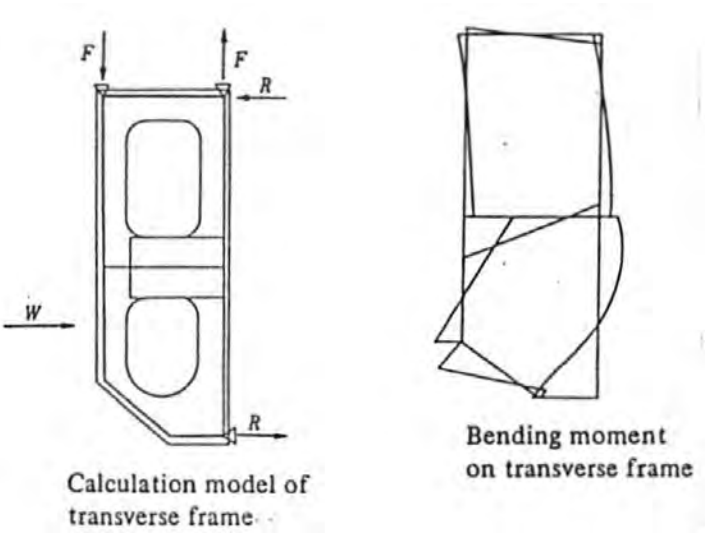

Fig. 3. 1－56

and also explained as follows. The tops of front and back shell panels whose shearing rigidity is much bigger than other two panels are fixed against vertical displacement and two coupling forces F and R are acting on the model as shown in the figure, and magnitude of R is determined according to the two condition i.e.: ① sum of the two couples equals torsion moment produced by the hydraulic pressure load on the model and the wooden seat reaction force and ② a ratio of F and R equals a ratio of the integrated shear flow values on the front and back panels (= 2 × L_H of Fig. 3. 1－55) and the other two panels (= 2 × L_W of Fig. 3. 1－55) and finally the obtained R is loaded on the top right corner of the frame model. Propriety of the assumption can be verified by comparing the reaction forces of restricted points with the results of structural analysis of whole gate structure.

［Center section］

There is a auxiliary support metal under the gate leaf center (hinge bracket in gate center) and it supports the gate leaf weight only. The gate leaf tends to deform as shown on Fig. 3. 1－57 since strain due to welding is released after the gate fabrication is completed. There is

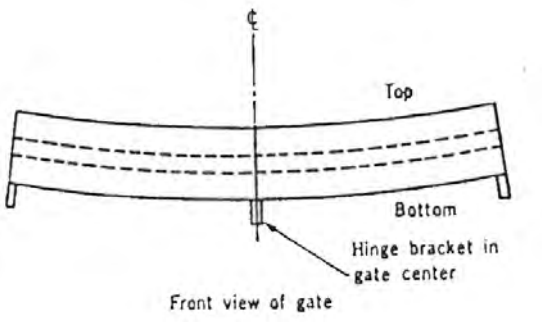

Deformation of gate due to welding

Fig. 3. 1－57

a possibility when the inside of the construction embankment is filled with water after the gate installation is over that the center section of the gate leaf deforms partially due to reaction of the gate weight concentration on the auxiliary support metal under the gate leaf center. Fig. 3. 1－58 shows structural analysis of the center section by 3-D finite element method. The a in the figure shows construction in the vicinity of the support metal, the b shows stress distribution and the c shows appearance of the deformation. The deformation appears only during the gate installation work and majority weight of the gate in service is compensated by buoyancy of water.

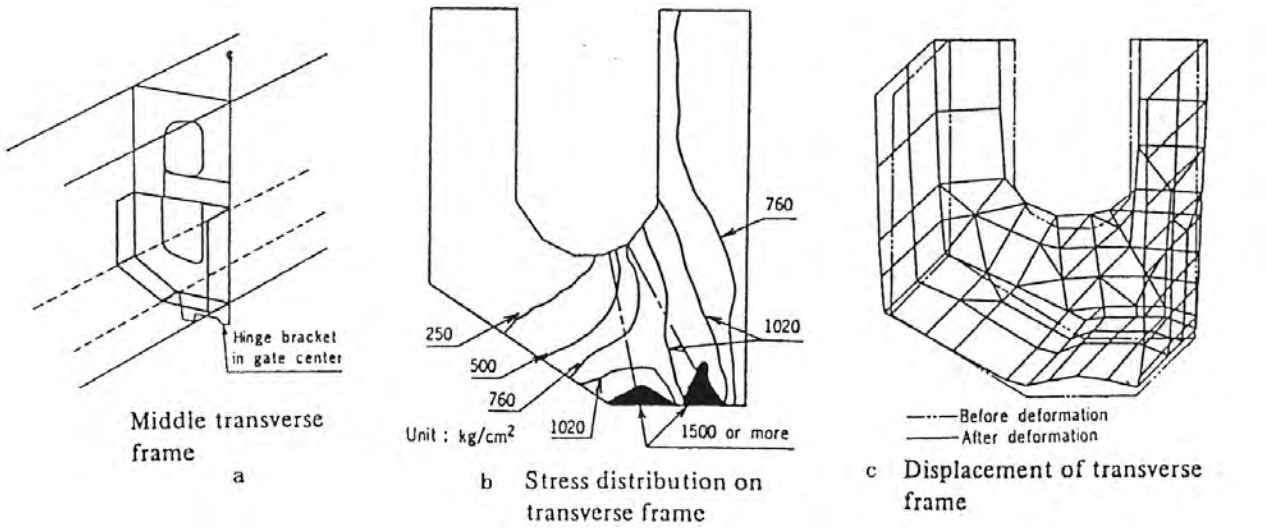

Fig. 3. 1－58

（5） Shear buckling

Precautions against shear buckling is very important for a torsion type structure because stress in shell members of closed sections is almost purely shear. Verification of buckling strength has to be done not only on the panel surrounded by stiffeners but also on various range of a panel including stiffeners and it is most important to find out that even the weakest buckling mode has enough strength. Bucking strength for shearing force can be verified by formulas listed in any

handbook[*1] for structural engineering. Openings are provided to shell members for various purposes and although their locations are selected from the less- important shell range from viewpoint of strength in general since the strength around openings will decrease, it can not help very often putting an opening on important strength member in case of the torsion type gate since whole shell panel of the gate is main strength member and most part of it is in critical state from viewpoint of strength especially in case of a large scale gate. The opening is usually strengthened by the plate doubling to mitigate stress concentration but the opening on the torsion type gate is often stiffened by a cylindrical stiffener to increase rigidity around the opening to prevent the panel from shear buckling. Study case on shear buckling of openings stiffened by cylindrical stiffeners is not so much[*2] and Fig. 3. 1－59 shows an example in which finite element method is applied for verification of the stiffening. It has been verified that the rigidity around the stiffened opening is much more than twice the rigidity of a panel without opening.

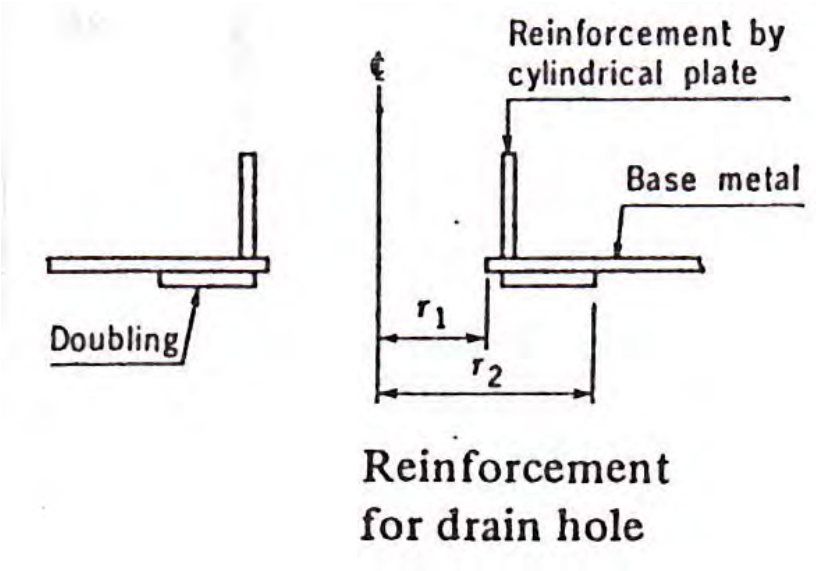

Fig. 3. 1－59

(6) Stress concentration at shell corners

The shell corner shown in Fig. 3. 1－8 is of a large circular shape to avoid shearing stress concentration on it. The corner shape in Fig. 3. 1－9 includes

[*1] For instance, bibliography (39)

[*2] Bibliography (26)

a right angle which was adopted to decrease the corner fabrication cost and whose stress concentration was taken into account for the gate leaf design. Fig. 3. 1－60 shows an example of stress concentration coefficient at a corner of the closed section.[*1] The results were obtained by the membrane theory where Eq(i) is a result obtained by solving the differential equation on the assumption that the corner membrane shape is a body of revolution, A is a result obtained by the method of finite difference without the assumption, the a is the inside radius of corner, δ is shell thickness, τo is stress of other than the corner and τmax is stress along the inside of corner.

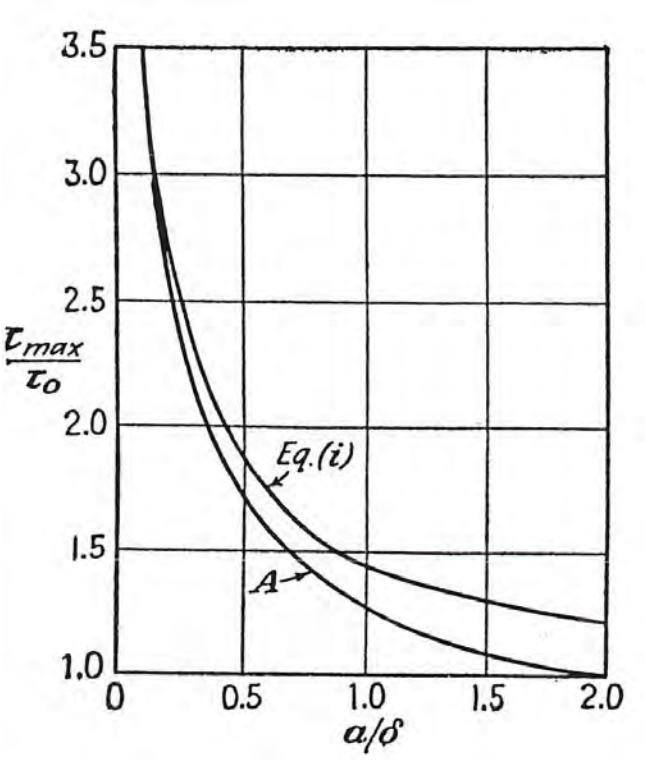

Fig. 3. 1－60

Fig. 3. 1－61 shows shape of the welded deposit metal on the corner where b b is the curve for a＝t and c c is the curve for a＝2t. According to the Fig. －60, τmax÷τo 1 for a＝2t and τmax÷τo 1.25 for a＝t. Field study on the corner fabrication to minimize total cost including stress concentration coefficient is necessary.

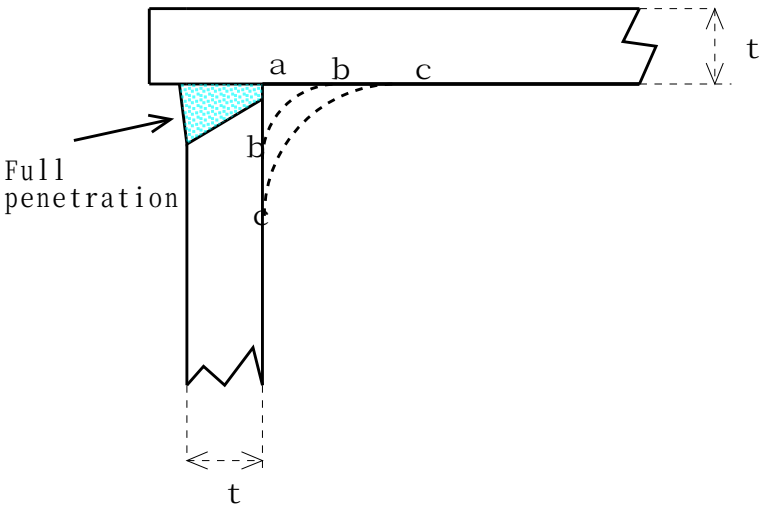

Fig. 3. 1－61

[*1] Cited from 301 page of bibliography (20).

3．1．4 Analysis based upon bending- torsion theory

Torsion phenomenon is a combination of the simple torsion and the bending- torsion and structural analysis including the bending- torsion is described in this section although only the simple torsion is considered in the preceding section. Phenomenon of the bending- torsion gives a big infulence upon stress distribution of a gate section. Basic theory of torsion in a closed thin shell section is shown at Appendix 3．1－2 and 3．1－3 and application results on the two kinds of section of the basic theory are shown at Appendix 3．1－4 and 3．1－5. The description in this section will start based upon these appendices. The formula which has an alphabetical number is a formula drawn from the appendix. Definition of terms in the drawn formula is shown in Appendix 3．1－1.

3．1．4．1 Stress distribution on a gate section

The bending- torsion theory includes both the simple torsion ane the bending- torsion and the all sectional stress described described in the section of the bending- torsion theory is reffered to in this section. In this section, distribution of shearing stress and vertical stress which come ouf due to the bending- torsion are made clear. A rectangular coordinate (x, y) is set coinciding with principal axes of a gate section. Sectional force is only bending- torsion moment T_w corresponding to the shearing stress and no bending moment and shearing force exists on the section since force and moment of the vertical stress are in balance on the section and no sectional force is composed. The shearing stress and the vertical stress are calculated for rotation angle θ of a section by following formulae.

[Bending- torsion section modulus]

$$C_{bd} = \Psi_0^2 J_0 - 2\Psi_0 J_1 + 4\Psi_0 a_i J_2 + J_3 - 4 a_i J_4 + 4 a_i^2 J_5 \quad \cdots\cdots (m)$$

where $a_i = A_s \div I_0$

$$J_0 = \oint t\,ds$$

$$J_1 = \oint R\,t\,ds$$

$$J_2 = \oint I\,t\,ds$$

$$J_3 = \oint R^2\,t\,ds$$

$$J_4 = \oint R\,I\,t\,ds$$

$$J_5 = \oint I^2\,t\,ds$$

$$I_0 = \oint \frac{1}{t}\,ds$$

$$R = \int_0^s r_s\,ds$$

$$I = \int_0^s \frac{1}{t}\,ds$$

Note 1. Original point of r_s is a shearing center.

[Bendin- torsion shear flow constant]

$$q_{w0} = -(\Psi_0 J_6 - J_7 + 2a_i J_8) \div I_0 \qquad \cdots\cdots(ae)$$

where Ψ_0 is given by formula (n) and a_i, I_0, R and I are defined at formula (m).

$$J_6 = \oint \frac{1}{t}\left(\int_0^s t\,ds\right) ds$$

$$J_7 = \oint \frac{1}{t}\left(\int_0^s R\,t\,ds\right) ds$$

$$J_8 = \oint \frac{1}{t}\left(\int_0^s I\,t\,ds\right) ds$$

[Bending- torsion shear flow]

$$q_w = \Psi_0 \int_0^s t\,ds - \int_0^s t\,R\,ds + 2a_i \int_0^s t\,I\,ds + q_{w0} \qquad \cdots\cdots(ac)$$

[Bending- torsion shearing stress]

$$\tau_w = \frac{q_w}{t} \cdot \frac{T_w}{C_{bd}} = -\frac{q_w}{t} E \frac{d^3\Theta}{dz^3} \qquad \cdots\cdots(ad)$$

[Warping constant]

$$\Psi_0 = \left(\oint t \int_0^s r_s\,ds - 2A_s \div \oint \frac{ds}{t} \cdot \oint t \int_0^s \frac{1}{t}\,ds\,ds\right) \div \oint t\,ds \qquad \cdots\cdots(n)$$

[Warping function]

$$\Psi = \Psi_0 - \int_0^s r_s\,ds + 2A_s \int_0^s \frac{1}{t}\,ds \div \oint \frac{ds}{t} \qquad \cdots\cdots(l)$$

[Bending- torsion vertical stress]

$$\sigma_z = E\Psi \frac{d^2\Theta}{dz^2} \qquad \cdots\cdots(aa)$$

［Distribution pattern on a section］

Distribution on a gate section of τ_w is defined by shear flow of bending- torsion and that of σ_z is defined by warping function Ψ. Fig. 3．1－62 thru 69 shows shear flow and warping function of various cases calculated on a fish- belly section and a box shape section shown on Fig. 3．1－12 and 13 respectively. All formulae being necessary in the calculation are shown in Appendix 3．1－4 (fish- belly) and 5 (box shape). They are results of applying above shown formulae of the general case to the two sectional sections. The original points of the x－y coordinate on Fig.－12 and 13 are determined for the sake of structural analysis carried out later, the original point of coordinate for above calculation has to be set at a gravity center of section. The calculated result is corresponds to the sectional shape and member scantlings shown on each figure and its magnitude is given by the calculated value multiplied by the rate shown on the figure. A sectional shape, a gravity center and a shearing center are also shown on each figure and outside of the section is the + zone of shear flow and warping function and clockwise shear flow is +. Fig. －62 thru 65 correspond to the fish- belly section of Fig. －12, and the remainders correspond to the box shape section of Fig.－13.

Let detail explanation of each figure be started. Fig. －62 shows bending- torsion shear flow and warping function of the case whose bending shear

flow is shown on Fig. －１４ or, in other words, both figures show results on the same section and the difference between bending shear flow and bending-torsion shear flow becomes very clear accordingly. The bending-torsion shear flow composes torsion moment around a shearing center just as the simple torsion shear flow dose and sum of the both torsion moments is in balance with the external torsion moment of a gate. Although impact degree of bending-torsion can be measured by a rate of bending-torsion moment among total torsion moment, shearing stress of bending-torsion is dramatically bigger than shearing stress of simple torsion when magnitude of both torsion moments is same since simple torsion shear flow is constant on a section whereas sign of bending-

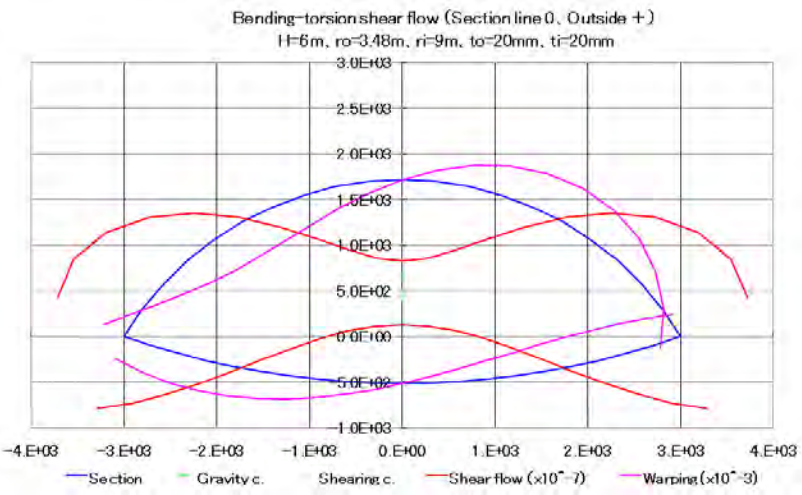

Fig. ３. １－６２

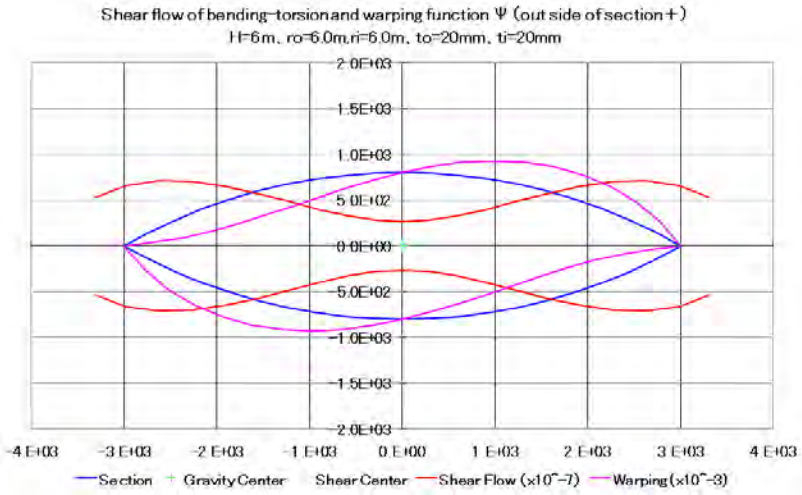

Fig. ３. １－６３

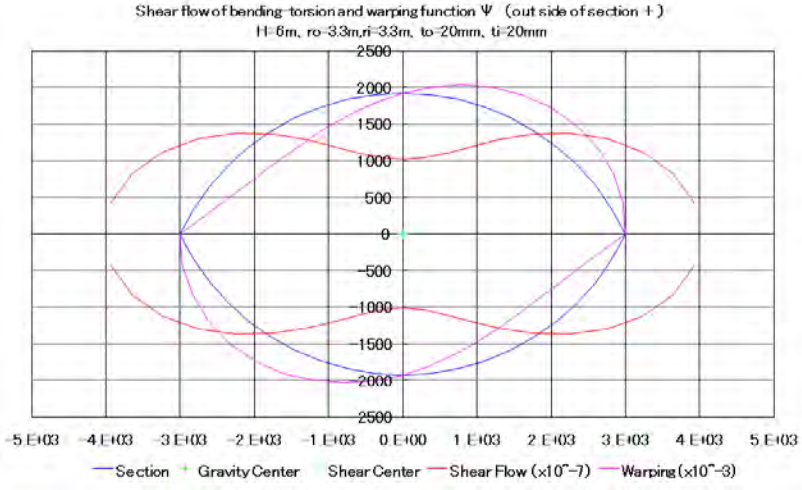

Fig. ３. １－６４

torsion shear flow on the section varys and value of bending-torsion moment is sum of the positive and negative moments. This is a cause of big sectional stress disturbance by bending-torsion phenomenon as it is shown in detail later. Fig. －63 thru 65 show effect of sectional shape and shear flow and warping function on a section of lens, ellipse and circular are shown. Shell thickness of a section is constant. In case of the circular section, both values are 0 and bending-torsion never comes out under any circumstance. Intensity of shear flow is supposed to decrease in sectional change approaching to a circular shape but it does not seem like so because the bending-torsion section modulus Cbd has increased as being described later. But it surely does so that the same comparison is made based on the formula (ad) which is a

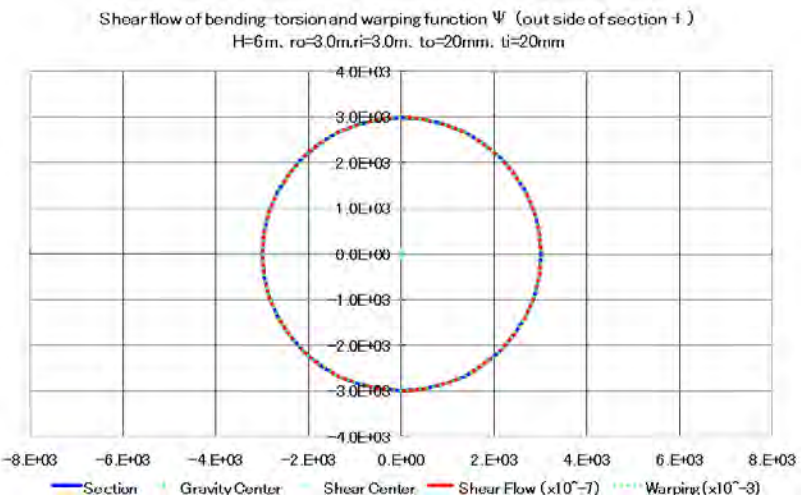

Fig. 3. 1－65

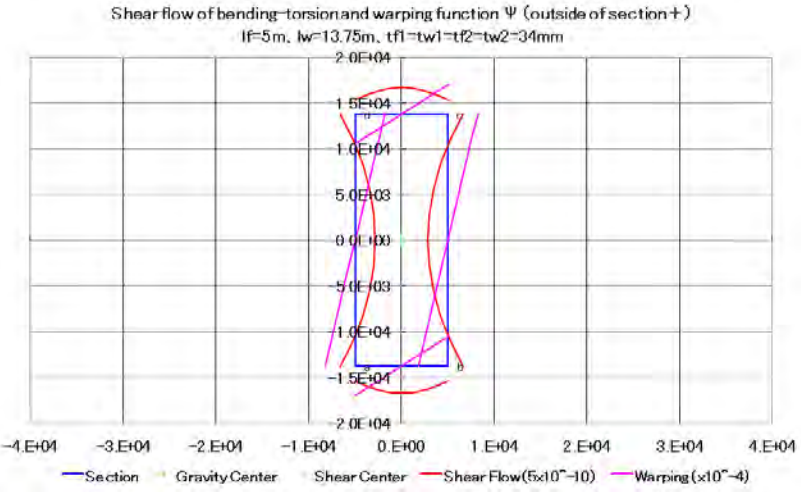

Fig. 3. 1－66

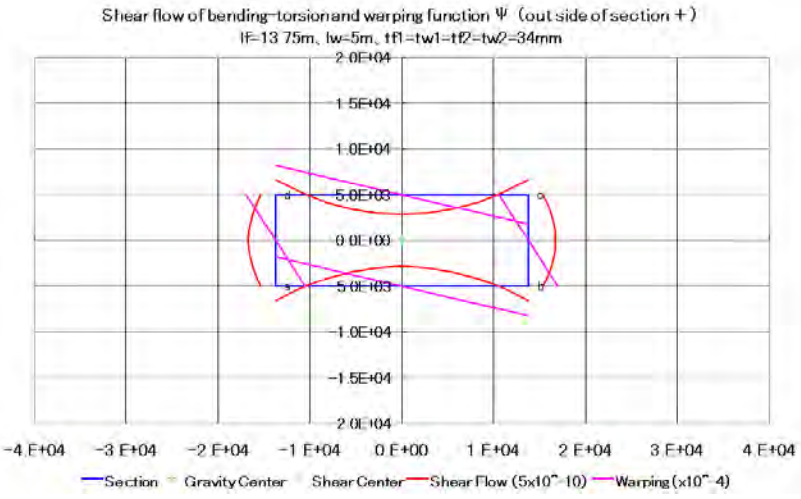

Fig. 3. 1－67

formula divided by the Cbd. For a reference, the shell plate thickness of Fig. －62 thru 65 is constant. Fig. －66 shows bending-torsion shear flow of the case whose bending shear flow is shown on Fig. －15 and difference between them is very clear here also. Fig. －67 shows the case whose has a invert slenderness ratio of Fig. －66 case and the difference of both figures indicates effect of sectional slenderness ratio since the shell thickness on both sections are constant. In short they indicate that negative shear flow appears on the longer side. Fig. －68 thru 70 show effect of shell thickness, and all shell sections are quadrate and their shell thickness distribution are as such that the bottom side is a half of other sides at Fig. －68, all sides are same at Fig. －69 and right side is a half of other sides at Fig. －70. Negative shear flow appears on

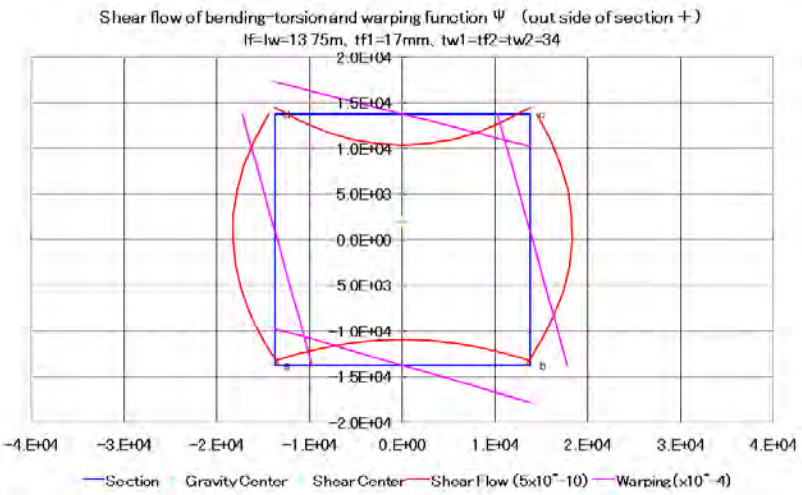

Fig. 3. 1－68

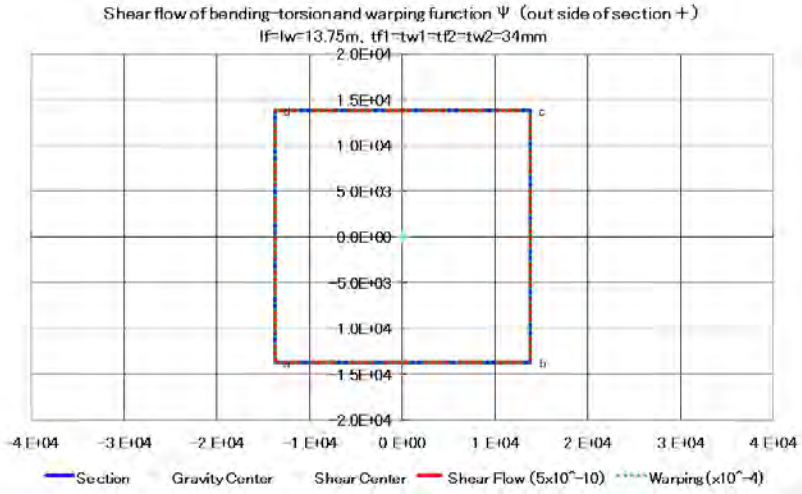

Fig. 3. 1－69

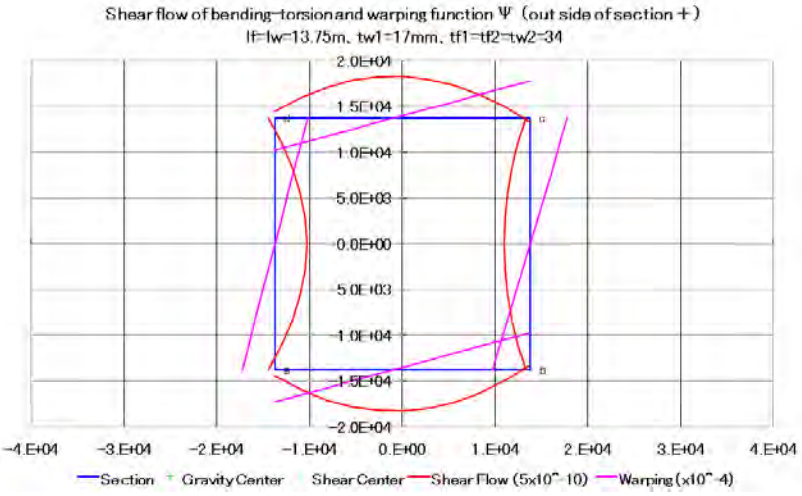

Fig. 3. 1－70

the thickness decreased side just like seen on the longer side of Fig. －６６ and ６７. The shear flow and the warping function equal ０ in case of constant shell thickness section of Fig. ６９ and bending-torsion never comes out under any circumstance just like the constant shell thickness circular. Impact degree of bending-torsion varies according to sectional shape including shell thickness and distribution of the θ since formula (aa) and (ad) which give shearing stress and vertical stress respectively include shear flow and warping function both of which are multiplied by a derivative of θ. On the other hand, sign of warping function is switching according to the first quadrant → the second quadrant → the third quadrant → the forth quadrant → the first quadrant in case of a quadrate.

３．１．４．２ Analysis by elastic equation

As the difference of the bending-torsion theory from the simple torsion theory is a calculation method of displacement due to twisting, formula (5) has to be replaced by a formula considering the bending-torsion so that the analysis by the elastic equation described at ３．１．３．２ may be expanded to the bending-torsion theory. Although the formula in general case will be obtained by solving following basic equation of the bending-torsion considering variable cross-

$$E C_{bd} \frac{d^4\Theta}{dz^4} - G J_t \frac{d^2\Theta}{dz^2} - m_t = 0 \qquad \cdots\cdots(e)$$

sections, description in this section will be concentrated on a uniform cross-section whose solution has been already obtained since the purpose of this thesis is to show a fundamental impact of bending-torsion phenomenon on analytical results.

（１） Analytical method

The same analytical model and external loads as for simple torsion theory is taken in analysis. The formulas of deformation due to concentrated torsion moment

are replaced by formulas including bending- torsion in addition to simple torsion. Following formulae which are Example 3 of the solutions shown in Appendix 3. 1

[Solution of basic equation]

$$\left.\begin{aligned} z \leqq c \quad \Theta &= \frac{T}{E C_{bd}} \left[\frac{z}{\alpha^2} - \frac{\mathrm{sh}\{\alpha(l-c)\}\mathrm{sh}(\alpha z)}{\alpha^3 \mathrm{sh}(\alpha l)} \right] \\ z \geqq c \quad \Theta &= \frac{T}{E C_{bd}} \left[\frac{c}{\alpha^2} - \frac{\mathrm{sh}\{\alpha(l-c)\}\mathrm{sh}(\alpha z)}{\alpha^3 \mathrm{sh}(\alpha l)} + \frac{\mathrm{sh}\{\alpha(z-c)\}}{\alpha^3} \right] \\ \text{where} \quad \alpha &= \sqrt{G J_t \div E C_{bd}} \end{aligned}\right\} \cdots\cdots (f3)$$

－2 are employed to calculate distortion angle Θ. Formulae (5) are not used and formulae (6) are replaced by following two formulae since a uniform cross- section

[Rotation angle at j support due to m_i on i section]

$$\left.\begin{aligned} \theta_{ij} &= \frac{m_i}{\alpha^3 E C_{bd}} \left\{ k j - \frac{\mathrm{sh}(k[n-i])\mathrm{sh}(k j)}{\mathrm{sh}(k n)} \right\} \quad (j \leqq i) \\ &\quad \frac{m_i}{\alpha^3 E C_{bd}} \left\{ k i + \mathrm{sh}(k[j-i]) - \frac{\mathrm{sh}(k[n-i])\mathrm{sh}(k j)}{\mathrm{sh}(k n)} \right\} \quad (j > i) \\ \text{where} \quad k &= \alpha l_s \end{aligned}\right\}$$

$\cdots\cdots (34)$

[Displacement at j support due to m_i on i section]

$$\left.\begin{aligned} \xi_{tij} &= \theta_{ij} l_{py} \\ \eta_{tij} &= \theta_{ij} l_{px} \end{aligned}\right\} \cdots\cdots (35)$$

is premise. And formulae (11) are also not used since there is no internal torsion moment due to bending because of the premise.

(2) Example of analytical resuit

The procedure to obtain internal forces from statically indeterminate reactions

given as results of the elastic equation is exactly the same as simple torsion theory. But the internal torsion moment given by formula (21) is a sum of the bending-torsion moment T_w and the simple torsion moment T_s and they have to be obtained separately. In addition to new formulas for T_w and T_s, formulas are necessary to obtain the vertical stress σ_z which newly comes out due to the bending- torsion and the θ instead of formula (22). The following formulas satisfy all needs above where θ_{kj} is rotation angle of j section due to m_{ek} acting at k section and ' denotes ordinary differentiation.

[External torsion moment acting on i section]

$$m_{ei} = m_{si} + X_i l_{py} + Y_i l_{px} \qquad \cdots\cdots(36)$$

[Rotation angle at j section and its derivatives due to m_{ei} acting on i section]

$$\theta_{ij} = \text{formula}(34) \text{ where } m_i \text{ is replaced by } m_{ei} \text{ in formula } (36) \qquad \cdots\cdots(37)$$

$$\left.\begin{aligned} \theta'_{ij} &= \frac{m_{ei}}{\alpha^2 E C_{bd}} \left\{1 - \frac{sh(k[n-i])ch(kj)}{sh(kn)}\right\} && (j \leqq i) \\ &\frac{m_{ei}}{\alpha^2 E C_{bd}} \left\{ch(k[j-i]) - \frac{sh(k[n-i])ch(kj)}{sh(kn)}\right\} && (j > i) \end{aligned}\right\} \cdots\cdots(38)$$

$$\left.\begin{aligned} \theta''_{ij} &= \frac{m_{ei}}{\alpha E C_{bd}} \left\{- \frac{sh(k[n-i])sh(kj)}{sh(kn)}\right\} && (j \leqq i) \\ &\frac{m_{ei}}{\alpha E C_{bd}} \left\{sh(k[j-i]) - \frac{sh(k[n-i])sh(kj)}{sh(kn)}\right\} && (j > i) \end{aligned}\right\} \cdots\cdots(39)$$

$$\left.\begin{aligned} \theta'''_{ij} &= \frac{m_{ei}}{E C_{bd}} \left\{- \frac{sh(k[n-i])ch(kj)}{sh(kn)}\right\} && (j \leqq i) \\ &\frac{m_{ei}}{E C_{bd}} \left\{ch(k[j-i]) - \frac{sh(k[n-i])ch(kj)}{sh(kn)}\right\} && (j > i) \end{aligned}\right\} \cdots\cdots(40)$$

where $\theta'_{ij} = \left(\frac{d\Theta}{dz}\right)_{ij}$、$\theta''_{ij} = \left(\frac{d^2\Theta}{dz^2}\right)_{ij}$、$\theta'''_{ij} = \left(\frac{d^3\Theta}{dz^3}\right)_{ij}$

[Rotation angle at i section and its derivatives]

$$\theta_j = \sum_{k=0}^{n} \theta_{kj} \qquad \cdots\cdots(41)$$

$$\theta'_j = \sum_{k=0}^{n} \theta'_{kj} \qquad \cdots\cdots(42)$$

$$\theta''_j = \sum_{k=0}^{n} \theta''_{kj} \qquad \cdots\cdots(43)$$

$$\theta'''_j = \sum_{k=0}^{n} \theta'''_{kj} \qquad \cdots\cdots(44)$$

[Simple torsion moment at j section]

$$T_{sj} = G J_t \theta'_j \qquad \cdots\cdots(45)$$

[Bending- torsion moment at j section]

$$T_{wj} = -E C_{bd} \theta'''_j \qquad \cdots\cdots(46)$$

θ, T_{sj} and T_{wj} vary along a bottom support interval at variance with the simple torsion theory and they can be obtained by handling the j in the formulae as a real number. Stress distribution is obtained by inserting sectional forces and derivatives of θ into formulae shown at clause 3．1．4．1．

Following two examples correspond to the cases shown in the simple torsion theory and their numbers are as same as the corresponding cases. Description on the gate section and calculation condition are not shown here.

[Example 1]

This is a case that a fish belly flap is supported at its one end. Fig.3．1－7 1 thru 7 7 shows the results of analysis by the bending- torsion theory. The Fig. 7 1 shows θ and its derivatives of the bending- torsion theory. The marks x in the figure indicate θ of the simple torsion theory. The lateral axis represents section numbers. Vertical axis represents calculated results after multiplied by rates shown. θ is in a rather smooth curve and exactly agrees with the simple torsion theory at free end of the gate. θ' is in proportion to T_s, which is apparently different from the simple torsion theory. θ'' is in proportion to σ_z due to bending- torsion

and its move is approximately periodic except for both terminal compartments. θ‵‵‵ is in proportion to bending-torsion moment Tw and shows same periodicity as θ‵‵ except that its sign is in reverse on both sides of the section including a bottom support. It is estimated that the reversals resulted from abrupt changes in direction of sectional warp change due to existence of the support reaction force. The Fig. 7.2 and 7.3 show sectional force. The Fig. 7.2 is results of bending moment and relating forces and there is no big difference from the simple torsion theory that is because the statically indeterminate reaction force which is basic data of sectional force calculation has no big change between the results of the both theories shown on Table 3.1-4. The Fig. 7.3 shows torsion moment. Simple torsion moment Ts and

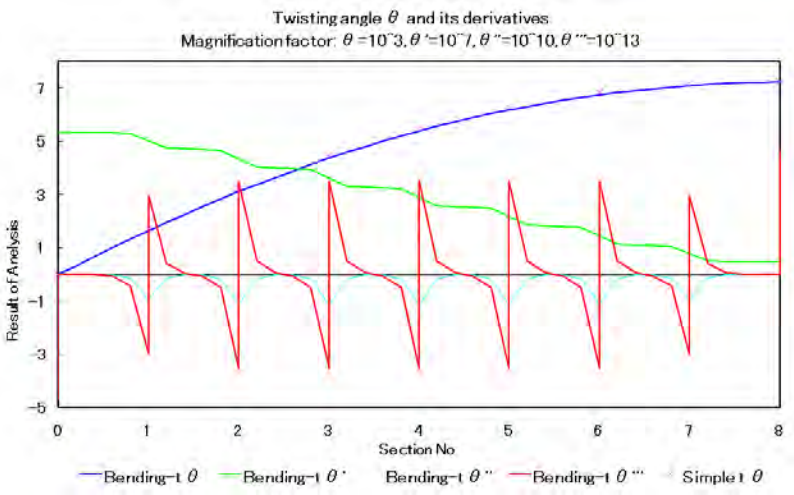

Fig. 3.1-71

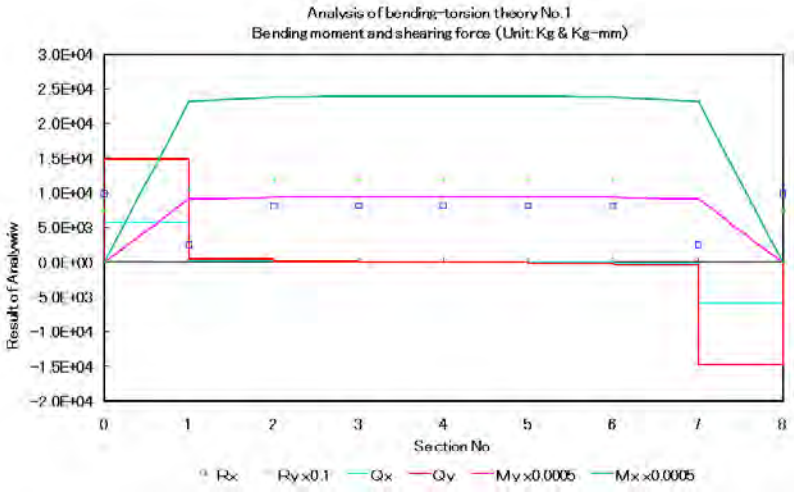

Fig. 3.1-72

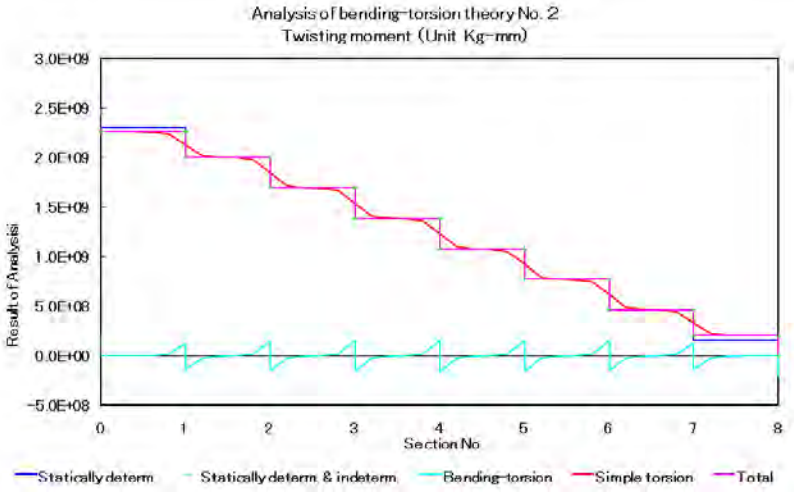

Fig. 3.1-73

Section No.	X (Kg)		Y (Kg)	
	Bending- torsion	Simple torsion	Bending- torsion	Simple torsion
0	- 5843	- 6059	- 14832	- 15381
1	5684	6070	14429	15408
2	112	- 11	285	- 27
3	47	0	120	0
4	- 2	0	- 5	0
5	48	0	121	0
6	112	- 11	285	- 27
7	5684	6070	14429	15408
8	- 5843	- 6059	- 14832	- 15381

Table 3. 1－4

bending- torsion moment Tw vary between bottom supports but their sum is constant and equals the internal torsion moment (＋ mark) calculated by formula (21). This indicates that the mean amplitude of bending- torsion moment is controlled by the number of bottom supports (or compartments) rather than the sectional particulars. In short, it is estimated that the greater the number of bottom supports, the less the mean amplitude of bending- torsion moment. It has to be emphasized that magnitude of bending- torsion moment is much less than simple torsion moment. The Fig 7 4 thru 7 7 show sectional stress distribution. The Fig. 7 4 thru 7 6 show shearing stress, vertical stress and principal stress. They show section 0 and section 1 outside (left hand side) and inside (right hand side) respectively. Although

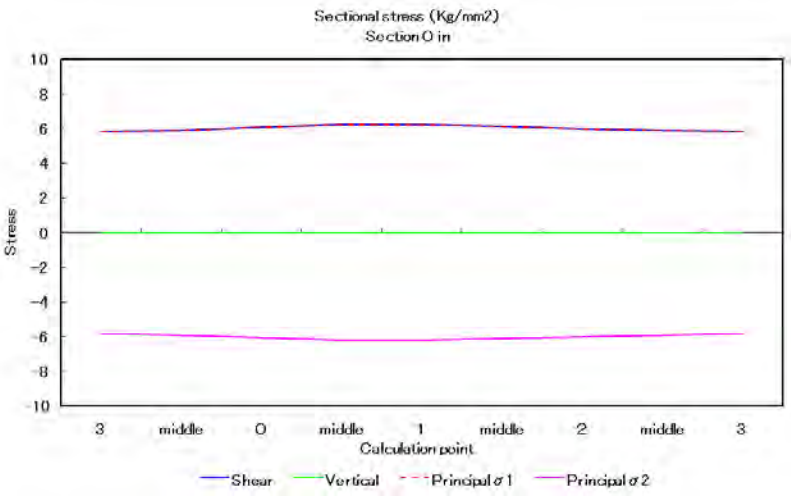

Fig. 3. 1－7 4

stress distribution on section 0 is flat since impact of bending-torsion is small, that of section 1 outside is not same and the degree of stress distribution disturbance due to bending-torsion will become quite clear when these stresses are compared to Fig. 3. 1-29 which is results of stress analysis by the simple torsion theory on the same section. The disturbance on section 1 inside is at the same level but in the reverse direction. Even if a big disturbance were to exist, the stress over all is still almost in pure shearing state. The Fig. 7 7 shows distribution of the element stresses which compose the sectional shearing and normal stresses. The element stresses shown are those on section 1 outside and can be compared with those on Fig. 3. 1－31 of the simple torsion theory where τ s is simple torsion shearing stress, τ w is bending-torsion shearing stress,

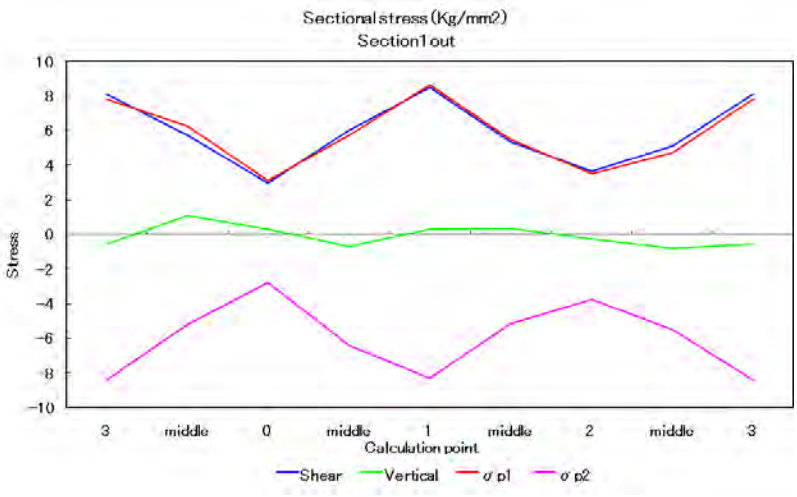

Fig. 3. 1－75

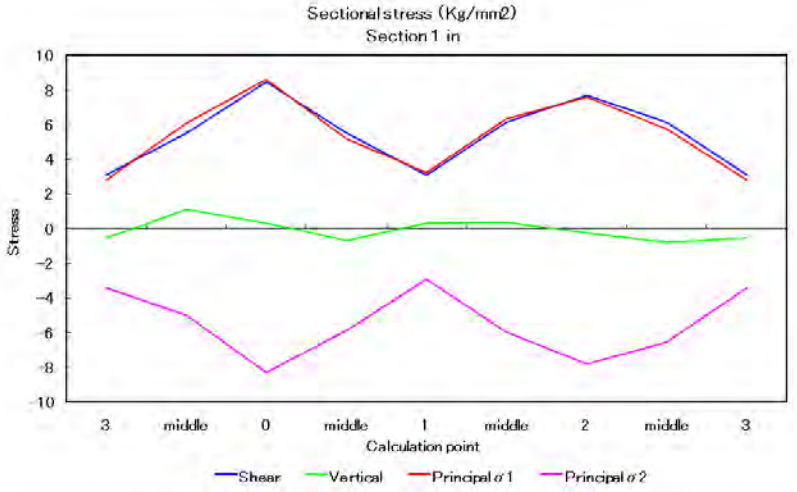

Fig. 3. 1－76

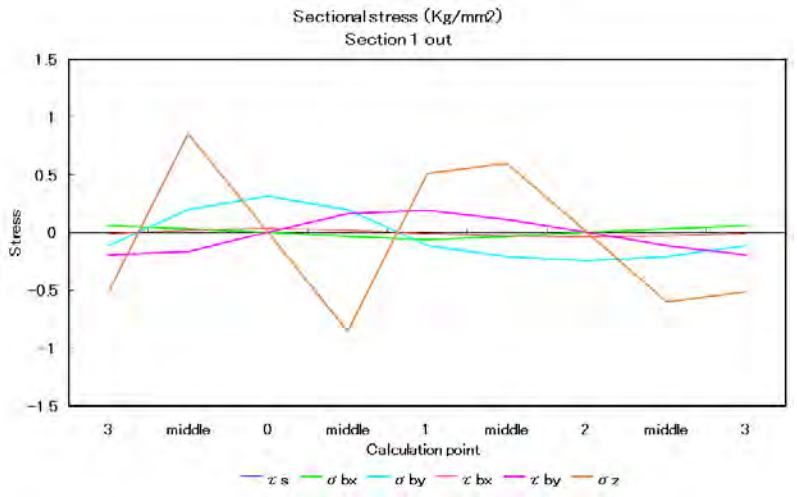

Fig. 3. 1－77

τ_{bx} and τ_{by} are bending shearing stress, σ_{by} is bending normal stress and σ_z is bending- torsion vertical stress. Causes of the disturbance are shearing stress τ_w and vertical stress σ_z due to bending- torsion and its intensity is much greater than disturbance by stresses due to bending. It is noticeable that the effect of T_w on stress distribution is very large although T_w is very small in comparison to T_s. Effect of bending- torsion is more remarkable at middle or free terminal section because the moment of simple torsion decreases towards the free terminal whereas moment of bending- torsion varies periodically with almost a constant amplitude throughout the gate length. In case of a small scale gate, neglect of bending- torsion will have no effect on the strength problem because the middle or free terminal portion of the gate usually has a big strength margin. In case of super large scale gates, a design without considering bending- torsion cannot hold good because the greater portion of the gate body is in a critical state of stress due to decrease in plate thickness for economic reason toward free terminal. Impact of bending- torsion phenomenon on sectional force of a torsion type gate is not so much but its sectional stress distribution is subject to a big influence from bending- torsion and the influence can not be neglected in case of the super large scale gates.

［Example 5］

This is a case which a box section gate is supported at one end. Fig. 3. 1－78 thru 83 shows analytical results by the bending-torsion theory. The Fig. 78 shows deformation and Fig. 79 and 80 show internal force. General tendency including internal forces is the same as Example 1 except that there is a little difference in details. Curves of θ`` and θ``` between bottom supports of Example 1 have a tendency of keeping it close to the 0 axis, whereas those of Example 5 deviate from it. It has been confirmed that this different tendency mainly stems from a difference of k values which was defined by formula (34). k equals 9.73 in Example 1 whereas K equals 3.07 in Example 5. There is a tendency that θ`` deviates more from the 0 axis and the intersect angle of θ``` and the 0 axis becomes larger for

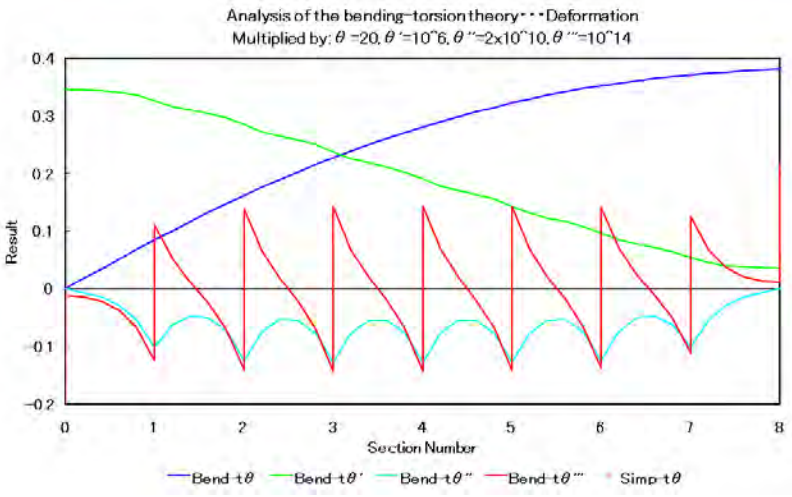

Fig. 3. 1－78

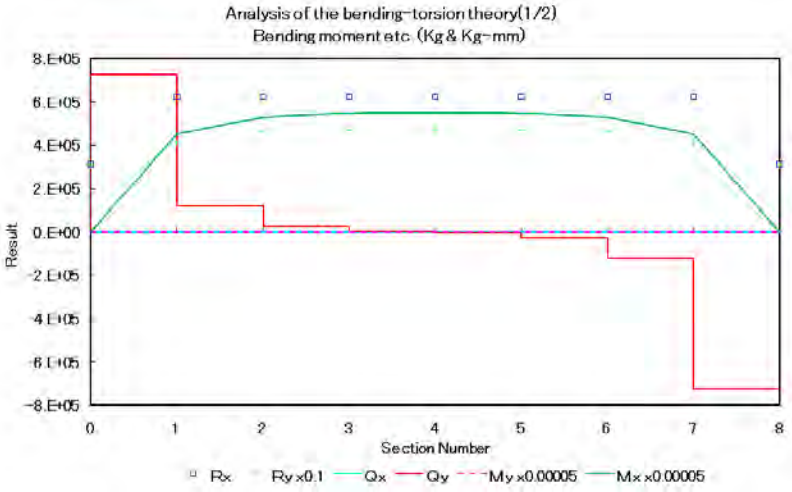

Fig. 3. 1－79

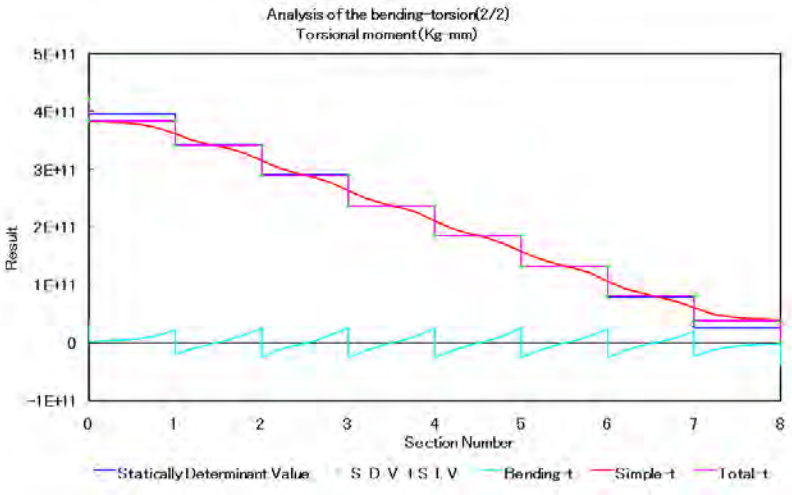

Fig. 3. 1－80

less k than 3.07. And also it was confirmed that the range of θ'' and θ''' being in close contact with the 0 axis becomes larger for more k than 9.73. In short, the influence range of bending-torsion becomes restricted in vicinity of the gate section including a support when k becomes larger and vice versa. The longer the gate support space becomes, the bigger the bending-torsion moment become whereas the less its influence range become since k is in linear to the gate support space. The influence range becomes larger for larger bending-torsion section modulus since k is divided by the modulus. The k becomes infinitive when α is infinitive which corresponds to the case that Cbd equals 0 according to formula (e) or, in other word, "simple torsion" and application of the formula obtained by the simple torsion theory is necessary. Fig. 3. 1

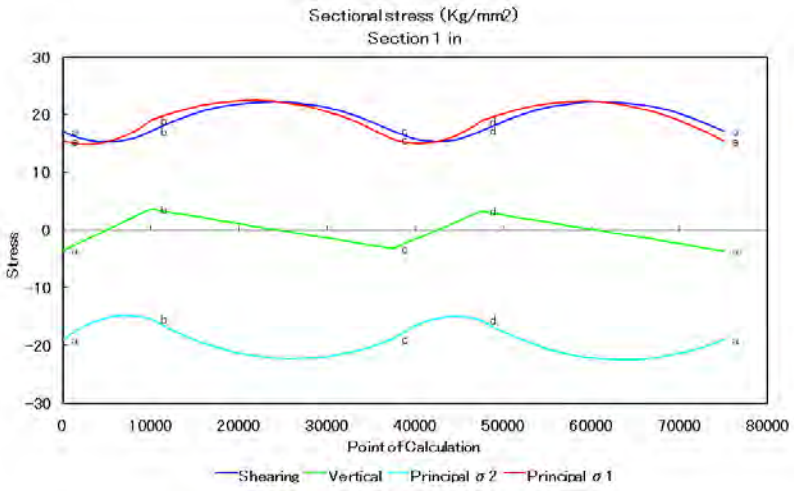

Fig. 3. 1－81

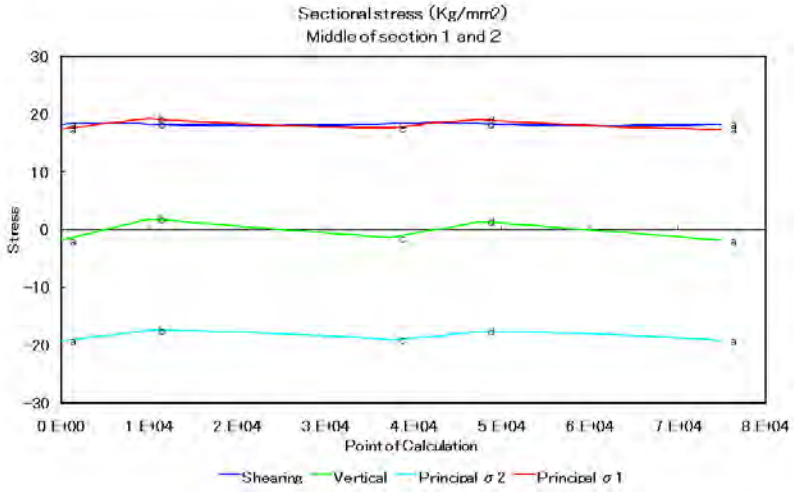

Fig. 3. 1－82

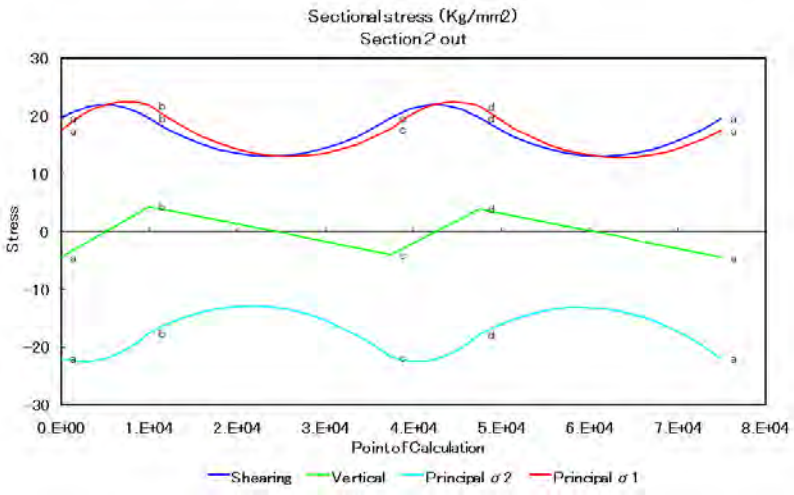

Fig. 3. 1－83

- 8 1 thru 8 3 show shearing stress, normal stress and principal stress. Each figure corresponds to section 1 inside, middle of the two section and section 2 outside. The stress disturbance is much and in reverse directions on section 1 and 2 and less on the middle section but their over all magnitude is less than Example 1. This difference is deemed to be caused by difference of their sectional shapes since average ratio of simple torsion moment and bending- torsion moment is supposed to be nearly equal because number of the gate supports in both case is same. In short, it seems to be right that rectangular shape can resist bending- torsion with higher efficiency than fish belly shape. The sectional efficiency factor against bending- torsion e_{bd} is given by following formula

$$e_{bd} = \left\{\frac{q_w}{t} \cdot \frac{1}{C_{bd}}\right\} \div \left\{\frac{q_s}{t} \cdot \frac{1}{J_t}\right\} = \frac{q_w}{q_s} \cdot \frac{J_t}{C_{bd}} = \frac{q_w \cdot 2A_s}{C_{bd}} \qquad \cdots\cdots(47)$$

which is a ratio of the coefficients included in formulae (ad) and (aj) to calculate shearing stress due to bending- torsion and simple torsion since average amplitude

no	Form		Thickness	A_s(mm ^{2})	$q_w$max(mm ^{4})	C_{bd}(mm ^{6})	e_{bd}
1	Circle		Uniform	28274333	0	0	0
2	F- belly			9366847	8.37E + 9	2.09E+ 16	7.50
3	Lens			6522197	6.13E + 9	1.03E+ 16	7.76
4	Ellipse			16604449	1.03E+ 10	2.43E+ 16	14.08
5	B		Uniform	275000000	5.91E+ 12	8.75E+ 20	3.71
6	o			275000000	5.91E+ 12	8.75E+ 20	3.71
7	x		Uniform	756250000	0	0	0
8			Btm . t/ 2	756250000	9.07E+ 12	1.54E+ 21	8.91
9			Rgt . t/ 2	756250000	9.07E+ 12	1.54E+ 21	8.91

of bending- torsion moment is determined according to the number of

compartments as it was described before. The magnitude of q_w in the formula has to be a maximum one on the section. The less e_{bd} shows the less bending-torsion stress and the better sectional efficiency. Below table shows results of calculation on the sections described in section 3.1.4.1. Example 1 corresponds to no. 2 and Example 5 corresponds to no. 5.

(3) Model experiment

The analytical results of the bending-torsion theory are shown by the Δ mark on Fig. 3.1—45 which is a graph showing measured sectional stress of the experiment. Eventually the analytical results have agreed with the simple torsion theory since the strain measuring section is middle of section 0 and 1 where θ'' and θ''' equal 0 respectively because the k of experimental model equals 20.4 but it is seemingly-meaningful that the both analytical results indicate quantities very similar to the experimental results.

3．1．4．3 Analysis by finite element method

Development of a computer has been accelerated since late 1970 and today analysis of a super large scale structure by way of the finite element method can be carried out by a desk top personal computer. Accordingly the structure of torsion type gate can be analyzed more effectively than before. In this clause, an importance of the gate analysis by the finite element method is described referring to analysis of a super large scale gate shown in Fig. 3．1－11. The content of finite element method will not be referred to since it has been already well- known.

(1) Similarity of deformation

Finite element methods using various kinds of elements are now available for practical use and analyzed result by them shows good similarity to measured deformation at site as well as model experiments as long as a proper mesh is chosen for nature of analyzed structure and purpose of analysis[*1]. If the concept of bending- torsion theory accords with the natural phenomena, this will be expected to appear in the results of analysis by the finite element method. It will be shown that the analytical result can be understood only through the bending- torsion theory since the cited example has been analyzed as a whole and the obtained stress distribution is very complicated and can not be explained fully by the simple torsion theory even if deformation of the vertical sections or stiffeners are considered.

[*1] Bibliography (4).

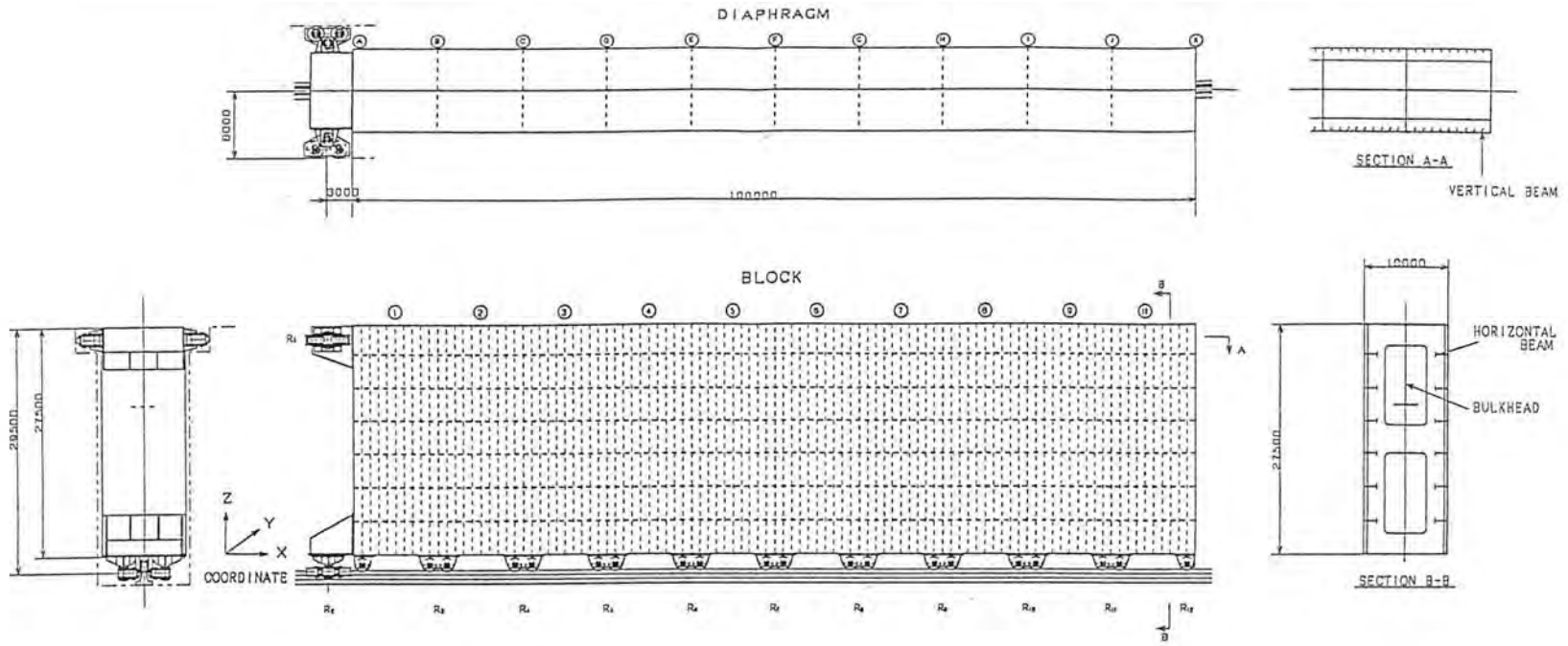

SKIN PLATE AND BEAM

+:TENTION
-:COMPRESSION

BLOCK		① ②	③ ④	⑤ ⑥	⑦ ⑧	⑨ ⑩
DIMENSION OF MEMBER(mm)	SKIN PLATE THICKNESS	34	16	14	12	12
	BULKHEAD THICKNESS	10	10	10	10	10
	HORIZONTAL BEAM SECTION	I 1500x721 x35/40	I 1500x699 x30/50	I 1000x546 x23/55	I 800x389 x10/36	I 600x244 x13/33
	VERTICAL BEAM SECTION	L 400x100x13/18				
MAXIMUM PRINCIPAL STRESS (kgf/mm²)	SKIN PLATE	+10.86 -13.08	+13.74 -14.44	+13.14 -14.18	+11.99 -13.28	+11.72 -12.77
	BULKHEAD	+4.54 -4.59	+4.40 -4.70	+4.44 -5.35	+4.76 -5.76	+5.16 -5.68
	HORIZONTAL BEAM	+13.15 -13.68	+16.85 -17.45	+6.19 -7.50	+9.41 -12.67	+10.52 -13.21
	VERTICAL BEAM	+9.38 -9.60	+12.10 -12.25	+10.70 -10.93	+8.81 -9.05	+9.48 -12.21
SHEARING STRESS (kgf/mm²)	SKIN PLATE	10.82	12.65	11.43	10.24	9.53
	BULKHEAD	3.92	3.85	3.35	3.54	3.74
	HORIZONTAL BEAM	1.59	1.35	3.35	5.49	8.80
	VERTICAL BEAM	8.67	0.43	0.38	0.64	1.54

DIAPHRAGM

	A	B C	D E	F G	H I	J	K
THICKNESS (mm)	22	11	10	10	10	10	10
MAXIMUM PRINCIPAL STRESS (kgf/mm²)	+11.25 -12.46	+9.45 -12.70	+6.11 -9.44	+6.09 -9.14	+5.37 -8.33	+5.06 -8.61	+9.31 -10.40
SHEARING STRESS (kgf/mm²)	11.66	9.28	6.84	6.42	5.84	6.31	7.18

REACTION FORCE

	R1	R2	R3	R4	R5	R6	R7	R8	R9	R10	R11	R12
Y-DIRECTION	-5192	+4036	+182	+326	-665	-928	-729	-929	-734	-717	-734	-1317
Z-DIRECTION	0	+137	+432	+312	+233	+218	+204	+187	+173	+164	+153	+79

Fig. 3.1-84 Result of Stractural Analysis of Tidal Gate (Torsion Type)
Principal Stress Table
Sea Level Canal 250000 DWT Canal Option

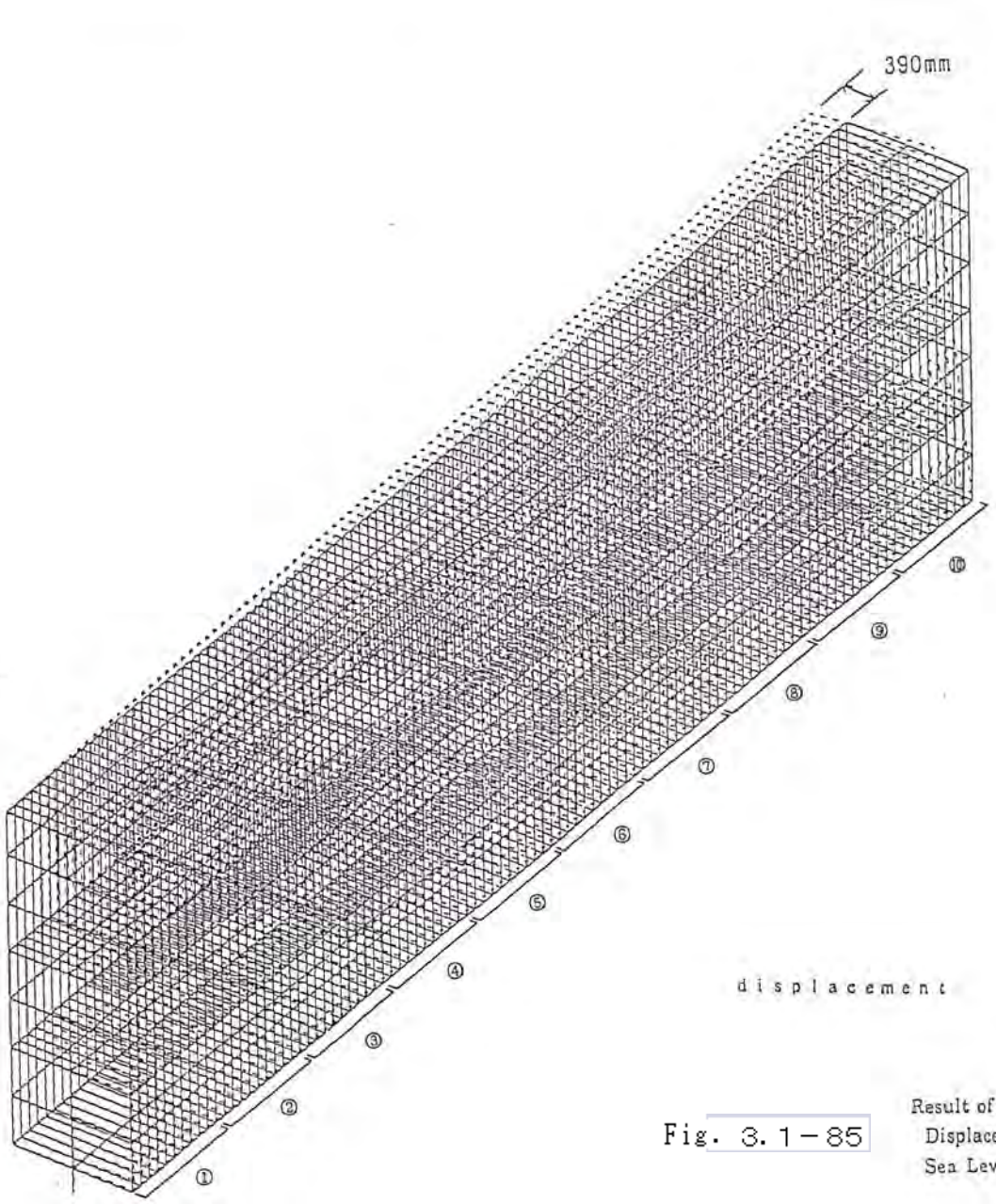

Fig. 3.1－85 Result of Stractural Analysis of Tidal Gate (Torsion Type)
Displacement Diagram
Sea Level Canal 250000 DWT Canal Option

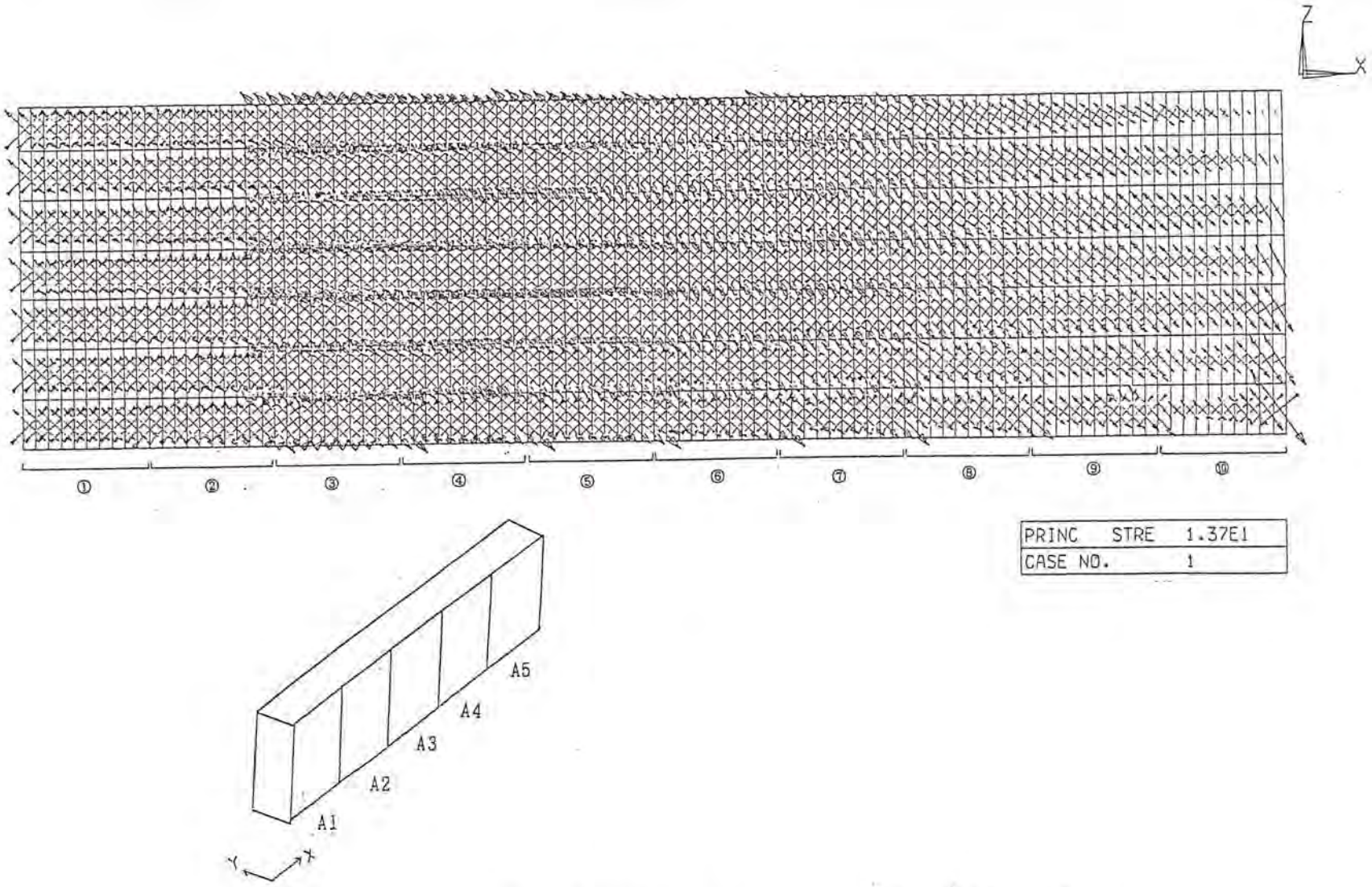

Fig. 3.1－86 principal stress A1－A5 (top)

Result of Stractural Analysis of Tidal Gate (Torsion Type)
Principal Stress Diagram
Sea Level Canal 250000 DWT Canal Option

（２） Analytical results

An explanation is given according to the reference[*1]. Gate shape of the cited case is shown on Fig. ３．１－１１. It is a rolling gate of 27.500m height x 200.000m width which is vertically divided at its center into two independent blocks and the left hand side block is shown on the figure. Each block is supported by its one end against huge water pressure force at its closed position (analysis condition). Top and bottom of the block end are supported directly by gate frames embedded in the concrete structure. The gate has a rectangular section whose shell plate is stiffened by auxiliary vertical girders arranged at 1m space and they are supported by six horizontal girders which in return are supported by web frames at 10m interval. The bottom of each web frame is supported by rollers instead of a bottom hinge support. Inside of the gate body is divided by bulkheads into many compartments each of which is used as a buoyancy tank. The tank has a longitudinal bulkhead at its center but has no bottom plate. In short, a shear flow loop of the gate body exists only on the vertical section. Analysis by the finite element method was carried out by IBM 9021 using "NASTRAN" which is a computer software developed at NASA. The degree of freedom at each joint of elements is 6 and elements can represent beam members also. Fig. ３．１－８４ thru ８６ show results of the analysis. The Fig. ８４ shows whole shape and member scantling of the gate body, principal and shearing stress on main parts of the gate and reaction force of the support rollers. The purpose of analysis is feasibility study and the shape and the member scantlings are preliminary ones. The Fig. ８５ shows meshing procedure of elements and over all deformation. The element breakdown is seven splits at six horizontal girders in vertical direction, two splits at the buoyancy tank longitudinal bulkhead in the tank width direction and one hundred sprits at the auxiliary vertical girders in the gate width direction, and the whole gate body was replaced by about 2500 plate elements and about 2000 beam elements. Water

[*1] Bibliography (9).

pressure acts on the shell plate but no partial bending arises on the plate elements because all joints of plate elements are located on beam elements. The Fig. 8 6 shows an example of the results and gives the magnitude and direction of principal stress on the shell plate. Stress on whole gate body is almost in a state of pure shear.

（3） Comparison of sectional stress

The analytical result by the finite method is compared with the stress obtained through elastic equations. For this comparison, stress on all surfaces of the gate is necessary while only principal stress on the skin plate is shown at the previous clause （2） of the finite element method. New analysis by finite element method was carried out with exactly the same structural members and meshing as the Fig. 8 4 and 8 5 using the same program software as the reference but by IBM 750 personal computer and it was confirmed that principal stresses on the skin plate agree with the values given in the Fig. 8 6. As stress on the top and bottom sides of a plate element were obtained and difference existed between them due to deformation of the auxiliary girders etc., the mean value of them was deemed as the stress of the element. And also the calculated stress on a plate element corresponds to a value at the center of element and all stress comparison was made on sections cut through element centers except that stress in the intermediate section between roller supports was deemed to be equal to mean value of elements which are located on both sides of the section because the section coincides with the element boundaries. Fig. 3. 1－8 7 shows plate thickness of gate section and its number

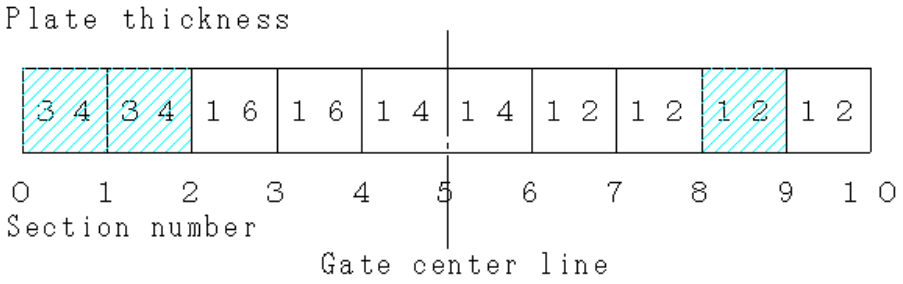

Fig. 3. 1－8 7

which is different from the roller number shown on the Fig. 8 4. Plate thickness of each section is constant. The compartments marked by inclined lines in the figure were selected for stress comparison because of the consideration that elastic equations are applicable only to a sectionally homogeneous structure. The comparison was made on the left side, middle and right side sections of each compartment. The two analytical models of the elastic equation are of the same external dimensions as the finite element model, supported by one end and of 34mm and 12mm shell thickness respectively and the section 0 thru 2 of the finite element model is compared with the 34mm model sections whose location from the supported end of the model is as same as the finite model and the section 8 thru 9 of the finite model is compared with the 12mm model section whose location from the free end of the model is as same as the finite model. The 34mm model has the section of which stress distribution is shown on the Fig. 1 5 and 6 6 and same profile as the finite model except that no auxiliary members such as vertical and horizontal girders are included. The 12mm model is different in shell thickness from the 34mm model but its stress distribution pattern is applicable. Fig. 3. 1 －8 8 thru 9 0 show comparison of principal stress σ_1 and σ_2 between the bending- torsion theory, the finite element method and the simple torsion theory which are shown in the figure by marks "bending", "finite" and "simple" respectively. The Fig. 8 8 corresponds to a section between 0 and 1、the Fig. 8 9 corresponds to a section between 1 and 2 and the Fig. 9 0 corresponds to a section between 8 and 9. The "inside" or "outside" in the figure refers to whether the section shown is located on the gate center line side (see fig. 8 7) or the opposite side respectively, and a ～ d represent points on a section and corresponds to those in Fig. 1 5 or 6 6. Bending- torsion theory is much more explanatory of the results by the finite element method than simple torsion theory. Fig. 3. 1－9 1 thru 9 3 show comparison of shearing stress τ and normal stress σ between the bending- torsion theory, the finite element method and the simple torsion theory. The Fig. 9 1 corresponds to a section between 0 and 1、the Fig. 9 2 corresponds to a section between 1 and 2 and the Fig. 9 3 corresponds to a

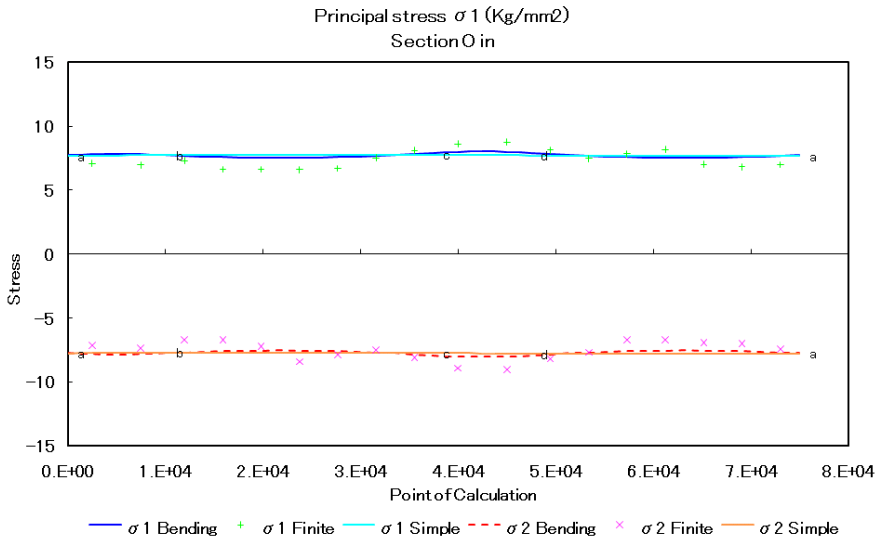

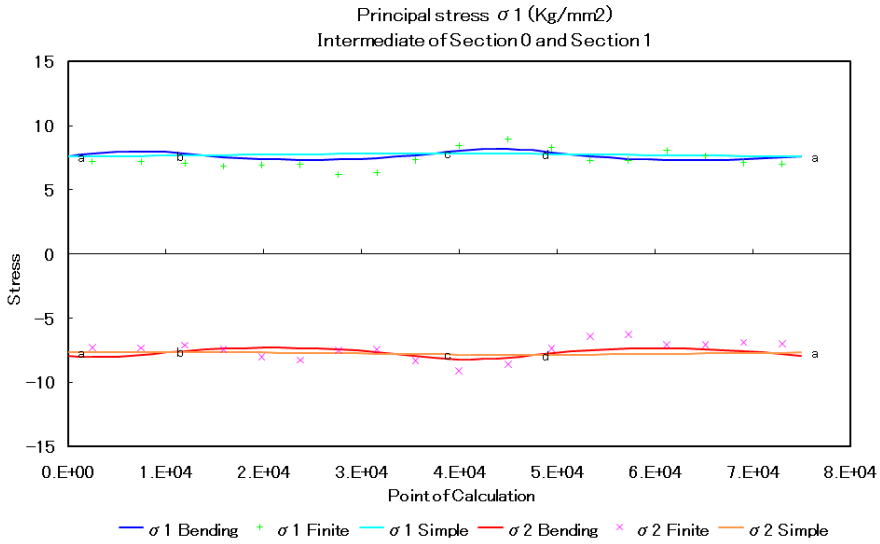

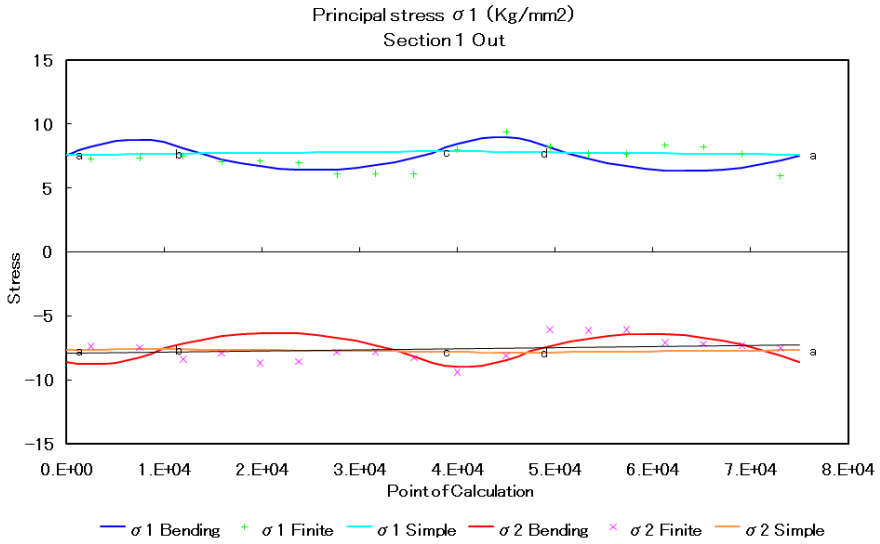

Fig. 3. 1－88 Principal stress Section 0～1

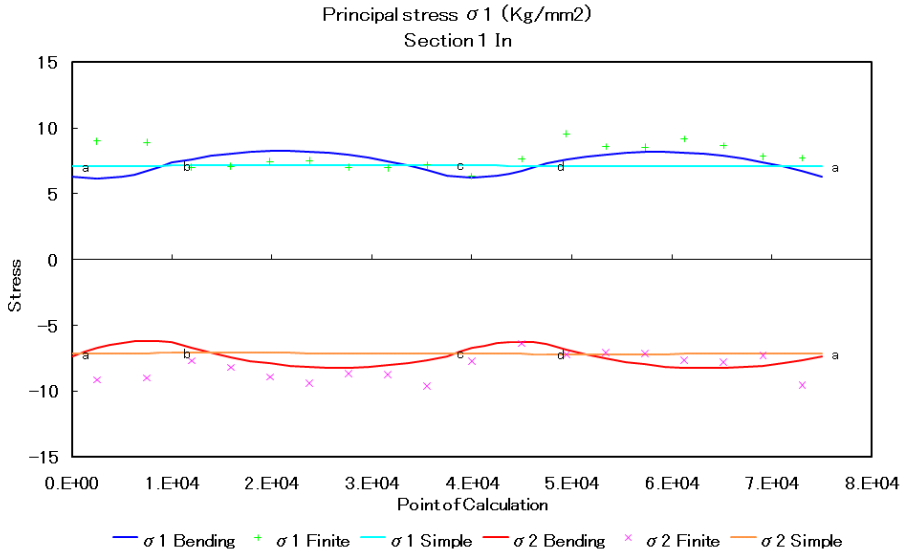

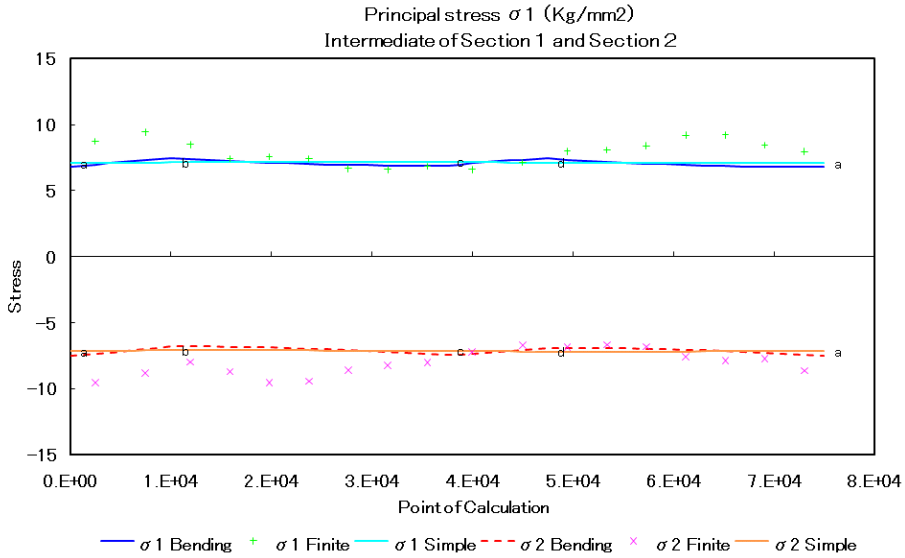

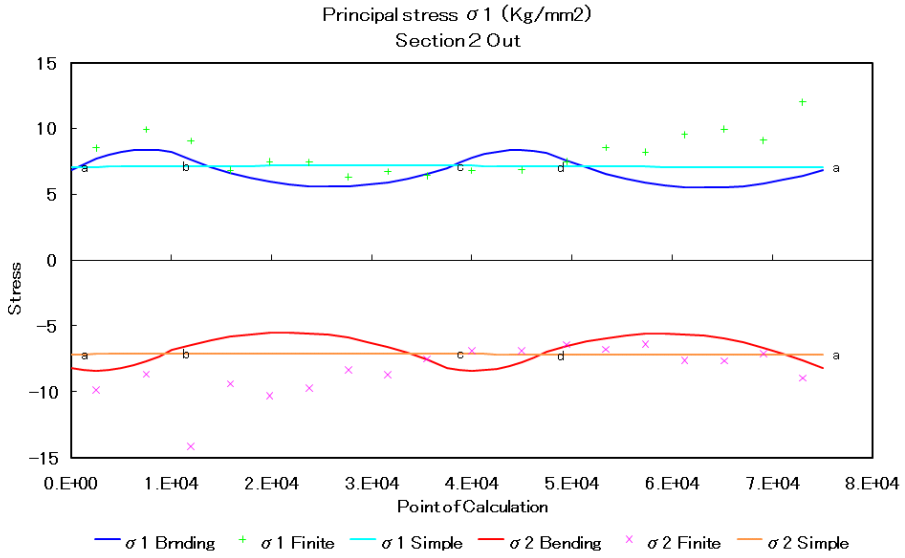

Fig. 3. 1－89 Principal stress Section 1～2

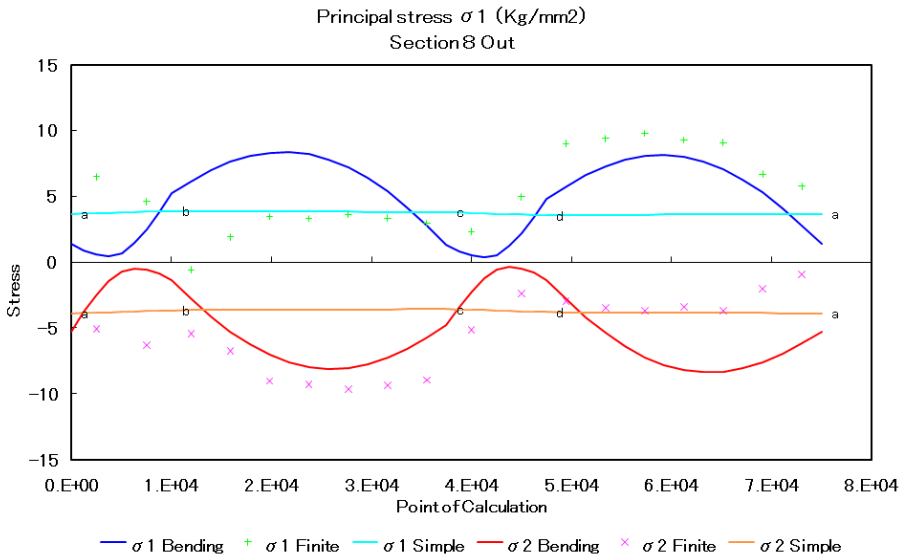

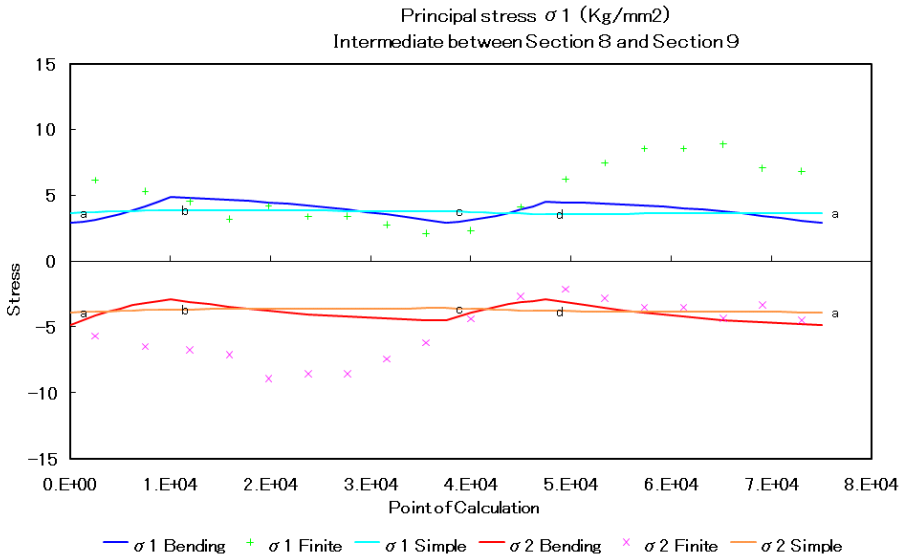

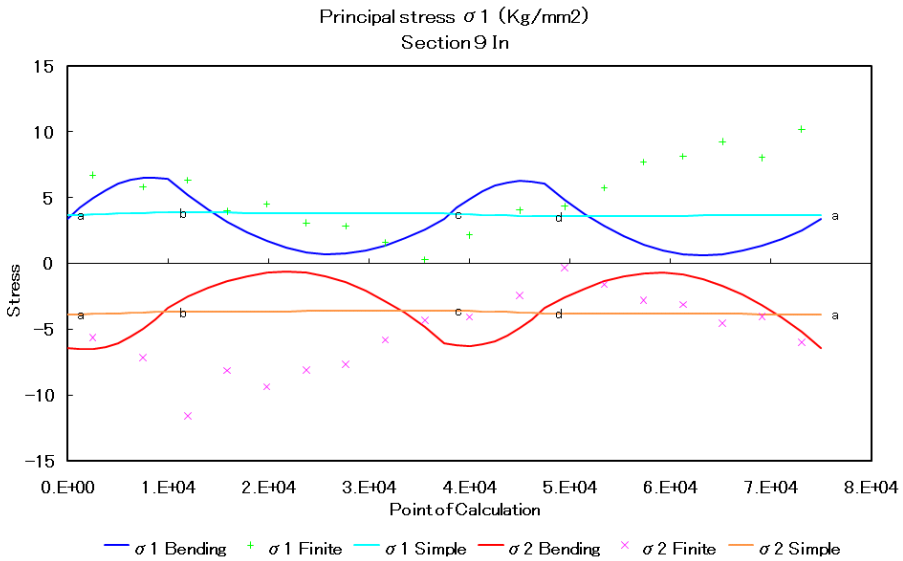

Fig. 3. 1－90 Principal stress Section 8～9

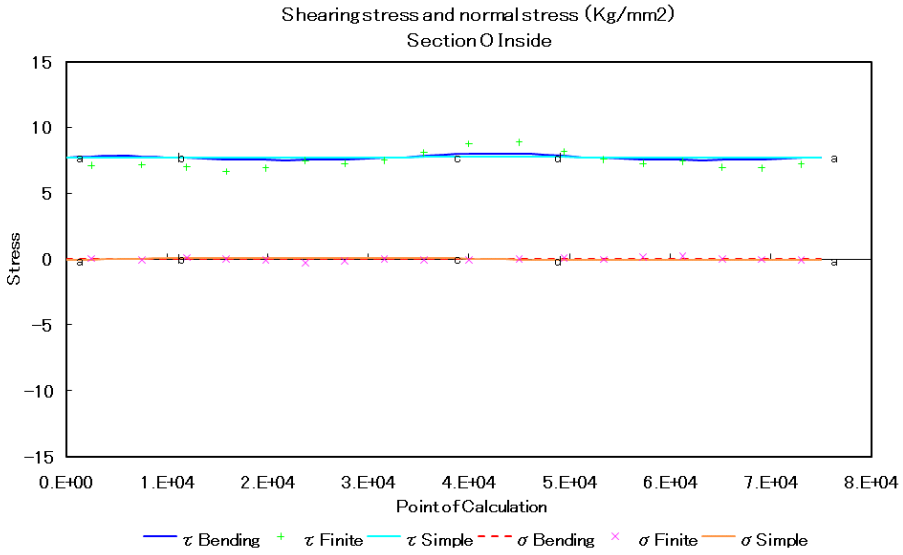

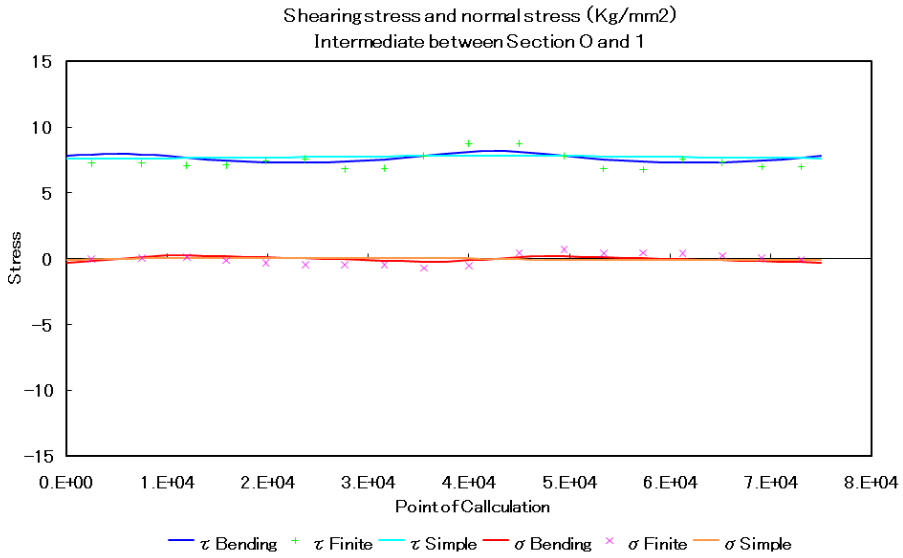

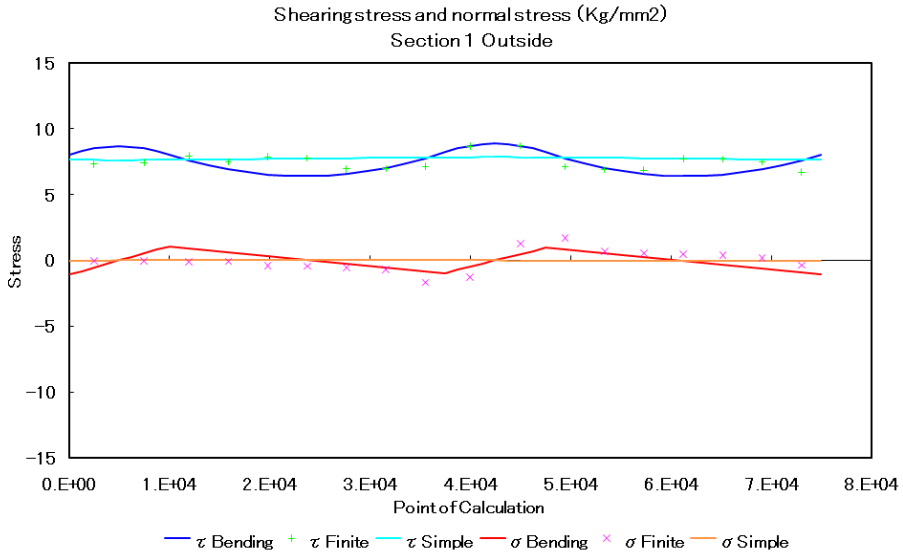

Fig. 3. 1－91 Shearing・normal stress Section 0～1

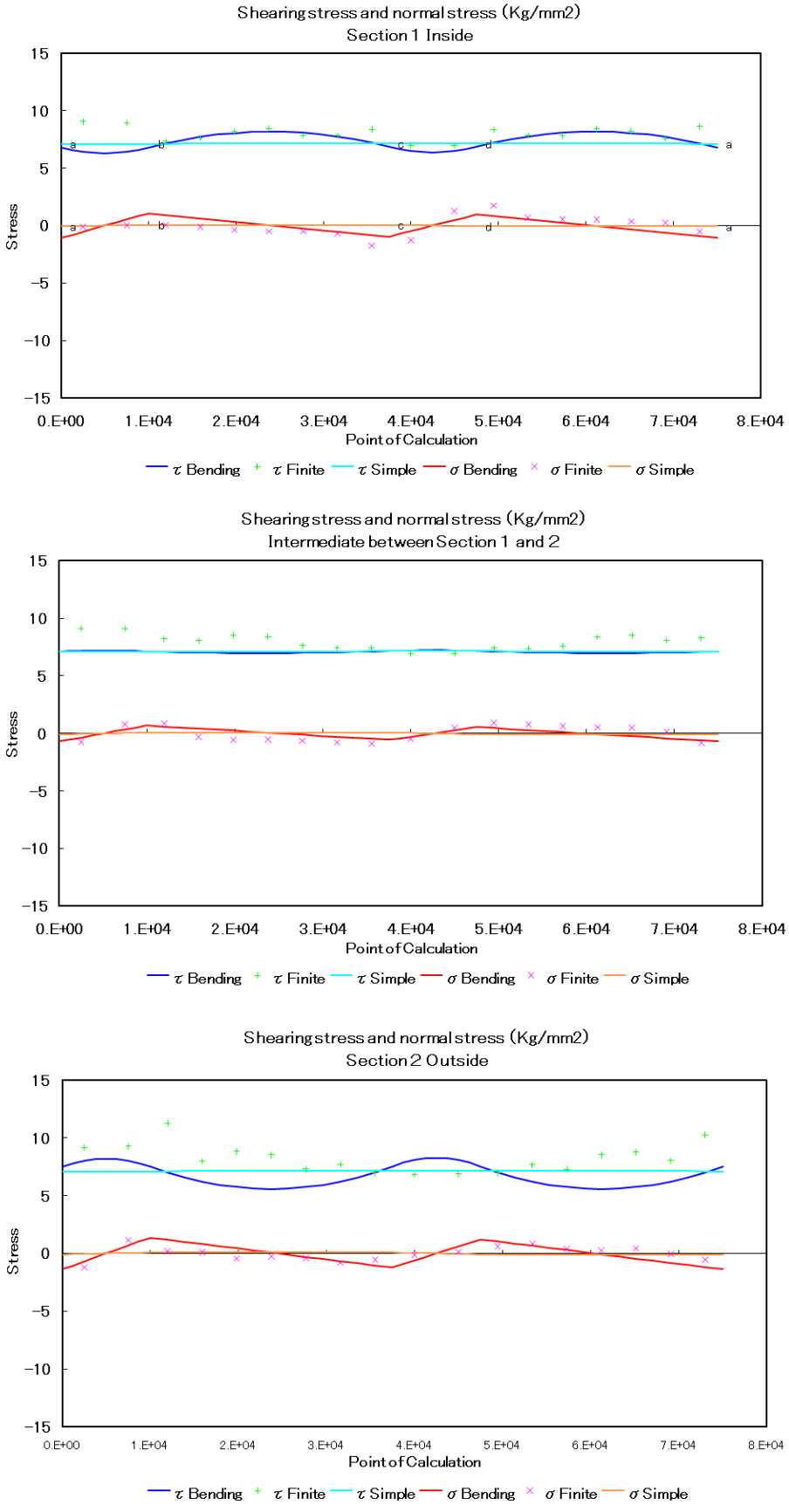

Fig. 3. 1－92 Shearing・normal stress Section 1～2

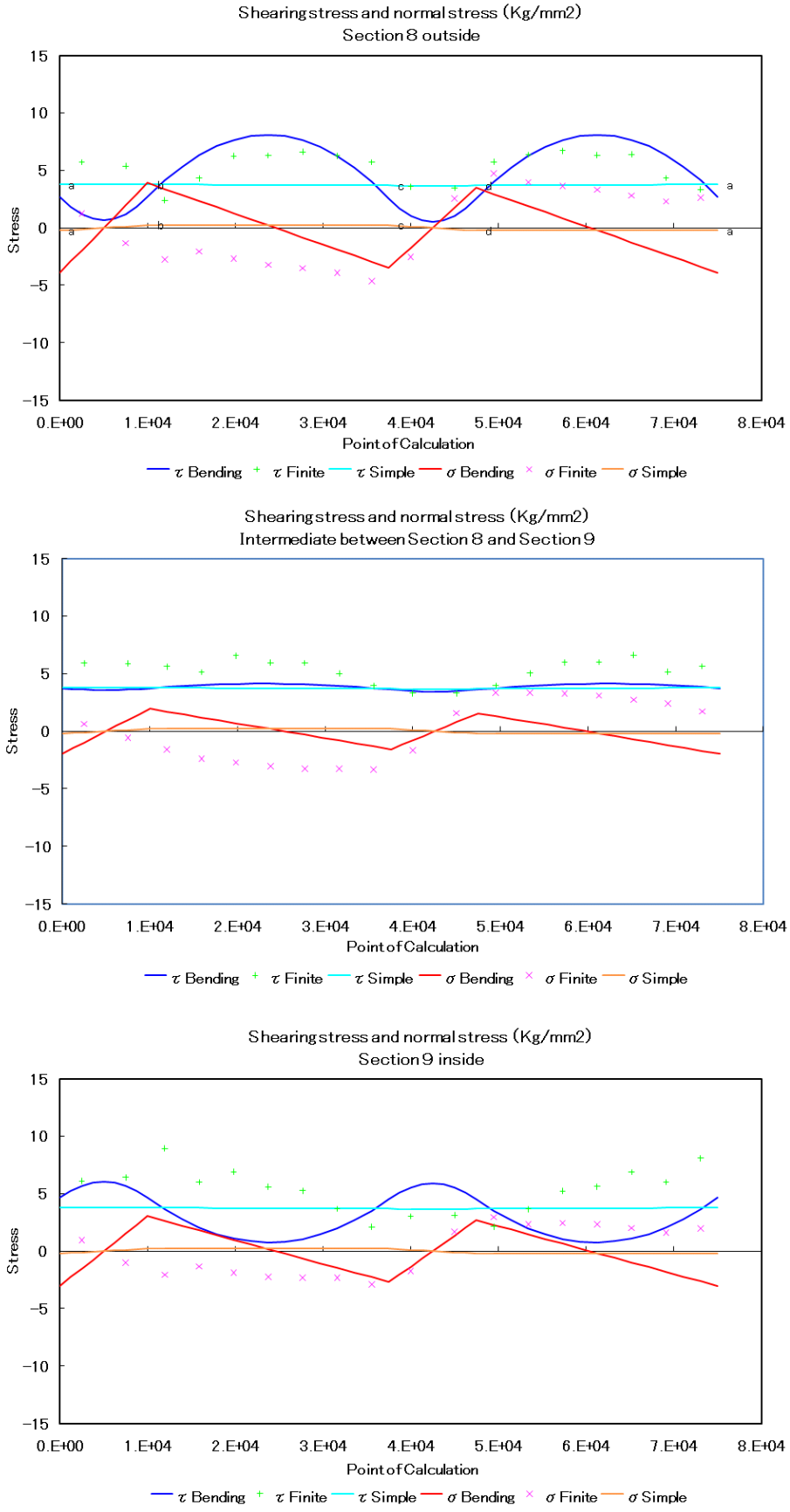

Fig. 3. 1－93 Shearing・normal stress Section 8～9

section between 8 and 9. It is more clear that bending- torsion theory is much more explanatory of the results by the finite element method than simple torsion theory. The results by the finite element method and by the bending- torsion theory are supposed to agree with each other but detailed observation of them disclose fairly large discrepancies on the outside of section 2 and sections between 8 and 9. It is estimated that the discrepancies mainly come from the analytical model of the elastic equation. In the model, ① deformation of vertical gate sections was not considered, ② distribution load was replaced by concentrated loads on web frames and ③ discontinuity in plate thickness over gate length was not considered. It can be expected that a vertical section including a roller support deforms to certain extent due to water pressure load, roller reaction force, shear flow variation etc. and auxiliary members between rollers deforms partially due to water pressure load, and the impact of deformation appears strongly on a section between 8 and 9 since the magnitude of concerned loads are approximately constant through out the gate width and the structural rigidity of the section is comparatively less. The disturbance of the finite element stress around the a and b points on the section suggests that there is a big possibility of roller reaction force impact. It would be quite expectable if the effect of the thickness discontinuity appears noticeably on section 2 where a big jump in plate thickness exists since the thickness discontinuity makes a big impact on statically indeterminate reaction force. The elastic equation of the bending- torsion theory can not respond to partial deformation and sectional discontinuity of the gate body but the approximate calculation method described at close (4) of the simple torsion theory is applicable to the partial deformation.

It cannot be denied that bending- torsion has an important influence on stress distribution even if there is a regardless of lack of uniformity in the comparison and it will be concluded that analysis by finite element method is inevitable in design of super large scale torsion type structures as long as elastic equations are not applicable for sectionally variable structures.

3．1．5 Conclusion

① A fabrication record shows the fish belly flap of torsion type structure was in operation at 1931 in Europe. The first application of this type in Japan was much later but its development seems to be in a somewhat different direction and its gate shape sometimes differs from fish belly shape. This is the reason why the expression "torsion type structure" or "torsion type gate" was introduced in this thesis.

② Characteristics of torsion type structure： (1) External force can compose torsion moment. (2) Sectional torsion rigidity is big. (3) Gate weight is small in case horizontally long. (4) Strong fatigue strength.

③ Erection of elastic equation： (1) Basic model is one end support. Both ends support is resolved as an applied problem. (2) Move of free end is unknown factor which is given as a solution of the equation. (3) The equation consists of torsion deformation and bending deformation.

④ Torsion type gate can be analyzed as a space frames. Problem of discrepancy between gravity and shearing centers of a member disappears due to the assumption that the web frame is a rigid body.

⑤ Analytical results of simple torsion theory： (1) Bending deformation of one end support and both ends support are equal in case of a uniform cross section. (2) Although shearing force and bending moment increase abruptly and their distributions are disturbed due to a variable cross section, its impact on internal torsion moment is small. (3) Impact of maximum I will be considerably mitigated by restriction release in maximum I direction of the bottom support. (4) Impact of maximum I will disappears when the bottom support location in minimum I direction coincides with sectional shearing center. (5) The main gate deflection of a double gate dose not spoil its flap gate function except that partial stress on the gate may increase. (6) Stress concentration appears at closed thin shell corners. (7) Above items are applicable to bending- torsion theory.

⑥ Analytical results of bending- torsion theory： (1) A solution of basic equation

for bending- torsion has been obtained for a uniform cross section and a set of elastic equation can be erected by it. (2) Bending- torsion does not make big impact on sectional force distribution. (3) Bending- torsion moment varies along a gate width with approximate periodicity and average amplitude depends on the support number. The more number the less amplitude. (4) Shearing stress due to bending- torsion moment shows much bigger value than that of simple torsion moment whose is same amount as the bending- torsion moment. The amount is small but eventual impact on sectional stress can not be neglected. (5) A rectangular section can resist bending- torsion more efficiently than a fish- belly section. (6) The effect of bending- torsion on sectional stress is more remarkable in the vicinity of non- supported gate end where torsion moment is comparatively small. Gate design without considering bending- torsion cannot hold good in the case of super large scale torsion type gates whose most of the surface is in a critical state of stress and stress due to bending- torsion is dominant in member selection over a large portion of the gate.

⑦ Analytical method : Behavior of a torsion type structure can not be fully explained by analysis of simple torsion theory. Analysis including bending- torsion is necessary and finite element method and elastic equation method can do it but finite element method is deemed to be the most appropriate procedure as long as elastic equation method can not respond to a variable cross section.

Appendix 3．1－1　Table of terms in cited formulae

（Cited formulae：formulae cited from the appendix to the body text）

The cited formulae in the text are (e), (f3), (l), (m), (n), (y), (aa), (ac), (ad), (ae), (aj), (ba), (bf), (bh) and (bj). A term of the formulae is defined at their appendices and main of the terms are shown below also.

x, y, z：Rectangular coordinate. x & y and sectional principal axes agree. s　：Girth axis around a thin shell section (clockwise is +).
θ　：Rotation angle of a section at z = z (clockwise is +). Θ　：Function which gives θ. ξ、η：The x and y components of displacement of a section (deflection)
E：Young's modulus G：Shearing elastic modulus t：Thickness of a thin shell section l：Overall length of a beam
A_s　：Area of a closed section M_x, M_y：Integration up to s of sectional 1st degree m. around x and y axes. I_x、I_y：Sectional 2nd degree moment around the x and y axes. J_t　：Section modulus of simple torsion C_{bd}　：Section modulus of bending- torsion
Q_x、Q_y：Sectional shearing force in the x and y directions m_x、m_y：Sectional bending moment around the x and y axes T_w　：Sectional bending- torsion moment T_s　：Sectional simple torsion moment m_t　：External distributed moment T　：External concentrated moment c　：Working location of T (on z axis)
r_s、r_0：Distance between shearing or coordinate center and tangent to ds. (The distance is + when moment of ds around the center is +.) $\oint ds$　：Full circle integration along s axis.

Appendix 3．1－2 Stress distribution of thin shell beam subject to twisting

Torsion shearing stress exists on a cross section of beam subject to twisting. Magnitude of moment composed by torsion shearing stress of a closed thin shell circled or regular polygon section beam of constant shell thickness equals torsion moment externally applied on it. A cross section of the beam only rotates around the beam axis and has no deformation in direction of the axis but a cross section of many other cases is bound to bring out deformation called "warping" as shown on Fig. 3．1－100[*1] Even if warping exists there will be no change of torsion shearing stress as long as the warping is constant along the beam axis but the stress distribution will change by in-plane bending of members composing the section if the warping changes along the axis due to internal torsion moment change or existence of external restriction. This phenomenon is called bending-torsion. Stress distribution of bending-torsion is completely different from those of bending beam theory or simple torsion theory. Vertical stress on the cross sections of top, bottom, sides etc. which are members of the beam section will compose a bending moment on each member whereas their integration over the beam section equals 0. Nevertheless of it, shearing stress on the member sections composes a torsion moment on the beam section and it is in balance with a part of the external torsion moment. Rate of the torsion moments shared by simple torsion and bending-torsion changes according to warping distribution along the axis. Many

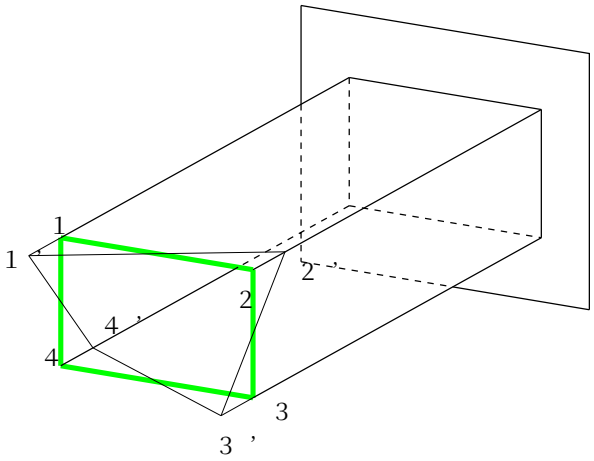

Fig 3．1－100

[*1] This figure was cited from page 239 of bibliography (32). Rectangle section 1234 moves to 1'2'3'4' due to warping. It is given by the reference on possible cause of the warping that the cross section keeps being in state of a right shape without crumpled up after the beam is twisted and also that, in short, right angled intersection condition between generatrices on the section and generatrices in parallel with the beam axis maintains after the beam is deformed.

papers which relate stress distribution of a beam including bending-torsion phenomenon have been written and this appendix intends to edit fragmentary information of the papers so as to provide consistent content which concentrates on a thin shell section beam and meets purpose of the study theme. In this study, torsion phenomenon is separated into simple torsion and bending-torsion, internal torsion moment of each group is called simple torsion moment and bending-torsion moment and analytical theory of torsion type structure is divided into simple torsion theory which neglects bending-torsion and bending-torsion theory which considers bending-torsion.

（１） Distribution of simple torsion and bending- torsion

［Displacement］

The original point of coordinate is set at gravity center（G）of the beam terminal and x, y and z axes are set as shown on Fig. ３. １－１０１. Rotation angle at z＝z is denoted by θ which is given by function Θ（z）as below.

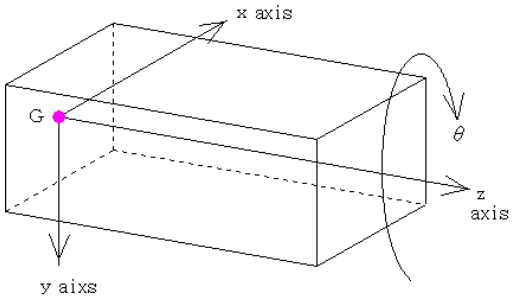

Fig. ３. １－１０１

$$\theta = \Theta(z)$$

Components u and v in the x and y direction of displacement caused by the θ can be given by following formulae since assumption that the section rotates around the gravity center dose not influence the stress components[*1] although the

$$\left.\begin{aligned} u &= -\Theta y \\ v &= \Theta x \end{aligned}\right\} \quad \cdots\cdot(a)$$

rotation takes place around the shearing center. Warping function Ψ（x, y）denotes the warping pattern of a section which crosses the z axis by right angle. The w which is displacement in the z direction of a point（x、y）on the section (refer to the right figure) is proportional to intensity of the sectional twisting and given by following formula.

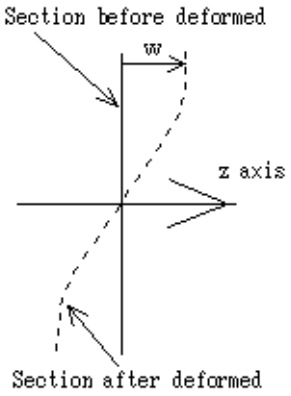

$$w = \frac{d\Theta}{dz}\Psi(x, y) \qquad \cdots\cdot(b)$$

[*1] Page 181 of bibliography (21).

［Strain and stress］

Let normal stress and shearing stress be σ and τ respectively, and let temsile strain and shearing strain be ε and γ respectively and let their applied surface and direction be identified by a suffix[*1], then the strain and stress are given by following formulae. E is Young's modulus and G is shearing elastic modulus.

$$\left.\begin{aligned} &\varepsilon_x=\varepsilon_y=0 \ 、\quad \varepsilon_z=\frac{\partial w}{\partial z} 、\ \gamma_{xy}=\frac{\partial v}{\partial x}+\frac{\partial u}{\partial y} \\ &\gamma_{xz}=\frac{\partial w}{\partial x}+\frac{\partial u}{\partial z}=\frac{d\Theta}{dz}\left(\frac{\partial \Psi}{\partial x}-y\right) \\ &\gamma_{yz}=\frac{\partial w}{\partial y}+\frac{\partial v}{\partial z}=\frac{d\Theta}{dz}\left(\frac{\partial \Psi}{\partial y}+x\right) \end{aligned}\right\} \quad \cdots\cdots(c)$$

$$\left.\begin{aligned} &\sigma_x=\sigma_y=0 \ 、\quad \sigma_z=E\varepsilon_z=E\frac{\partial w}{\partial z} 、\ \tau_{xy}=G\gamma_{xy}=G\left(\frac{\partial v}{\partial x}+\frac{\partial u}{\partial y}\right) \\ &\tau_{xz}=G\gamma_{xz}=G\frac{d\Theta}{dz}\left(\frac{\partial \Psi}{\partial x}-y\right)=G\left(\frac{\partial w}{\partial x}-\frac{d\Theta}{dz}y\right) \\ &\tau_{yz}=G\gamma_{yz}=G\frac{d\Theta}{dz}\left(\frac{\partial \Psi}{\partial y}+x\right)=G\left(\frac{\partial w}{\partial y}+\frac{d\Theta}{dz}x\right) \end{aligned}\right\} \quad \cdots\cdots(d)$$

Direction of positive shearing stress on the surface whose normal line agree with direction of coordinate axis coincides with direction of shearing stress. Vice versa.

［Equation of equality］

Let the equation be obtained by potential energy of torsion. Torsion shearing strain in proportion to $\frac{d\Theta}{dz}$ and vertical strain $\frac{\partial w}{\partial z}$ comes out on the section of

[*1] σ_x is normal stress in x direction of the surface whose normal line is in x direction, τ_{xy} is shearing stress in y direction of the surface whose normal line is in x direction, ε_x is tensile strain in x direction of the surface whose normal line is in x direction and γ_{xy} is shearing strain corresponding to shearing stress in y direction of the surface whose normal line is in x direction.

twisted beam and corresponding strain energy is stored[*1]. Suppose uniform torsion moment m_t exists along the z axis, then over all potential energy Π is given as follows since potential energy of the load due to the beam rotation is also stored.

$$\Pi = -\int_0^l m_t \Theta \, dz + \int_0^l \int \frac{E}{2} \left(\frac{\partial w}{\partial z}\right)^2 t \, ds \, dz + \int_0^l \frac{GJ_t}{2} \left(\frac{d\Theta}{dz}\right)^2 dz$$

In above formula, s is distance along the thin shell section, t is shell thickness, the l is over all length of the beam and J_t is section modulus of torsion. Formula (b) is inserted into above formula and $\int \Psi^2 t \, ds = C_{bd}$ is replaced then following formula obtained.

$$\Pi = -\int_0^l m_t \Theta \, dz + \frac{EC_{bd}}{2} \int_0^l \left(\frac{d^2\Theta}{dz^2}\right)^2 d + \int_0^l \frac{GJ_t}{2} \left(\frac{d\Theta}{dz}\right)^2 dz$$

C_{bd} is section modulus of bending-torsion. The theorem by variation of displacement is applied to above formula and following formula is obtained[*2].

$$\delta\Pi = \int_0^l \left(-m_t \delta\Theta + EC_{bd} \frac{d^2\Theta}{dz^2} \cdot \delta \frac{d^2\Theta}{dz^2} + GJ_t \frac{d\Theta}{dz} \cdot \delta \frac{d\Theta}{dz}\right) dz$$

$$= \int_0^l \left(-m_t \delta\Theta + EC_{bd} \frac{d^2\Theta}{dz^2} \cdot \frac{d^2\delta\Theta}{dz^2} + GJ_t \frac{d\Theta}{dz} \cdot \frac{d\delta\Theta}{dz}\right) dz$$

Operation of partial integration is made twice on the second term and once on the third term in the integration mark of above formula and following results will be obtained.

[*1] Although shearing stress comes out due to bending-torsion, let it be neglected at this stage.

[*2] Refer to page 59 of bibliography (18). Same result will be obtained by Taylor expansion after definitely small terms of more than second degree are deleted.

$$\int_0^l \frac{d^2\Theta}{dz^2} \cdot \frac{d^2\delta\Theta}{dz^2} dz = \left[\frac{d^2\Theta}{dz^2} \cdot \frac{d\delta\Theta}{dz}\right]_0^l - \left[\frac{d^3\Theta}{dz^3}\delta\Theta\right]_0^l + \int_0^l \frac{d^4\Theta}{dz^4}\delta\Theta dz$$

$$\int_0^l \frac{d\Theta}{dz} \cdot \frac{d\delta\Theta}{dz} dz = \left[\frac{d\Theta}{dz}\delta\Theta\right]_0^l - \int_0^l \frac{d^2\Theta}{dz^2}\delta\Theta dz$$

They are inserted into the formula of $\delta\Pi$ and following formula is obtained after

$$\delta\Pi = \left[EC_{bd}\frac{d^2\Theta}{dz^2} \cdot \frac{d\delta\Theta}{dz}\right]_0^l - \left[\left(EC_{bd}\frac{d^3\Theta}{dz^3} - GJ_t\frac{d\Theta}{dz}\right)\delta\Theta\right]_0^l$$

$$+ \int_0^l \left(EC_{bd}\frac{d^4\Theta}{dz^4} - GJ_t\frac{d^2\Theta}{dz^2} - m_t\right)\delta\Theta dz = 0$$

their terms are organized. The first and second terms in above formula equal 0 since quantity of their factors is determined by the end conditions of Θ as shown below formulae and one of two factors in each term becomes 0.

$$\text{First term} = \left[\text{Vertical stress} \cdot \text{Warping}\right]_0^l$$

$$\text{Second term} = \left[\text{Torsion moment} \cdot \text{Rotation angle}\right]_0^l$$

Eventually, the third term has to be 0 because $\delta\Pi = 0$ and following basic equation of the bending- torsion is obtained. The rotation angle Θ of a section is obtained by solving this formula and Θ', Θ'' and Θ''' are calculated one right after the other, then distribution of simple torsion moment, warping, vertical stress due to the warping and bending- torsion moment will be made known.

$$EC_{bd}\frac{d^4\Theta}{dz^4} - GJ_t\frac{d^2\Theta}{dz^2} - m_t = 0 \qquad \cdots\cdots(e)$$

［End condition］

End conditions of warping and rotation are necessary as it became clear in the previous explanation. Table 3.1－101 shows formulae and values of the conditions.

Condition	Warping	Rotation
Free	$EC_{bd}\dfrac{d^2\Theta}{dz^2}=0$	$EC_{bd}\dfrac{d^3\Theta}{dz^3}-GJ_t\dfrac{d\Theta}{dz}=0$
Restricted	$\dfrac{d\Theta}{dz}=0$	$\Theta=0$

Talbe 3.1－101

［Exampe of solution 1］*1

Example of Fig. 3.1－102a is a beam of length l with free condition for warping and restricted condition for rotation at both beam ends and a concentrated torsion moment $T=T_1+T_2$ is acting at $z=c$ of the beam. Let m_t in formula (e) be set at 0 and following two formulae are obtained after integration.

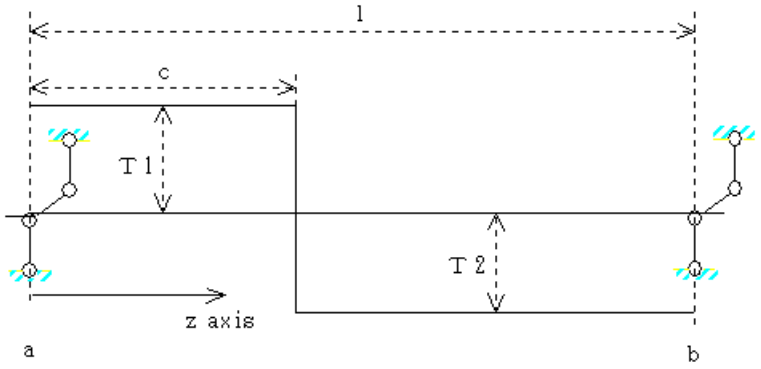

Fig. 3.1－102a

where $z \leqq c$ $\quad EC_{bd}\dfrac{d^3\Theta}{dz^3}-GJ_t\dfrac{d\Theta}{dz}=-T_1$

where $z \geqq c$ $\quad EC_{bd}\dfrac{d^3\Theta}{dz^3}-GJ_t\dfrac{d\Theta}{dz}=-T_2$

*1 The same solution is given in bibliography (27) and (28).

One more condition necessary to eliminate internal torsion moment T_1 and T_2 is a continuity condition of above two formulae at $z = c$. And their solution is given by following formula.

$$z \leqq c \quad \Theta = \frac{T}{E C_{bd}} \left[\frac{\mathrm{sh}\{\alpha(l-c)\}\mathrm{sh}(\alpha z)}{\alpha^3 \mathrm{sh}(\alpha l)} - \frac{l-c}{\alpha^2} z - \frac{\mathrm{sh}\{\alpha(z-c)\}}{\alpha^3} + \frac{z-c}{\alpha^2} \right]$$

$$z \geqq c \quad \Theta = \frac{T}{E C_{bd}} \left[\frac{\mathrm{sh}\{\alpha(l-c)\}\mathrm{sh}(\alpha z)}{\alpha^3 \mathrm{sh}(\alpha l)} - \frac{l-c}{\alpha^2} z \right]$$

where $\alpha = \sqrt{G J_t \div E C_{bd}}$

·····(f1)

[Example of solution 2] *1

Example of Fig. 3. 1−102 b is a beam of length l with free condition for warping and restricted condition for rotation at both beam ends and a distributed torsion moment t is acting between $z = c$ and end b of the beam. A solution is given as below.

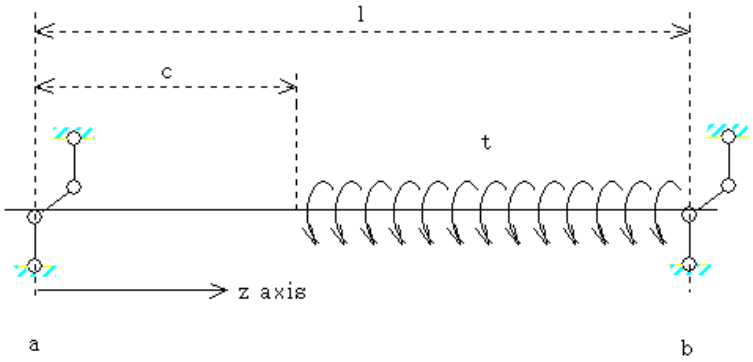

Fig. 3. 1−102 b

$$z \leqq c \quad \Theta = \frac{t}{E C_{bd}} \left[\frac{(1-\mathrm{ch}\{\alpha(l-c)\})\mathrm{sh}(\alpha z)}{\alpha^3 \mathrm{sh}(\alpha l)} - \frac{(l-c)^2}{2\alpha l} z \right]$$

$$z \geqq c \quad \Theta = \frac{t}{E C_{bd}} \left[\frac{(1-\mathrm{ch}\{\alpha(l-c)\})\mathrm{sh}(\alpha z)}{\alpha^3 \mathrm{sh}(\alpha l)} - \frac{(l-c)^2}{2\alpha l} z - \frac{1-\mathrm{ch}\{\alpha(z-c)\}}{\alpha^3} - \frac{(z-c)^2}{2\alpha} \right]$$

where $\alpha = \sqrt{G J_t \div E C_{bd}}$

·····(f2)

*1 Cited from bibliography (27)。

［Example of solution 3］[*1]

Example of Fig. 3. 1－102c is a beam of length l with free condition for warping and restricted condition for rotation at beam end a and free condition for warping and rotation at beam end b and a concentrated torsion moment T is acting at $z = c$ of the beam. A solution is given as below.

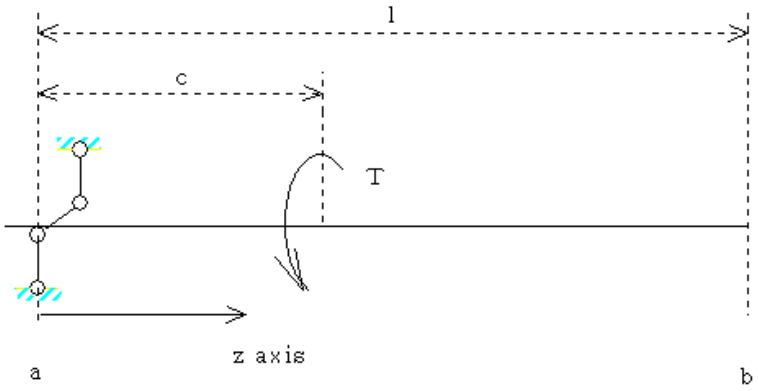

Fig. 3. 1－102c

$$z \leqq c \quad \Theta = \frac{T}{EC_{bd}} \left[\frac{z}{\alpha^2} - \frac{sh\{\alpha(l-c)\})sh(\alpha z)}{\alpha^3 sh(\alpha l)} \right]$$

$$z \geqq c \quad \Theta = \frac{T}{EC_{bd}} \left[\frac{c}{\alpha^2} - \frac{sh\{\alpha(l-c)\})sh(\alpha z)}{\alpha^3 sh(\alpha l)} + \frac{sh\{\alpha(z-c)\}}{\alpha^3} \right]$$

where $\alpha = \sqrt{GJ_t \div EC_{bd}}$

·····(f3)

［Example of solution 4］[*2]

Example of Fig. 3. 1－102d is a beam of length l with restricted condition for warping and rotation at beam end a and free condition for warping and rotation at beam end b and a concentrated torsion moment T is acting at $z = c$ of the beam. A solution is given as below.

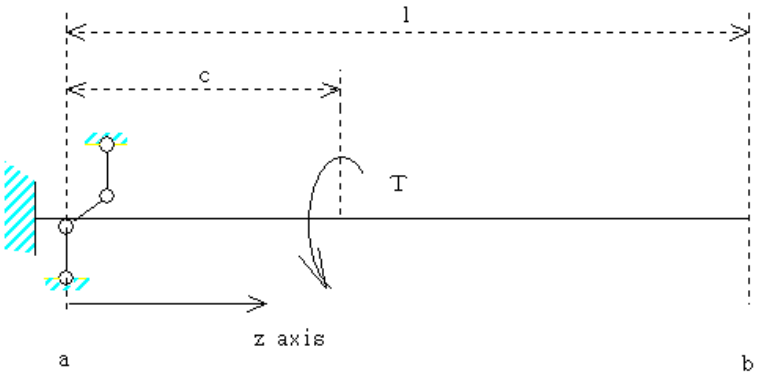

Fig. 3. 1－102d

[*1] Cited from bibliography (28)。
[*2] Cited from bibliography (28)。

$$z \leqq c \quad \Theta = \frac{T}{\alpha^3 E C_{bd}} \left[\left\{ sh(\alpha l) - sh\{\alpha(l-c)\} \right\} \frac{ch(\alpha z) - 1}{ch(\alpha l)} - sh(\alpha z) + \alpha z \right]$$

$$z \geqq c \quad \Theta = \frac{T}{\alpha^3 E C_{bd}} \left[\alpha c - \frac{sh(\alpha l) - sh\{\alpha(l-c)\} + sh\{\alpha(l-z)\}\{ch(\alpha c) - 1\}}{ch(\alpha l)} \right]$$

where $\alpha = \sqrt{GJ_t \div EC_{bd}}$

·····(f4)

[Example of solution 5] *1

Example of Fig. 3.1−102e is a beam of length l with free condition for warping and restricted condition for rotation at the beam end a and free condition for warping and rotation at the beam end b and a distributed torsion moment t is acting all over the beam. A solution is given as below.

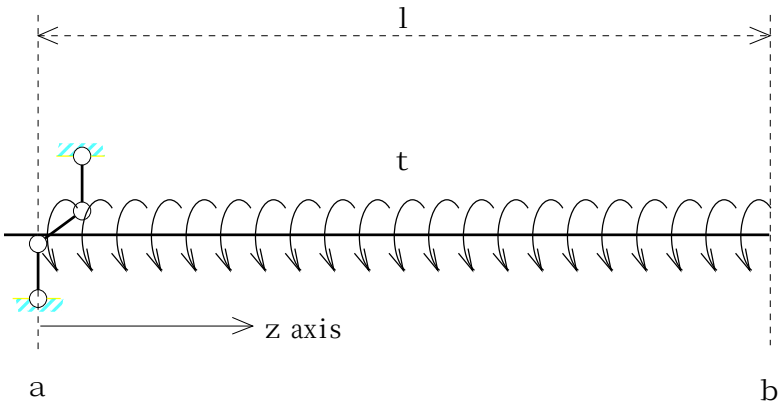

Fig. 3.1−102e

$$\Theta = \frac{t}{\alpha^4 E C_{bd}} \left[\alpha^2 z (l - z/2) + \frac{ch\{\alpha(l/2 - z)\}}{ch(\alpha l/2)} \right]$$

where $\alpha = \sqrt{GJ_t \div EC_{bd}}$

·····(f5)

*1 Cited from bibliography (28)。

［Example of solution 6］[*1]

Example of Fig. 3. 1－102f is a beam of length l with restricted condition for warping and rotation at the beam end a and free condition for warping and rotation at the beam end b and a distributed torsion moment t is acting all over the beam. A solution is given as below.

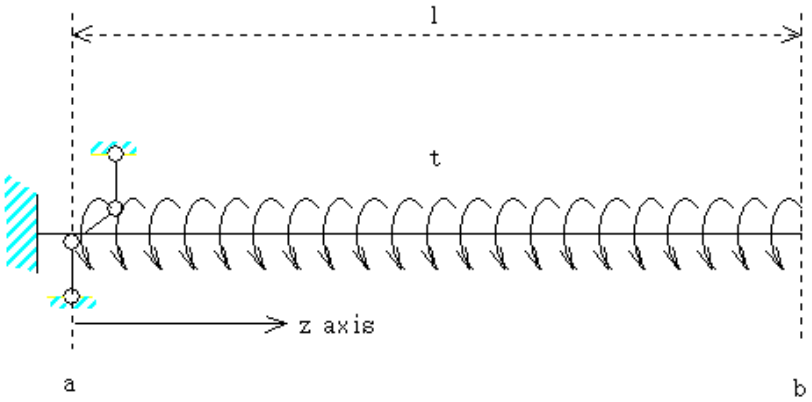

Fig. 3. 1－102f

$$\Theta = \frac{t}{\alpha^4 E C_{bd}} \left[\alpha^2 z (l - z/2) + \frac{ch(\alpha z) - 1 - \alpha l \, sh(\alpha l) + \alpha l \, sh\{\alpha (l - z)\}}{ch(\alpha l)} \right]$$

where $\alpha = \sqrt{GJ_t \div EC_{bd}}$ ·····(f6)

Many solutions are available for loading conditions and end conditions other than above examples[*2].

[*1] Cited from bibliography (28)。
[*2] Bibliography (28) shows solutions of 36cases including above cited examples。Bibliography (29) and (30) are their abstracts in Japnese version。

（2） Calculation method of C_{bd} and J_t

Section moduli C_{bd} and J_t of bending-torsion and simple torsion are necessary to calculate quantity of torsion and bending-torsion by the solution of formula (e).

2－1）C_{bd}： Section modulus of bending-torsion

C_{bd} was defined as follows in the process of deriving formula (e).

$$C_{bd} = \int \Psi^2 t \, ds \qquad \cdots\cdots(g)$$

Ψ is called a warping function which describes a pattern of warping. Quantity of warping w is given by Ψ multiplied by intensity of twisting as shown in formula (b). Ψ has to be obtained ahead of deriving formula of C_{bd}. The s axis is set along the center line of thin shell section as shown on Fig. 3. 1－103 and ds, dx and dy denote an imperceptible length of the s and components of the ds in the x and y directions respectively. The + direction of s is clockwise as same as θ. Suppose the section considered is closed one and τ_s denotes shearing stress on the ds, then τ_s is approximately constant over the thickness of thin shell and given by following formula according to the definitions on the figure.

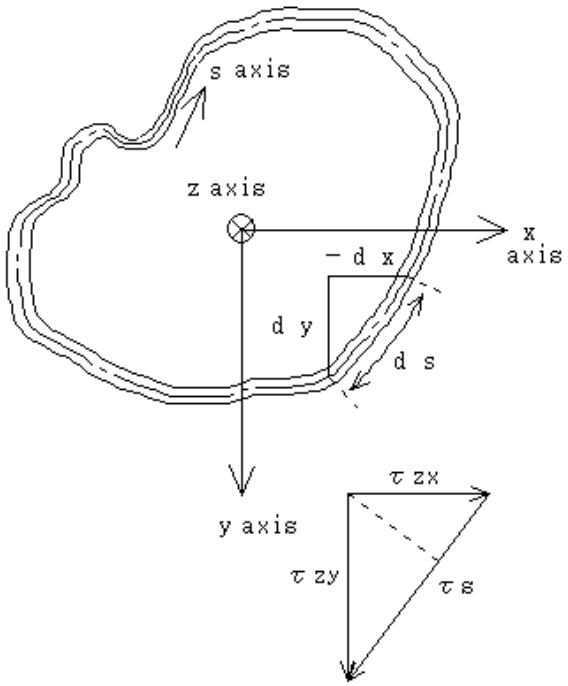

Fig. 3. 1－103

$$\tau_s = \tau_{zx}\frac{dx}{ds} + \tau_{yz}\frac{dy}{ds} = \tau_{xz}\frac{dx}{ds} + \tau_{zy}\frac{dy}{ds} \qquad \cdots\cdots(h)$$

Formulae (d) are inserted into τ_{xz} and τ_{zy} of formula (h) and integration along s is made on the both sides of re-organized formula (h), then following formula is obtained.

$$\int_0^s \tau_s ds = G\int_0^s \left(\frac{\partial w}{\partial x}\cdot\frac{dx}{ds}+\frac{\partial w}{\partial y}\cdot\frac{dy}{ds}\right)ds + G\frac{d\Theta}{dz}\int_0^s (x\,dy - y\,dx)$$

.....(i)

The expression in the integration mark of first term on right side of the formula is a form of composite function of x and y after differentiated by s[*1] and that of the second term is geometrically replaced according to $x\,dy - y\,dx = r_s\,ds$[*2]. The r_s is a distance between the shearing center and tangent to ds. Although the coordinate origin can be set at arbitrary point[*3], it is supposed to be the gravity center and formula (i) is transformed to get following formula. Integration of

$$\int_0^s \tau_s ds = G\int_0^s \frac{dw}{ds}ds - G\frac{d\Theta}{dz}\int_0^s r_s\,ds = G(w-w_0) + G\frac{d\Theta}{dz}\int_0^s r_s\,ds$$

.....(j)

the formula is made on whole circumference of the section, then the right hand side first term becomes $w - w_0 = 0$ and the second term equals sectional area A_s multiplied by 2, and since τ_s of the left hand side is shearing stress due to simple torsion, τ_s multiplied by t equals shear flow of simple torsion which is constant. Eventually τ_s becomes as follows.

$$\oint \tau_s ds = \tau_s t \oint \frac{ds}{t} = 2GA_s\frac{d\Theta}{dz} \quad \text{従って、} \quad \tau_s = \frac{2GA_s}{t}\cdot\frac{d\Theta}{dz}\div\oint\frac{ds}{t}$$

[*1] Refer to page 67 of bibliography (15)。

[*2] It can be confirmed on a simple sketch and also it has been verified on page 157 of bibliography (17)。

[*3] Its reason is as same as the reason of formula (a) whose rotation center can be shiftted arbitrary。

$\cdots\cdots(k)$

Formula of w is obtained by using fromula (j) and (k) and then warping function of closed section Ψ is obtained after the w_0 in w is replaced by $w_0 = \Psi_0 \frac{d\Theta}{dz}$ and formula (b) is inserted into w. The formula in the ( ) is expression based on the definitions at formula (m). The r_s is a quantity which has + or - sign and is + when $r_s ds$ gives positive moment around the shearing center[*1].

$$\Psi = \Psi_0 - \int_0^s r_s ds + 2A_s \int_0^s \frac{1}{t} ds \div \oint \frac{ds}{t} \quad (= \Psi_0 - R + 2a_1 I) \qquad \cdots\cdots(l)$$

At the begining of this section, a section on which no warping exists was touched of which more concrete explanation can be given based upon formula (l). As warping function $\Psi \equiv 0$ then $\Psi_0 = 0$. Accordingly Ψ is rewritten as follows. Owing to Ψ

$$\Psi = \int_0^s \{ - r_s + (2A_s \div \oint \frac{ds}{t}) \frac{1}{t} \} ds$$

equals 0 for any s, the inside of integration mark has to be 0. Accordingly a condition of no warping becomes as follows[*2]. The formula in the ( ) is expression

$$r_s = \frac{1}{t} (2A_s \div \oint \frac{ds}{t}) \quad (= \frac{2a_1}{t})$$

based on the definitions at formula (m). A circular section and a regular tetragon section satisfy this condition when t is constant and any section can satisfy this condition if distribution of the t satisfies the equation $t \times r_s$ = constant.

[*1] Page 239 of bibliography (32)。

[*2] $\Psi_0 = 0$ is true when this condition is satisfied。

C_{bd} is given as follows after formula (l) is inserted into formula (g). The center of r_s is at shearing center of a section.

$$C_{bd} = \Psi_0^2 J_0 - 2\Psi_0 J_1 + 4\Psi_0 a_i J_2 + J_3 - 4 a_i J_4 + 4 a_i^2 J_5 \quad \cdots\cdots (m)$$

where $a_i = A_s \div I_0$

$$J_0 = \oint t\,ds$$
$$J_1 = \oint R\,t\,ds$$
$$J_2 = \oint I\,t\,ds$$
$$J_3 = \oint R^2 t\,ds$$
$$J_4 = \oint R\,I\,t\,ds$$
$$J_5 = \oint I^2 t\,ds$$

$$I_0 = \oint \frac{1}{t} ds$$

$$R = \int_0^s r_s ds$$

$$I = \int_0^s \frac{1}{t} ds$$

Note 1. The center of r_s is at shearing center of a section.

Ψ_0 is value of Ψ at a starting point of circumferential integration and the value is obtained by the condition that there is no external force in direction of the axis. In short, integration of the Ψ over the section has to be 0 since there is no external force in direction of the axis. Following formula is obtained from formula (l) after

$$\oint \Psi t\,ds = \Psi_0 \oint t\,ds - \oint t \int_0^s r_s ds\,ds + 2A_s \div \oint \frac{ds}{t} \cdot \oint t \int_0^s \frac{1}{t} ds\,ds = 0$$

this condition is applied to it and accordingly formula of Ψ_0 becomes following which consists of the marks of formula (m).

$$\Psi_0 = \left(\oint t \int_0^s r_s ds\,ds - 2A_s \div \oint \frac{ds}{t} \cdot \oint t \int_0^s \frac{1}{t} ds\,ds \right) \div \oint t\,ds$$
$$= (J_1 - 2 a_i J_2) \div J_0 \quad \cdots\cdots (n)$$

Section modulus of bending- torsion C_{bd} can be calculated from formula (n) and (m). Shearing center (x_s、y_s) which are used in the calculation is given by following formulae based on the condition that moments around the coordinate

origin of sectional shearing force and shearing stress due to bending are equal[*1]. The x and y axes are supposed to coincide with sectional principal axes.

$$\left.\begin{aligned} y_s &= (J_{11} + 2A_s c_x) \div I_y \\ x_s &= -(J_{12} + 2A_s c_y) \div I_x \end{aligned}\right\} \quad \cdots\cdots (o)$$

where $c_x = -J_9 \div I_0$

$c_y = -J_{10} \div I_0$

$$J_9 = \oint \frac{M_y}{t} ds \qquad M_y = \int_0^s x\, t\, ds$$

$$J_{10} = \oint \frac{M_x}{t} ds \qquad M_x = \int_0^s y\, t\, ds$$

Note 1. Center of r_0 is at a gravity center.

$$J_{11} = \oint \frac{r_0 M_y}{t} ds$$

$$J_{12} = \oint \frac{r_0 M_x}{t} ds$$

$$I_y = \oint x^2 t\, ds$$

$$I_x = \oint y^2 t\, ds$$

I_0、A_s is as same as definition for formula (m).

r_0 is a distance between coordinate origin and tangent to the integrating point. Examples of calculated C_{bd} are shown in Appendix 3. 1－4 and 5 which are application results of formulae (o), (n) and (m) on a fish belly section and a rectangular section. Numerical computation formula of simple section form is very complicated as shown on the examples and numerical integral by a computer on a line elements model is necessary for a practical purpose.

Calculation method of closed section modulus for bending- torsion is described above. In case of open section, shearing stress along the center line of thin shell

[*1] Detail of their derivation is shown in appendiz 3. 1. 3.

can be deemed to be 0 since amount of the shearing stress varies approximately in liner along the thickness of the thin shell and the stresses at inside and outside of the shell are supposed to be equal in their absolute figure but have different sign. Suppose τ_s is stress along a center line of the thin shell, right hand side of formula (j) can be replaced by 0 and warping function along the thin shell center line of open section Ψ is given as follows since a term including A_s of formula (l)

$$\Psi = \Psi_0 - \int_0^s r_s \, ds \qquad \cdots\cdots(p)$$

disappears. C_{bd} is given as follows since terms including a_i of formula (m)

$$C_{bd} = \Psi_0^2 J_0 - 2\Psi_0 J_1 + J_3 \qquad \cdots\cdots(q)$$

where J_0, J_1 and J_3 are formulae in formula (m) after $\oint$ is replaced by $\int_0^u$ and 0 corresponds to one end of the open section and u corresponds to other end.

disappear. Ψ_0 is given as follows since a term including a_i of formula (n) disappears. Marks in the formula are as same as definitions of formula (q). C_{bd}

$$\Psi_0 = J_1 \div J_0 \qquad \cdots\cdots(r)$$

becomes following by inserting formula (r) into formula (q). A shearing center of

$$C_{bd} = (J_3 J_0 - J_1^2) \div J_0 \qquad \cdots\cdots(s)$$

open cross- section can be represented as following since it corresponds to formula

$$\left.\begin{aligned} y_s &= J_{11} \div I_y \\ x_s &= -J_{12} \div I_x \end{aligned}\right\} \qquad \cdots\cdots(t)$$

where J_{11}, J_{12}, I_y, I_x and I_0 are formulae in formula (o) after $\oint$ is replaced by $\int_0^u$ and 0 corresponds to one end of the open section and u corresponds to other end.

(o) except $c_x = c_y = 0$. In case of an equal angle steel, the shearing center is at the intersection of its legs, which means all sectional members run toward the shearing center and C_{bd} becomes 0 since r_s becomes 0 at calculation of coefficients included in integration formula (s). It is not sufficient in such case that a warping function only along the shell thickness center line just like formula (q) is considered and a variation of Ψ along the thickness has to be considered. After going back to formula (h), let the n axis be set in direction normal to s and the same mathematical operation as r_s is made on shearing stress in the n direction τ_n.

$$\tau_n = \tau_{zx}\frac{dx}{dn} + \tau_{yz}\frac{dy}{dn} = \tau_{xz}\frac{dx}{dn} + \tau_{zy}\frac{dy}{dn} \qquad \cdots\cdots(u)$$

Formula (d) is inserted into τ_{xz} and τ_{zy} of above formula and after its both hand sides are reorganized and integrated in the n direction, following formula is obtained.

$$\int_0^n \tau_n dn = G\int_0^n \left(\frac{\partial w}{\partial x}\cdot\frac{dx}{dn} + \frac{\partial w}{\partial y}\cdot\frac{dy}{dn}\right) dn + G\frac{d\Theta}{dz}\int_0^n (x\,dy - y\,dx) \qquad \cdots\cdots(v)$$

The expression in the integration mark of first term on right side of the formula is a form of composite function of x and y after differentiated by n and that of the second term is geometrically replaced according to $x\,dy - y\,dx = r_n dn$. The r_n is a distance between the shearing center and tangent to n axis. The coordinate origin is supposed to be at the gravity center for a convenience of subsequent calculation. The w is replaced by w_n which denotes difference of warping displacement at arbitrary n from that on the thin shell center line. Accordingly w_n at the origin of n axis equals 0. Formula (v) is transformed to get following formula.

$$\int_0^n \tau_n dn = G\int_0^n \frac{dw}{dn} dn - G\frac{d\Theta}{dz}\int_0^n r_n\, dn = Gw_n + G\frac{d\Theta}{dz}\int_0^n r_n dn$$

w_n can be obtained by putting the right hand side equals 0 since τ_n is always 0. Warping function Ψ is replaced by Ψ_n which corresponds to w_n and formula (b) after transformed is inserted into w_n of above formula to get Ψ_n.

$$\Psi_n = -\int_0^n r_n dn \qquad \cdots\cdots(w)$$

Ψ in formula (g) is replaced by $\Psi+\Psi_n$, the integration is made both on the s direction and n direction, C_{bd} is replaced by C_{bdt} where C_{bdt} equals $C_{bd}+C_{bdn}$ and C_{bdn} is section modulus corresponding to Ψ_n, the whole formula is reorganized and formula (w) is inserted into Ψ_n to get following result.

$$C_{bdt} = \int_0^u \int_{-2/t}^{+t/2} (\Psi+\Psi_n)^2 t\, dn\, ds$$

$$= \int_0^u \Psi^2 t\, ds + 2\int_0^u \Psi \int_{-2/t}^{+t/2} \Psi_n dn\, ds + \int_0^u \int_{-2/t}^{+t/2} \Psi_n^2 dn\, ds = C_{bd} + \int_0^u r_n^2 \frac{t^3}{12} ds$$

$$= C_{bd} + C_{bdn}$$

$$\text{i.e.: } C_{bdn} = \int_0^u r_n^2 \frac{t^3}{12} ds$$

$\cdots\cdots(x)$

Section modulus of bending-torsion for thin shell open cross section can be calculated either by formula (s) of (x) according to its shape as explained above and result of widely used sectional shapes is given on a design handbook etc. Table 3.1−102 shows its examples.

2－2）J_t：Section modulus of simple torsion

Only results are shown since calculation method of the section modulus of simple torsion is well known. Result of widely used sectional shapes is formulated in many design handbooks. Table 3. 1－102 shows its examples.

For closed cross section: $$J_t = 4A_s^2 \div \oint \frac{ds}{t} = \frac{4A_s^2}{I_0} \quad \cdots\cdots(y)$$

For open cross section: $$J_t = \int_0^u \frac{t^3}{3} ds \quad \cdots\cdots(z)$$

e:shearing center S C:torsion rigidity Γ:bending-torsion rigidity

断面形	e, C, Γ
1. 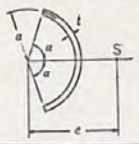	$e=\frac{2a(\sin\alpha-\alpha\cos\alpha)}{\alpha-\sin\alpha\cos\alpha}$ $C=\frac{2}{3}Ga\alpha t^3$ $\Gamma=\frac{2}{3}Ea^5t\left\{\alpha^3-\frac{6(\sin\alpha-\alpha\cos\alpha)^2}{\alpha-\sin\alpha\cos\alpha}\right\}$
2. 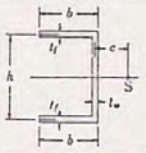	$e=\frac{3b^2t_f}{6bt_f+ht_w}$ $C=\frac{G}{3}(2bt_f^3+ht_w^3)$ $\Gamma=\frac{Eb^3h^2t_f}{12}\frac{3bt_f+2ht_w}{6bt_f+ht_w}$
3. 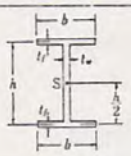	$C=\frac{G}{3}(2bt_f^3+ht_w^3)$ $\Gamma=\frac{E}{24}b^3h^2t_f$
4. 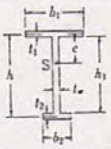	$e=\frac{I_2}{I_1+I_2}h,\quad I_1=\frac{1}{12}b_1^3t_1,\quad I_2=\frac{1}{12}b_2^3t_2$ $C=\frac{G}{3}(h_1t_w^3+b_1t_1^3+b_2t_2^3)$ $\Gamma=\frac{E}{12}\{b_1^3t_1e^2+b_2^3t_2(h-e)^2\}$
5. 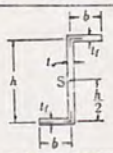	$C=\frac{G}{3}(2bt_f^3+ht_w^3)$ $\Gamma=\frac{Eb^3h^2}{12(2b+h)^2}\{2(b^2+bh+h^2)t_f+3bht_w\}$
6. 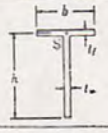	$C=\frac{G}{3}(bt_f^3+ht_w^3)$ $\Gamma=E\left(\frac{b^3t_f}{144}+\frac{h^3t_w}{36}\right)$
7. 	$C=\frac{2}{3}Ght^3$ $\Gamma=\frac{1}{18}Eh^3t^3$

a. Section modulus of simple torsion and bending- torsion (open section)[*1]

Sectional shape	Torsion sectional modulu1 J_t
Constant t. hollow pipe 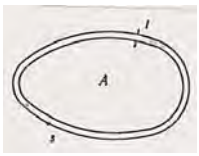	$\frac{4A^2t}{s}$
Tetragon hollow pipe 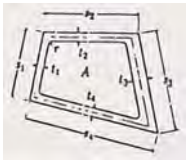	$4A^2\sum\frac{t1}{s1}+\frac{t2}{s2}+\frac{t3}{s3}+\frac{t4}{s4}$

b. Section modulus of simple torsion (closed section)[*2]

Table 3. 1－102 Section modulus formula of thin shell section

[*1] Page 105 of bibliography (35)。
[*2] Page 103 of bibliography (35)。

（３） Calculation method of stress

After sectional rigidity of simple torsion and bending- torsion is determined a distribution of twisting angle appears, and warping displacement and bending- torsion and simple torsion moments will be found out in sequence and then shearing stress and vertical stress of bending- torsion and shearing stress of simple torsion can be calculated.

３－１） Stress distribution of bending- torsion

Vertical stress due to bending- torsion is given as follows by inserting formula (b) into the 2nd expression of formula (d). It commons to open and closed cross

$$\sigma_z = E\Psi \frac{d^2\Theta}{dz^2} \qquad \cdots\cdots(aa)$$

sections and Ψ is given by $\Psi = \Psi + \Psi_n$ just like formula (l), (p) or (x).

Shearing stress can be obtained by a condition that the stress is in balance with the vertical stress. Let the stress of closed section be found out first. Fig. ３．１－１０４ shows stress on a small piece ds x dz x t cut out from the section. The τ_w denotes shearing stress due to bending- torsion (being separated from τ_s which is shearing stress due to simple torsion). Following formula is obtained by an equilibrium of force in

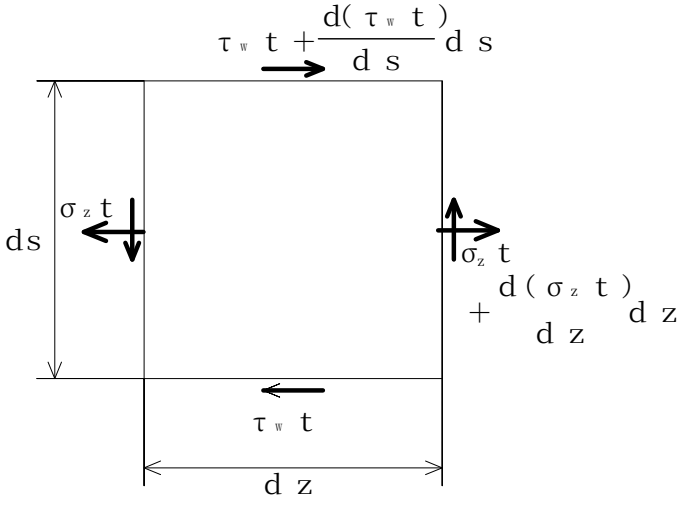

Fig. ３．１－１０４

the z direction.

$$\frac{\partial(\tau_w t)}{\partial s} = -\frac{\partial(\sigma_z t)}{\partial z}$$

Formula (aa) is inserted into the right hand side of above formula and both hand sides of the formula is integrated along the s axis to get τ_w of following formula.

$$\tau_w = -\frac{E}{t}\left(\int_0^s \Psi t\, ds + q_{w0}\right)\frac{d^3\Theta}{dz^3} \qquad \cdots\cdots(ab)$$

The inside of ( ) in this formula is shear flow which shows a distribution of shearing stress of bending- torsion. Let q_w denote the shear flow and formula (1) is inserted into the Ψ to get following formula where q_{w0} is value of the shear flow at a starting point of integration.

$$q_w = \Psi_0 \int_0^s t\, ds - \int_0^s t\, R\, ds + 2a_i \int_0^s t\, I\, ds + q_{w0}$$

$$= \Psi_0 J_{0s} - J_{1s} + 2a_1 J_{2s} + q_{w0} \qquad \cdots\cdots(ac)$$

where Ψ_0 is given by formula (n), a_i, R and I are same definition as those of formula (m) and J_{0s}, J_{1s} and J_{2s} are J_0, J_1 and J_2 of formula (m) after their one round integration is replaced by the integration up to the s respectively.

The shearing stress can be given by formula (ad) which includes the shear flow where T_w is a moment of bending- torsion.

$$\tau_w = -\frac{q_w}{t} E \frac{d^3\Theta}{dz^3} = \frac{q_w}{t} \cdot \frac{T_w}{C_{bd}} \qquad \cdots\cdots(ad)$$

Let q_{w0} be settled next. Before that, let the condition which is necessary for the settlement be found out. τ_w can be expressed as τ_{sz} according to the expression method defined for formulae (c) and (d). Let the relation between τ_w and strain be formulated referring to these formulae and let the geometric relation of stresses shown on Fig. 3.1-103 be applied to that of strains to get following formula where q is a displacement in the s direction.

$$\tau_w = G\gamma_{sz} = G\left(\frac{\partial w}{\partial s} + \frac{\partial q}{\partial z}\right) = G\left(\frac{\partial w}{\partial s} + \frac{\partial u}{\partial z}\cdot\frac{\partial x}{\partial s} + \frac{\partial v}{\partial z}\cdot\frac{\partial y}{\partial s}\right)$$

Following formula which is a condition to settle q_{w0} is obtained by integrating above formula along the s axis giving consideration to that u and v are rigid displacement of sections.

$$\oint \tau_w ds = \oint \frac{\partial w}{\partial s} ds + \frac{\partial u}{\partial z}\oint \frac{\partial x}{\partial s} ds + \frac{\partial v}{\partial z}\oint \frac{\partial y}{\partial s} ds = 0$$

To get q_{w0}, both hand sides of formula (ab) is integrated along the s axis and the integrated right hand side is set as 0. This is solved for q_{w0} which is a function of Ψ. Formula (l) is inserted into the Ψ and integration of the function is carried out. The result is given as follows.

$$q_{w0} = -(\Psi_0 J_6 - J_7 + 2a_i J_8) \div I_0 \qquad \cdots\cdots(ae)$$

where Ψ_0 is given by formula (n) and a_i, I_0, R and I correspond to the definition at formula (m).

$$J_6 = \oint \frac{1}{t}\left(\int_0^s t\, ds\right) ds$$

$$J_7 = \oint \frac{1}{t}\left(\int_0^s R\, t\, ds\right) ds$$

$$J_s = \oint \frac{1}{t}\left(\int_0^s I\,t\,ds\right) ds$$

For a closed cross section, a shear flow constant is calculated by formula (ae) and it is inserted into formula (ac) to establish shear flow, and then shearing stress at arbitrary point of the section is calculated by formula (ad). Appendix 3. 2－5 shows an calculated example of shear flow constant and shear flow on a rectangular section. Calculation formula is very complicated even in case of simple sectional shape like this and numerical integral by a computer on a line elements model is necessary for a practical purpose.

Let a open cross section be described next. Suppose a starting point of integration on the section is at an end of sectional members then shear flow of the point equals 0 since shearing stress in the s direction at the point has to be 0. Accordingly q_{w0} in the formula (ab) which gives shearing stress disappears and the formula is rewritten as follows.

$$\tau_w = -\frac{E}{t}\int_0^s \Psi\,t\,ds\,\frac{d^3\Theta}{dz^3} \qquad \cdots\cdots(af)$$

A term including a_i of formula (ac) which gives shear flow disappears in addition to q_{w0} and the formula is rewritten as follows.

$$q_w = \Psi_0 \int_0^s t\,ds - \int_0^s t\,R\,ds \qquad \cdots\cdots(ag)$$

where Ψ_0 is given by formula (s) and R corresponds to definition at formula (m).

There is no change in the procedure that shearing stress is calculated by formula (ad) including shear flow. Shear flow of I section is given by formula (ag) as a

parabolic formula as shown following where l_f is flange width, l_w is web height, A_f is flange area and ν is non dimensional figure between 0 and 1 which corresponds to a point on flange.

$$q_w = l_f l_w A_f (\nu - \nu^2) \div 4$$

In case that all sectional members run toward the shearing center such as an equal angle steel which was described at preceding clause (2) for Cbd, a variation of Ψ along the thickness had to be considered to get Cbd, and as the shear flow in this case also becomes approximately 0, Calculation method of shearing stress has to be so expanded that a variation of Ψ along the shell thickness may be considered. According to Cbd case, let $\Psi = \Psi + \Psi_n$ and $\tau_{wt} = \tau_w + \tau_{wn}$ be set where τ_{wn} is shearing stress corresponding to Ψ_n. Ψ in the formula (aa) is replaced by $\Psi + \Psi_n$ to get following formula (ah).

$$\sigma_z = E(\Psi + \Psi_n) \frac{d^2\Theta}{dz^2} \qquad \cdots\cdots (ah)$$

Although shearing stress can be obtained by a equilibrium of shearing stress and vertical stress, the equation of equilibrium is supposed to have following expression since warping function varies along shell thickness.

$$\int_{-2/t}^{+t/2} \frac{\partial(\tau_{wt})}{\partial s} dn = -\int_{-2/t}^{+t/2} -\frac{\partial(\sigma_z)}{\partial z} dn$$

Formula (ah) and $\tau_{wt} = \tau_w + \tau_{wn}$ are inserted into above formula and its both hand sides are integrated along the s axis to get following formula. A constant of the integration is naturally 0.

$$\tau_w t + \int_0^{s} \int_{-2/t}^{+t/2} \frac{\partial(\tau_{wn})}{\partial s} \, dn \, ds = -E \int_0^{s} \Psi t \, ds \, \frac{d^3\Theta}{dz^3} - E \int_0^{s} \int_{-2/t}^{+t/2} \Psi_n dn \, ds \, \frac{d^3\Theta}{dz^3}$$

The first terms of both hand sides of above formula are deleted since they are equal according to formula (af) and it is transformed to get following formula.

$$\int_0^{s} \int_{-2/t}^{+t/2} \left(\frac{\partial(\tau_{wn})}{\partial s} + E\Psi_n \frac{d^3\Theta}{dz^3} \right) dn \, ds = 0$$

The inside of double integration has to be 0 owing to that above formula is true for any value of s since t is a function of s. In short,

$$\frac{\partial(\tau_{wn})}{\partial s} + E\Psi_n \frac{d^3\Theta}{dz^3} = 0$$

This relation is integrated along the s axis and following formula by which τ_{wn} can be calculated is obtained.

$$\tau_{wn} = -E \int_0^{s} \Psi_n ds \, \frac{d^3\Theta}{dz^3} \qquad \cdots\cdots (ai)$$

Integration constant of τ_{wn} equals 0 because of the same reason as the shear flow. The τ_{wt} is obtained by adding the τ_{wn} to τ_w which is calculated by formula (af).

A result of the application on equal angle steel shown on Fig. 3. 1－105 is presented next. The τ_w in this cas is 0. The stress distribution is parabolic where l is a distance from the flange tip to the shearing center, t is flange thickness, ν is non dimensional figure between 0 and 1 which corresponds to a

point on the flange, its origin is a starting point of each interval and ± corresponds to outside and inside of the angle respectively .

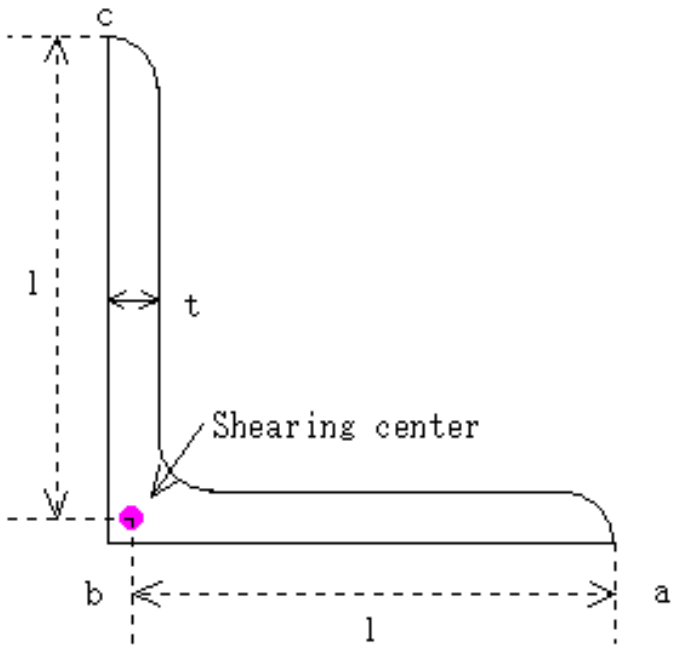

Fig. 3. 1－105

a ～ b $\quad \tau_{wn} = \pm \dfrac{E t l^2}{2} \left(\nu - \dfrac{\nu^2}{2} \right) \dfrac{d^3 \Theta}{d z^3}$

b ～ c $\quad \tau_{wn} = \pm \dfrac{E t l^2}{4} (1 - \nu^2) \dfrac{d^3 \Theta}{d z^3}$

3－2）Stress distribution of simple torsion

Only results are shown since calculation method of shearing stress due to simple torsion is well known. T_s is simple torsion moment and equals a difference between internal torsion moment and bending- torsion moment.

For a closed cross section,

$$\tau_s = \frac{1}{2A_s t} T_s = \frac{q_s}{t} \cdot \frac{T_s}{J_t} = \frac{q_s}{t} G \frac{d\Theta}{dz} \qquad \cdots\cdots(aj)$$

where $I_0 = \oint \frac{ds}{t}$

$$q_s = \frac{2A_s}{I_0} = \text{shear flow corresponding to simple torsion}$$

For an open cross section,

$$\tau_s = \frac{t}{J_t} T_s = \frac{t}{J_t} G J_t \frac{d\Theta}{dz} = G t \frac{d\Theta}{dz} \quad \text{where} \quad J_t = \int_0^u \frac{t^3}{3} ds \cdots\cdots(ak)$$

In the right hand side of above formula, T_s was replaced by GJ_t multiplied by a twisting intensity $\frac{d\Theta}{dz}$ which is calculated from solution of formula (e); i. e. equation of equilibrium for bending- torsion. Result which corresponds to moment of widely used sectional shapes is formulated in many design handbooks. Table 3. 1－103 shows its examples.

	Sectional shape	Calculation formula
Closed cross section	Constant t. hollow pipe 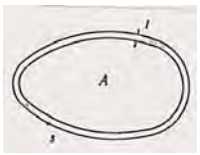	$\tau_s = \dfrac{T_s}{2A_s t}$
	Tetragon hollow pipe 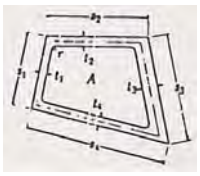	$\tau_{s1} = \dfrac{T_s}{2A_s t_1}$、$\tau_{s2} = \dfrac{T_s}{2A_s t_2}$ ……
Open cross section	Angle 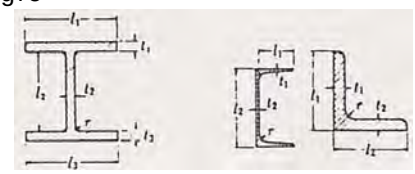	$\tau_{s1} = \dfrac{3T_s t_1}{\sum t_n^3 l_n}$、$\tau_{s2} = \dfrac{3T_s t_2}{\sum t_n^3 l_n}$ ……
	Split circular pipe 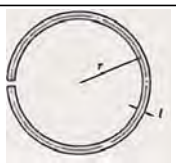	$\tau_{smax} = \dfrac{3T_s}{2\pi r t}$

Table 3．1－103 Torsion shearing stress formulae of thin shell section[*1]

[*1] For instance page 102 and 103 of bibliography (35)。

（４） Characteristics of stress distribution

Fig. ３. １－１０６ shows characteristics of shearing stress distribution on various sectional shapes. This is an assumed characteristics for stress formulation

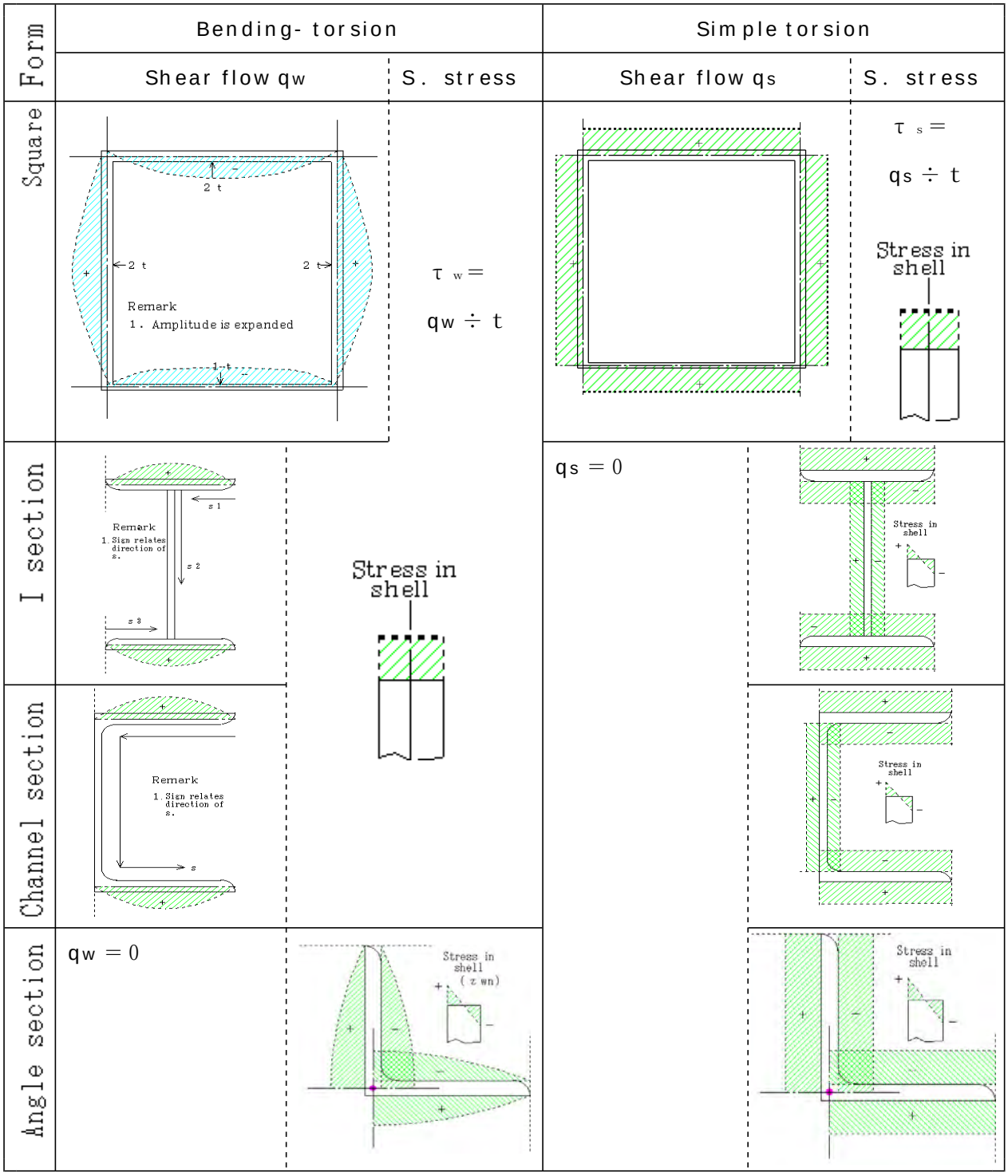

Fig. ３. １－１０６

and actual detail of them is supposed to be just a bit different. τ_{wn} due to bending-torsion on square, I and channel sections are abbreviated because of their quantities although they are supposed to exist. In case of a square section of simple torsion, stress component which varies on a shell thickness section is supposed to exist but they can be neglected in general. Shearing stress distribution due to bending-torsion and that of bending are completely different. Fig. 3.1－107 shows distribution pattern of shearing stress due to bending where Q indicates a loading direction, G is a gravity center and S is a shearing center.

Rectangular	I section	Channel	Angle
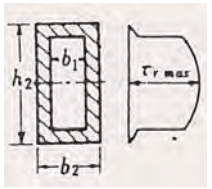	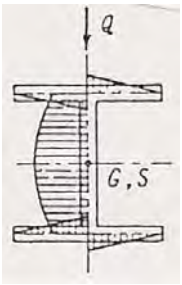	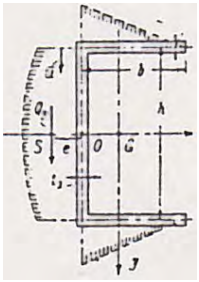	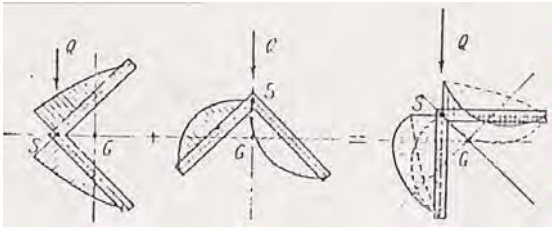

Fig. 3.1－107[*1]

[*1] For instance page 66 of bibliography (35) and page 45 and 46 of bibliography (38)。

Appendix 3．1－3　Stress distribution of thin shell section subject to bending

Formulae to calculate stress distribution and a shearing center of a thin shell closed cross section beam are presented[*1]

(1)　Shearing stress distribution

The x and y axes are set coinciding with principal axes of a beam cross section such as shown on Fig.3．1－103．Normal bending stress σ_b and sectional moment of inertia are given by following formulae where m_x and m_y are bending moment around the x axis and the y axis respectively and I_x and I_y are sectional moment of inertia around the x axis and the y axis respectively．

$$\sigma_b = \frac{m_y}{I_y} x + \frac{m_x}{I_x} y = \sigma_{bx} + \sigma_{by} \qquad \cdots\cdots(ba)$$

$$\left.\begin{aligned} I_y &= \oint x^2 t \, ds \\ I_x &= \oint y^2 t \, ds \end{aligned}\right\} \qquad \cdots\cdots(bb)$$

Let τ_b denote shearing stress which is in equilibrium with $\sigma_b t$, then relation between the two stress is expressed by following formula since the relation equals relation between σ_z and τ_w shown of Fig．3．1－104．

$$\frac{\partial(\tau_b t)}{\partial s} = -\frac{\partial(\sigma_b t)}{\partial z} \qquad \cdots\cdots(bc)$$

In above formula，t is thickness of the balanced small portion，z is a axis set normal to the section and s is a girth axis along the shell thickness center line of

[*1] Detail of derivation is，for instance，shown on page 201 201 of bibliography (17)。

the section defined on Fig. 3. 1－103. Let Q_x and Q_y denote shearing force in the x and y directions on the section, then the relation between shearing force and bending moment is expressed as follows.

$$\left.\begin{aligned} Q_x &= \frac{dm_y}{dz} \\ Q_y &= \frac{dm_x}{dz} \end{aligned}\right\} \qquad \cdots\cdots(bd)$$

Formula (ba) is separated into σ_{bx} which is a bending stress due to load in the x direction and σ_{by} which is a bending stress due to load in the y direction and they are inserted into formula (bc) to get formulae relating to shearing stress τ_{bx} and τ_{by} which correspond to each bending stress. The bending moments in the formulae are eliminated by using formulae (bd) and the integration along the s axis is made on them to get following two formulae which give shearing stress distribution.

$$\left.\begin{aligned} \tau_{bx}t &= -\frac{Q_x}{I_y}\left(\int_0^s x\,t\,ds + c_x\right) = -\frac{Q_x}{I_y}\left(M_y + c_x\right) \\ \tau_{by}t &= -\frac{Q_y}{I_x}\left(\int_0^s y\,t\,ds + c_y\right) = -\frac{Q_y}{I_x}\left(M_x + c_y\right) \end{aligned}\right\} \qquad \cdots\cdots(be)$$

In above formulae, definition of M_x and M_y is same as that of formula (o) in Appendix 3. 1－2 and the inside of ( ) is shear flow of bending and c_x and c_y in the ( ) are integration constants which are intensity of the shear flow at a starting point of integration. Let q_{bx} and q_{by} denote the shear flow corresponding to Q_x and Q_y respectively to express a formula for shearing stress as follows where ξ and η are displacement in the x and y directions of whole section, in short, deflection of the beam.

$$\left.\begin{aligned}\tau_{bx} &= -\frac{Q_x}{I_y}\cdot\frac{q_{bx}}{t} = -E\frac{q_{bx}}{t}\cdot\frac{d^3\xi}{dz^3}\\ \tau_{by} &= -\frac{Q_y}{I_x}\cdot\frac{q_{by}}{t} = -E\frac{q_{by}}{t}\cdot\frac{d^3\eta}{dz^3}\end{aligned}\right\} \quad \cdots\cdots(bf)$$

where $q_{bx} = M_y + c_x$ (shear flow of bending due to a load in the x direction)

$q_{by} = M_x + c_y$ (shear flow of bending due to a load in the y direction)

Condition to determin c_x and c_y can is derived according to the condition set to derive formula (ae) of Appendix 3. 1－2. In short, the relation between τ_w and γ_{sz} is set in relation between shearing stress τ_b and shearing strain γ_b and following two formulae for the condition are obtained.

$$\left.\begin{aligned}\oint \tau_{bx} ds &= 0\\ \oint \tau_{by} ds &= 0\end{aligned}\right\} \quad \cdots\cdots(bg)$$

Formula (be) is inserted into above formulae and they are solved for c_x and c_y, then following formulae are obtained. J_9, J_{10} and I_0 are same definition as that of formula (o) of Appendix 3. 1－2.

$$\left.\begin{aligned}c_x &= -\oint \frac{1}{t}\left(\int_0^s x\,t\,ds\right) ds \div \oint \frac{1}{t} ds = -J_9 \div I_0\\ c_y &= -\oint \frac{1}{t}\left(\int_0^s y\,t\,ds\right) ds \div \oint \frac{1}{t} ds = -J_{10} \div I_0\end{aligned}\right\} \quad \cdots\cdots(bh)$$

(2) Shearing center

A working point of resultant force of shearing stress given by formula (be) is not the origin (sectional gravity center) in general. This is a shearing center. Let moments around the origin of shearing stress and its resultant force be equilibrium to get coordinates of shearing center, x_s and y_s, and following formulae are

obtained where r_0 is a distance between the origin and tangent to an integrating point.

$$\left.\begin{aligned} \oint \tau_{bx} t \cdot r_0 ds &= Q_x \cdot y_s \\ \oint \tau_{by} t \cdot r_0 ds &= -Q_y \cdot x_s \end{aligned}\right\} \quad \cdots\cdots(bi)$$

Formula (be) is inserted into these formulae and integration is made on them to get following formulae by which shearing center can be calculated. J_{11}, J_{12} and A_s are same definition as that of formula (o) of Appendix 3. 1－2. The x and y axes adopted in this clause coincide with principal axis of beam cross section so that moment of inertia and product of inertia of the section equal 0. In above description subject matter is a closed cross section and a open cross section corresponds to the closed case except that $c_x = c_y = 0$ and $\oint$ in the formulae are replaced by $\int_0^u$ and starting point of the integration has to be at an end of the open section. Other end is supposed to be u.

$$\left.\begin{aligned} y_s &= \oint r_0 \left(\int_0^s x t ds + c_x\right) ds \div I_y = (J_{11} + 2A_s c_x) \div I_y \\ x_s &= -\oint r_0 \left(\int_0^s y t ds + c_y\right) ds \div I_x = -(J_{12} + 2A_s c_y) \div I_x \end{aligned}\right\} \quad \cdots\cdots(bj)$$

Appendix 3．1－4 Example 1 of bending- torsion section calculation

A result of formulae calculation on section modulus Cbd and shear flow of bending- torsion for a fish belly flap section shown on 3．1－108 is presented. The ti and to denotes shell thickness of the upstream side and the downstream side respectively and another marks are shown on the figure. Marks other than defined here are same definition as these of the based formulae. The x axis is vertical and passes through the intersection points of the upstream and downstream shells and the y axis coincides with a principal axis of the section.

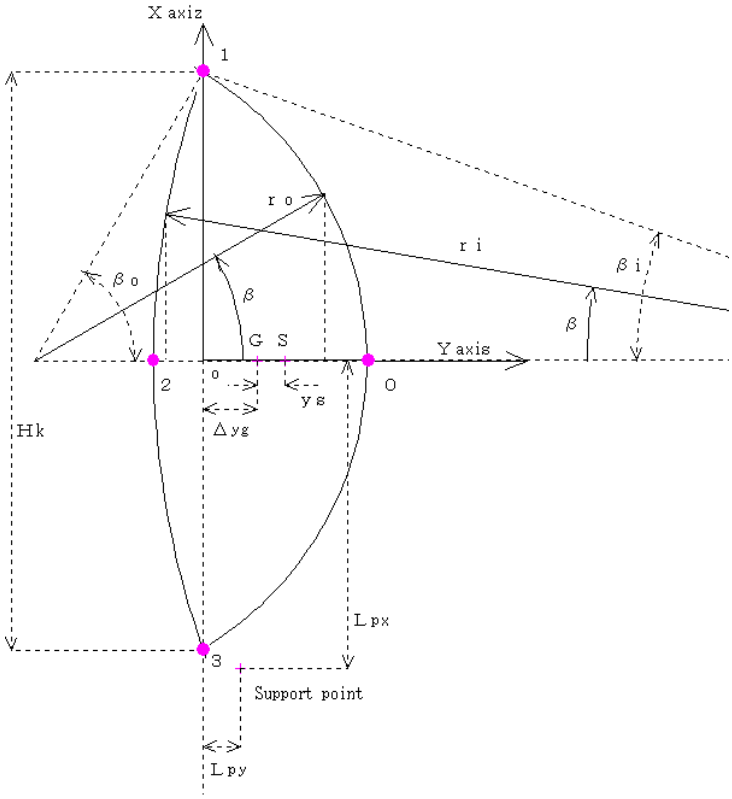

Fig．3．1－108

(1) Section modulus C_{bd}

This is a result of formulae calculation for section modulus Cbd of bending- torsion based on formula(m)、(n) and (o) in Appendix 3．1－2.

[Result of calculation]

Member area $\rightarrow J_0 = 2(r_i \beta_i t_i + r_o \beta_o t_o)$

Section area $\rightarrow A_s = \beta_i r_i^2 + \beta_o r_o^2 - (r_i^2 \sin(2\beta_i) + r_o^2 \sin(2\beta_o)) \div 2$

Gravity center $\rightarrow \triangle x = 0$

$\rightarrow \triangle y = M_{ox} \div A_s$

where $M_{ox} = 2 t_o r_o^2 f_2(\beta_o) - 2 t_i r_i^2 f_2(\beta_i)$, and

$f_2(\beta) = \sin(\beta) - \cos(\beta) \cdot \beta$

Shearing center

$$I_0 = 2(r_i\beta_i \div t_i + r_o\beta_o \div t_o)$$

$$J_9 = -2r_o^3 f_2(\beta_o) + 2r_i^3 f_2(\beta_i)$$

$$c_x = -J_9 \div I_0$$

$$I_y = 2t_o r_o^3 f_1(\beta_o) + 2t_i r_i^3 f_1(\beta_i)$$

$$f_1(\beta) = \beta/2 - \sin(2\beta)/4$$

$$J_{11} = 2t_o r_o^4 \{-f_1(\beta_o) - (\cos(\beta_o) + k_o)(\sin(2\beta_o)/4 - \beta_o/2)\}$$
$$-2t_i r_i^4 \{-f_1(\beta_i) - (\cos(\beta_i) + k_i)(\sin(2\beta_i)/4 - \beta_i/2)\}$$

$$\rightarrow y_s = -(J_{11} + 2A_s c_x) \div I_y$$

$$J_{10} = 2r_o^3 \beta_o f_8(\beta_o, k_o) + 4r_o^2 r_i \beta_i t_o/t_i f_8(\beta_o, k_o)$$
$$-2r_i^3 \beta_i f_8(\beta_i, k_i)$$

$$f_8(\beta, k) = \sin(\beta) - (\cos(\beta) + k)\beta$$

$$k_o = \Delta y \div r_o$$

$$k_i = \Delta y \div r_i$$

$$c_y = -J_{10} \div I_0$$

$$I_x = 2t_o r_o \{r_o^2 f_3(\beta_o) - 2r_o \Delta y f_2(\beta_o) + \Delta y^2 \beta_o\}$$
$$+2t_i r_i \{r_i^2 f_3(\beta_i) + 2r_o \Delta y f_2(\beta_i) + \Delta y^2 \beta_i\}$$

$$f_3(\beta) = \beta/2 + \beta\cos(2\beta) - 3\sin(2\beta)/4$$

$$\rightarrow x_s = 0$$

Integral constant of warping function

$$a_i = A_s \div I_0$$

$$\triangle x_s = \triangle x + x_s$$

$$\triangle y_s = \triangle y + y_s$$

$$J_1 = 2r_o^3 t_o \beta_o f_7(\beta_o, h_o) + 4r_o^2 r_i t_i \beta_i f_7(\beta_o, h_o)$$
$$+2r_i^3 t_i \beta_i f_7(\beta_i, h_i)$$

$$f_7(\beta, h) = \beta - \sin(\beta)(\cos(\beta) + h)$$

$$h_o = \triangle y_s \div r_o$$

$$h_i = \triangle y_s \div r_i$$

$$J_2 = 2\beta_o^2 r_o^2 + 4\beta_o \beta_i r_o r_i t_i/t_o + 2\beta_i^2 r_i^2$$

$$\rightarrow \Psi_0 = (J_1 - 2a_i J_2) \div J_0$$

Section modulus of bending- torsion

$$J_3 = 2r_o^5 t_o \beta_o f_7^2(\beta_o, h_o)$$
$$+ 2r_i^5 t_i \beta_i f_7^2(\beta_i, h_i)$$
$$+ 8r_o^2 r_i t_i \beta_i f_7(\beta_o, h_o)\{r_o^2 f_7(\beta_o, h_o) + r_i^2 f_7(\beta_i, h_i)\}$$
$$+ r_o^5 t_o \{2\beta_o^3/3 + 4[\cos(\beta_o) + h_o][\cos(\beta_o)\beta_o - \sin(\beta_o)]$$
$$+ [\beta_o - \sin(2\beta_o)/2][\cos(\beta_o) + h_o]^2\}$$
$$+ r_i^5 t_i \{2\beta_i^3/3 + 4[\cos(\beta_i) - h_i][\cos(\beta_i)\beta_i - \sin(\beta_i)]$$
$$+ [\beta_i - \sin(2\beta_i)/2][\cos(\beta_i) - h_i]^2\}$$
$$J_4 = 2r_o^4 \beta_o^2 f_7(\beta_o, h_o) + 2r_i^4 \beta_i^2 f_7(\beta_i, h_i)$$
$$+ 4r_o r_i \beta_i \{2r_o^2 \beta_o f_7(\beta_o, h_o) t_i/t_o + r_o r_i \beta_i f_7(\beta_o, h_o)$$
$$+ r_i^2 \beta_o f_7(\beta_i, h_i) t_i/t_o\}$$
$$+ r_o^4 \{2\beta_o^3/3 + 2[\cos(\beta_o)\beta_o - \sin(\beta_o)][\cos(\beta_o) + h_o]\}$$
$$+ r_i^4 \{2\beta_i^3/3 + 2[\cos(\beta_i)\beta_i - \sin(\beta_i)][\cos(\beta_i) - h_i]\}$$
$$J_5 = 8\beta_o^3 r_o^3/(3t_o) + 8\beta_i^3 r_i^3/(3t_i)$$
$$+ 8\beta_o \beta_i r_o r_i/t_o(\beta_i r_i + r_o \beta_o t_i/t_o)$$
$$\rightarrow C_{bd} = \Psi_0^2 J_0 - 2\Psi_0 J_1 + 4\Psi_0 a_i J_2 + J_3 - 4a_i J_4 + 4a_i^2 J_5$$

（2） Shear flow

This is a result of formulae calculation for shear flow constant and shear flow of bending- torsion based on formula(ac)、(ad) and (ae) in Appendix 3．1－2．

［Result of calculation］

Shear flow constant

$$J_6 = 2\beta_o^2 r_o^2 + 2\beta_i^2 r_i^2 + 4\beta_o \beta_i r_o r_i t_o/t_i$$
$$J_7 = -2(\beta_o^3 r_o^4 + \beta_i^3 r_i^4)/3 + 2[r_o^4 \beta_o^2 f_7(\beta_o, h_o)$$
$$+ r_i^4 \beta_i^2 f_7(\beta_i, h_i)$$
$$+ 4r_o^2 r_i \beta_i f_7(\beta_o, h_o)/t_i(r_i \beta_i t_i + r_o \beta_o t_o)$$
$$+ 2\{r_o^4[\cos(\beta_o) + h_o][\sin(\beta_o) - \cos(\beta_o)\beta_o]$$
$$+ r_i^4[\cos(\beta_i) - h_i][\sin(\beta_i) - \cos(\beta_i)\beta_i]\}$$

$$J_8 = 4[\beta_o^3 r_o^3 / t_o + \beta_i^3 r_i^3 / t_i]$$

$$+ 4\beta_o\beta_i r_o r_i / (t_o t_i)(r_i\beta_i t_i + r_o\beta_o t_o)$$

$$\rightarrow q_{w0} = -(\Psi_0 J_6 - J_7 + 2a_i J_8) \div I_0$$

Fig. 3. 1－109 is calculated examples of shear flow of bending, shear flow of bending-torsion and warping function and shows their distribution patterns. Marks are those shown on Fig. 3. 1－108. Each curve shows a calculated result multiplied by the figure shown on the figure. The shear flow of bending, the shear flow bending-torsion and the warping function were calculated by formula (f), (ac) and (l) of Appendix 3. 1－3 respectively.

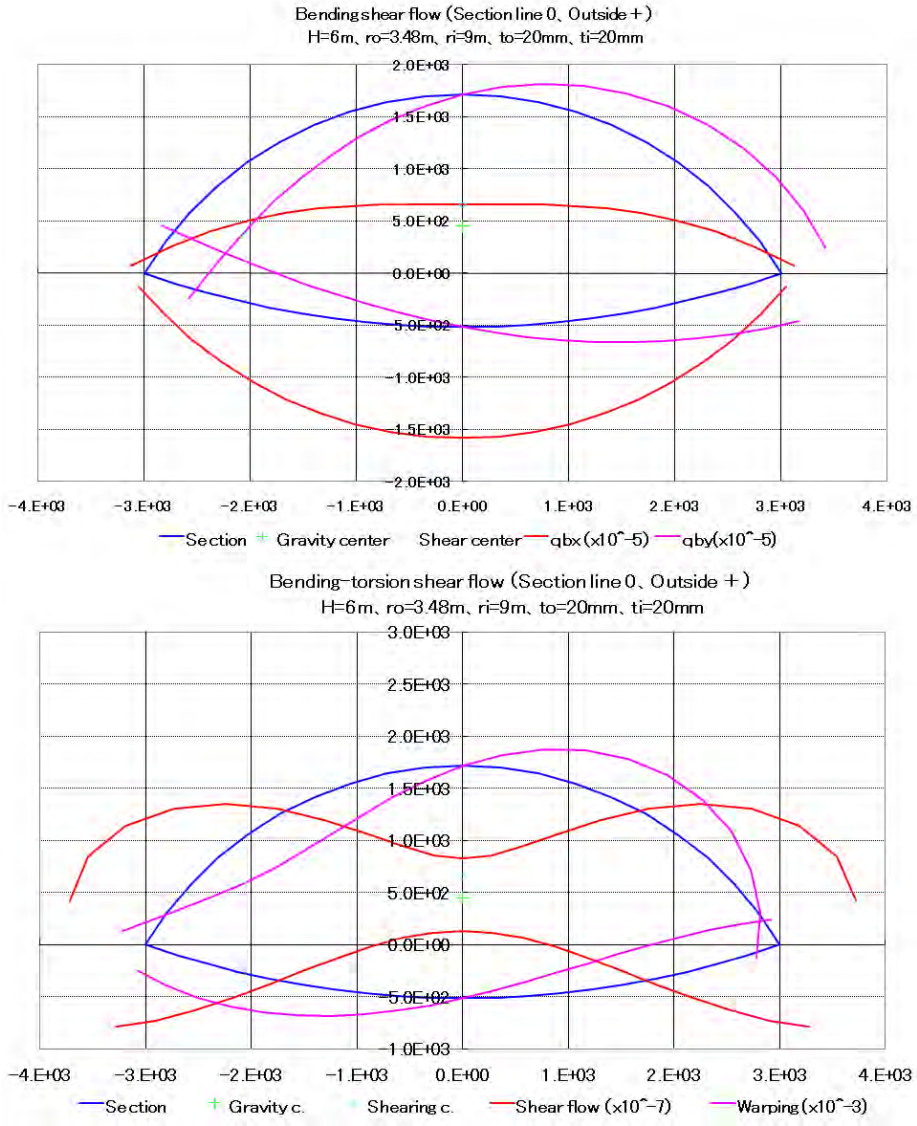

Fig. 3. 1－109

Appendix 3．1－5 Example 2 of bending- torsion section calculation

A result of formulae calculation on section modulus Cbd and shear flow of bending- torsion for a rectangular section shown on 3．1－110 is presented. 2×lw and 2×lf denote height and width of the section respectively and tf1, tw1, tf2 and tw2 are shell thickness as shown on the figure. The x and y axes coincide with principal axes of the section and △x and △y denote x and y components of distance between the centroid and the gravity center of the section. Marks other than defined here are same definition as these of based formulae.

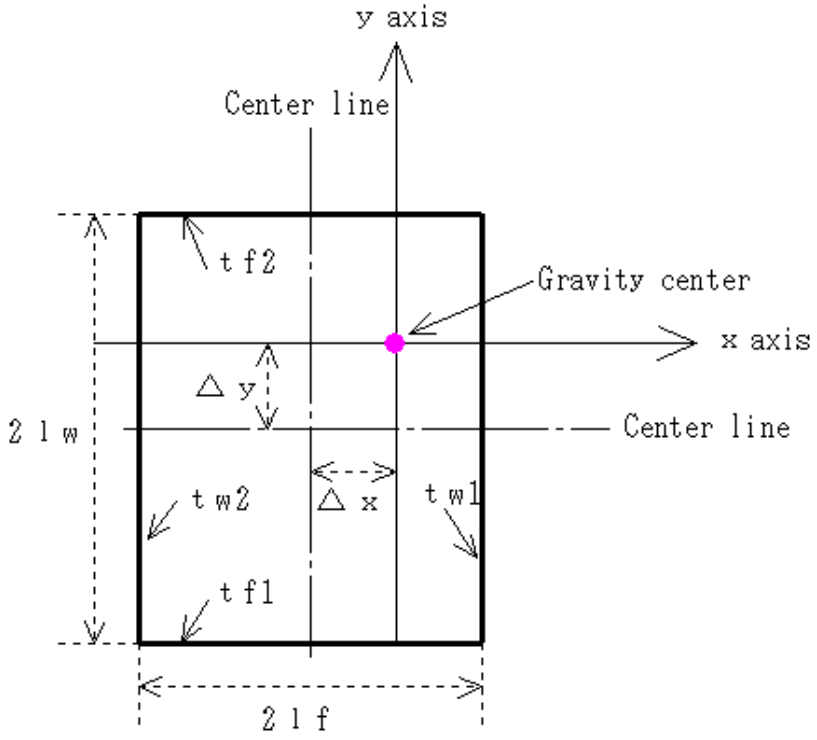

Fig．3．1－110

(1) Section modulus Cbd

This is a result of formulae calculation for section modulus Cbd of bending- torsion based on formula(m)、(n) and (o) in Appendix 3．1－2.

［Result of calculation］

Member area $\rightarrow J_0 = 2l_f(t_{f1}+t_{f2}) + 2l_w(t_{w1}+t_{w2})$

Sectional area $\rightarrow A_s = 4l_w l_f$

Gravity center $\rightarrow \triangle x = A_s(t_{w1}-t_{w2}) \div (2J_0)$

$\rightarrow \triangle y = A_s(t_{f2}-t_{f1}) \div (2J_0)$

Shearing center

$$I_0 = 2l_f(1\div t_{f1}+1\div t_{f2}) + 2l_w(1\div t_{w1}+1\div t_{w2})$$

$$J_9 = \oint \frac{1}{t}\left(\int_0^s x\,t\,ds\right) ds =$$

$$4\frac{t_{w1}}{t_{f2}} l_f^2 l_w + 4\frac{t_{w1}}{t_{w2}} l_f l_w^2 - \triangle x\left\{\left(4+4\frac{t_{f1}}{t_{f2}}\right) l_f^2 + \left(4\frac{t_{f1}}{t_{w1}} + 4\frac{t_{w1}}{t_{f2}} + 4\frac{t_{f1}}{t_{w2}} + 4\frac{t_{f2}}{t_{w2}}\right) l_f l_w + \left(4+4\frac{t_{w1}}{t_{w2}}\right) l_w^2\right\}$$

$$c_x = -J_9 \div I_0$$

$$I_y = (t_{f1}+t_{f2})(l_f^2\div 3+\triangle x^2)2l_f + t_{w1}(l_f-\triangle x)^2 2l_w + t_{w2}(l_f+\triangle x)^2 2l_w$$

$$J_{11} = \oint r_0\left(\int_0^s x\,t\,ds\right) ds = \sum_{i=1,\,j=1}^{i=4,\,j=4} A_i B_j C_{ij}$$

where A is an element of the first row, B is an element of the first column and C is other element of below table. The i is row number and j is column number.

$A_i\downarrow$ $B_j\rightarrow$	$l_w t_{w2}$	$l_f t_{f2}$	$l_w t_{w1}$	$l_f t_{f1}$
$(l_w+\triangle y)2l_f$				$-(l_f\div 3+\triangle x)$
$(l_f-\triangle x)2l_w$			$(l_f-\triangle x)$	$-2\triangle x$
$(l_w-\triangle y)2l_f$		$l_f\div 3-\triangle x$	$2(l_f-\triangle x)$	$-2\triangle x$
$(l_f+\triangle x)2l_w$	$-(l_f+\triangle x)$	$-2\triangle x$	$2(l_f-\triangle x)$	$-2\triangle x$

$\rightarrow y_s = (J_{11}+2A_s c_x)\div I_y$

$$J_{10} = \oint \frac{1}{t} \left(\int_0^s y\, t\, ds \right) ds = -4 \frac{t_{f1}}{t_{f2}} l_f^2 l_w$$

$$- \left(4 \frac{t_{f1}}{t_{w2}} + 4 \frac{t_{f1}}{t_{w1}} - 4 \frac{t_{f2}}{t_{w2}} \right) l_f l_w^2 - \triangle y \left\{ \left(4 + 4 \frac{t_{f1}}{t_{f2}} \right) l_f^2 \right.$$

$$\left. + \left(4 \frac{t_{f1}}{t_{w1}} + 4 \frac{t_{w1}}{t_{f2}} + 4 \frac{t_{f1}}{t_{w2}} + 4 \frac{t_{f2}}{t_{w2}} \right) l_f l_w + \left(4 + 4 \frac{t_{w1}}{t_{w2}} \right) l_w^2 \right\}$$

$$c_y = -J_{10} \div I_0$$

$$I_x = (t_{w1} + t_{w2}) \left(l_w^2 \div 3 + \triangle y^2 \right) 2 l_w + t_{f1} (l_w - \triangle y)^2 2 l_f$$

$$+ t_{f2} (l_w + \triangle y)^2 2 l_f$$

$$J_{12} = \oint r_0 \left(\int_0^s x\, t\, ds \right) ds = \sum_{i=1,\, j=1}^{i=4,\, j=4} A_i B_j C_{ij}$$

where A is an element of the first row, B is an element of the first column and C is other element of below table. The i is row number and j is column number.

$A_i \downarrow$ $B_j \rightarrow$	$l_w t_{w2}$	$l_f t_{f2}$	$l_w t_{w1}$	$l_f t_{f1}$
$(l_w + \triangle y) 2 l_f$				$-(l_w + \triangle y)$
$(l_f - \triangle x) 2 l_w$			$-(l_w \div 3 + \triangle y)$	$-2(l_w + \triangle y)$
$(l_w - \triangle y) 2 l_f$		$(l_w - \triangle y)$	$-2 \triangle y$	$-2(l_w + \triangle y)$
$(l_f + \triangle x) 2 l_w$	$l_w \div 3 - \triangle y$	$2(l_w - \triangle y)$	$-2 \triangle y$	$-2(l_w + \triangle y)$

$$\rightarrow x_s = -(J_{12} + 2 A_s c_y) \div I_x$$

Integral constant of warping function

$$a_i = A_s \div I_0$$

$$\triangle x_s = \triangle x + x_s$$

$$\triangle y_s = \triangle y + y_s$$

$$J_1 = (l_w + \triangle y_s) 2 l_f (l_f t_{f1} + 2 l_w t_{w1} + 2 l_f t_{f2} + 2 l_w t_{w2})$$

$$+ (l_f - \triangle x_s)\, 2 l_w (l_w t_{w1} + 2 l_f t_{f2} + 2 l_w t_{w2})$$

$$+ (l_w - \triangle y_s)\, 2 l_f (l_f t_{f2} + 2 l_w t_{w2})$$

$$+ (l_f + \triangle x_s)\, 2 l_w (l_w t_{w2})$$

$$J_2 = 2 l_f t_{f1} (l_f \div t_{f1})$$

$$+ 2 l_w t_{w1} (2 l_f \div t_{f1} + l_w \div t_{w1})$$

$$+ 2 l_f t_{f2} (2 l_f \div t_{f1} + 2 l_w \div t_{w1} + l_f \div t_{f2})$$

$$+ 2 l_w t_{w2} (2 l_f \div t_{f1} + 2 l_w \div t_{w1} + 2 l_f \div t_{f2} + l_w \div t_{w2})$$

$$\rightarrow \Psi_0 = (J_1 - 2 a_i J_2) \div J_0$$

Section modulus of bending- torsion

$$J_3 = 8 \sum_{i=1,\, j=1}^{i=4,\, j=4} A_i B_j C_{ij}$$

where A is an element of the first row, B is an element of the first column and C is other element of below table. The i is row number and j is column number.

$A_i \downarrow$	$l_w + \triangle y_s$	$l_f - \triangle x_s$	$l_w - \triangle y_s$	$l_f + \triangle x_s$
$l_w + \triangle y_s$	$l_f^3 (t_{f1} \div 3 + t_{f2}) + l_f^2 l_w (t_{w1} + t_{w2})$	$l_f^2 l_w 2 t_{f2} + l_f l_w^2 \cdot (t_{w1} + 2 t_{w2})$	$l_f^3 t_{f2} + l_f^2 l_w 2 t_{w2}$	$l_f l_w^2 t_{w2}$
$l_f - \triangle x_s$		$l_f l_w^2 t_{f2} + l_w^3 \cdot (t_{w1} \div 3 + t_{w2})$	$l_f^2 l_w t_{f2} + l_f l_w^2 2 t_{w2}$	$l_w^3 t_{w2}$
$l_w - \triangle y_s$			$l_f^3 t_{f2} \div 3 + l_f^2 l_w t_{w2}$	$l_f l_w^2 t_{w2}$
$l_f + \triangle x_s$				$l_w^3 t_{w2} \div 3$

$$J_4 = 8 \sum_{i=1,\, j=1}^{i=4,\, j=4} A_i B_j C_{ij}$$

where A is an element of the first row, B is an element of the first column and C is other element of below table. The i is row number and j is column number.

$A_i \downarrow$	$1 \div t_{f1}$	$1 \div t_{w1}$	$1 \div t_{f2}$	$1 \div t_{w2}$
$l_w +$ $\triangle y_s$	$l_f^3 (t_{f1} \div 3 + t_{f2})$ $+$ $l_f^2 l_w (t_{w1} + t_{w2})$	$l_f^2 l_w t_{f2}$ $+ l_f l_w^2 \cdot$ $(t_{w1} \div 2 + t_{w2})$	$l_f^3 t_{f2} \div 2$ $+$ $l_f^2 l_w t_{w2}$	$l_f l_w^2 t_{w2}$ $\div 2$
$l_f -$ $\triangle x_s$	$l_f^2 l_w t_{f2}$ $+ l_f l_w^2 \cdot$ $(t_{w1} \div 2 + t_{w2})$	$l_f l_w^2 t_{f2}$ $+ l_w^3 \cdot$ $(t_{w1} \div 3 + t_{w2})$	$l_f^2 l_w t_{f2} \div 2$ $+$ $l_f l_w^2 t_{w2}$	$l_w^3 t_{w2} \div 2$
$l_w -$ $\triangle y_s$	$l_f^3 t_{f2} \div 2 +$ $l_f^2 l_w t_{w2}$	$l_f^2 l_w t_{f2} \div 2$ $+ l_f l_w^2 t_{w2}$	$l_f^3 t_{f2} \div 3 +$ $l_f^2 l_w t_{w2}$	$l_f l_w^2 t_{w2}$ $\div 2$
$l_f +$ $\triangle x_s$	$l_f l_w^2 t_{w2} \div 2$	$l_w^3 t_{w2} \div 2$	$l_f l_w^2 t_{w2} \div 2$	$l_w^3 t_{w2} \div 3$

$$J_5 = 8 \sum_{i=1,\ j=1}^{i=4,\ j=4} A_i B_j C_{ij}$$

where A is an element of the first row, B is an element of the first column and C is other element of below table. The i is row number and j is column number.

$A_i \downarrow$	$1 \div t_{f1}$	$1 \div t_{w1}$	$1 \div t_{f2}$	$1 \div t_{w2}$
$\frac{1}{t_{f1}}$	$l_f^3 (t_{f1} \div 3 + t_{f2})$ $+$ $l_f^2 l_w (t_{w1} + t_{w2})$	$l_f^2 l_w 2 t_{f2}$ $+ l_f l_w^2 \cdot$ $(t_{w1} + 2 t_{w2})$	$l_f^3 t_{f2}$ $+$ $l_f^2 l_w 2 t_{w2}$	$l_f l_w^2 t_{w2}$
$\frac{1}{t_{w1}}$		$l_f l_w^2 t_{f2}$ $+ l_w^3 \cdot$ $(t_{w1} \div 3 + t_{w2})$	$l_f^2 l_w t_{f2}$ $+$ $l_f l_w^2 2 t_{w2}$	$l_w^3 t_{w2}$
$\frac{1}{t_{f2}}$			$l_f^3 t_{f2} \div 3 +$ $l_f^2 l_w t_{w2}$	$l_f l_w^2 t_{w2}$
$\frac{1}{t_{w2}}$				$l_w^3 t_{w2} \div 3$

$$\rightarrow C_{bd} = \Psi_0^2 J_0 - 2\Psi_0 J_1 + 4\Psi_0 a_i J_2 + J_3 - 4 a_i J_4 + 4 a_i^2 J_5$$

Table 3. 1－104 shows formulae of section modulus in case of simplified conditions as shown on the table.

S. Condition		Formula							
Frm	thickness	$\triangle_x$	$\triangle_y$	c_x	c_y	x_s	y_s	Ψ_0	C_{bd}
$l_f = l$	$t_{f1} = t$ other 2t	0	$\frac{1}{l-7}$	$-8 \div 5 \times l^2 t$	$8 \div 7 \times l^2 t$	0	$\frac{256}{1050} l$	$-\frac{16}{75} l^2$	$0.185 \times l^5 t$
$l_w = l$	all 2t	0	0	$-2 \times l^2 t$	$2 \times l^2 t$	0	0	0	0

Fig 3. 1－104

（2） Shear flow

This is a result of formulae calculation for shear flow constant and shear flow of bending- torsion based on formula(ac)、(ad) and (ae) in Appendix 3．1－2．

［Result of calculation］

Shear flow constant

$$J_6 = \left(4+4\frac{t_{f1}}{t_{f2}}\right) l_f^2 + \left(4\frac{t_{f1}}{t_{w1}} + 4\frac{t_{w1}}{t_{f2}} + 4\frac{t_{f1}}{t_{w2}} + 4\frac{t_{f2}}{t_{w2}}\right) l_f l_w + \left(4+4\frac{t_{w1}}{t_{w2}}\right) l_w^2$$

$$J_7 = 4\sum_{i=1,\ j=1} A_i B_j C_{ij}$$

where A is an element of the first row, B is an element of the first column and C is other element of below table. The i is row number and j is column number.

$A_i \downarrow B_j \rightarrow$	l_f^3	$l_f^2 l_w$	$l_f l_w^2$	l_w^3
$l_w + \triangle y_s$	$\frac{4}{3} + \frac{t_{f1}}{t_{f2}}$	$\frac{t_{f1}}{t_{w1}} + 2\frac{t_{w1}}{t_{f2}} + 2\frac{t_{f2}}{t_{w2}} + \frac{t_{f1}}{t_{w2}}$	$2 + 2\frac{t_{w1}}{t_{w2}}$	
$l_f - \triangle x_s$		1	$\frac{t_{w1}}{t_{f2}} + 2\frac{t_{f2}}{t_{w2}}$	$\frac{4}{3} + \frac{t_{w1}}{t_{w2}}$
$l_w - \triangle y_s$	$\frac{1}{3}$	$\frac{t_{f2}}{t_{w2}}$	1	
$l_f + \triangle x_s$				$\frac{1}{3}$

$$J_8 = \frac{16}{3} l_f^3 \left(\frac{1}{t_{f1}} + \frac{1}{t_{f2}}\right) + 8 l_f^2 l_w \left(\frac{t_{w1}}{t_{f1} t_{f2}} + \frac{t_{f2}}{t_{f1} t_{w2}} + \frac{1}{t_{w1}} + \frac{1}{t_{w2}}\right)$$

$$+ 8 l_f l_w^2 \left(\frac{t_{w1}}{t_{f1} t_{w2}} + \frac{t_{f2}}{t_{w1} t_{w2}} + \frac{1}{t_{f1}} + \frac{1}{t_{f2}}\right) + \frac{16}{3} l_w^3 \left(\frac{1}{t_{w1}} + \frac{1}{t_{w2}}\right)$$

$$\rightarrow q_{w0} = -\left(\Psi_0 J_6 - J_7 + 2 a_i J_8\right) \div I_0$$

Shear flow

Table 3．1－105 shows formulae of shear flow in case of simplified condition as shown on the table. Fig. 3．1－111 shows the shear flow in condition ① of the table after its value was divided by $(24l^2t)$ to let it be dimensionless and be compressed in magnitude.

S. condition		Position	Formula	
Frm	Thickness		$\int_0^s \Psi t\,ds \quad (1 \leqq \nu \leqq 0)$	q_{w0} :summing
$l_f = l$ $l_w = l$	① $t_{f1} = t$ other 2t	t_{f1} side	$(-224\nu + 224\nu^2)\ l^3t \div 525$	$-0.021333\,l^3t$
		t_{w1} side	$(448\nu - 420\nu^2)\ l^3t \div 525$	
		t_{f2} side	$(28 - 392\nu + 392\nu^2)\ l^3t \div 525$	
		t_{w2} side	$(28 + 392\nu - 420\nu^2)\ l^3t \div 525$	
	② all 2t	All sides	0	0

Table 3．1－105

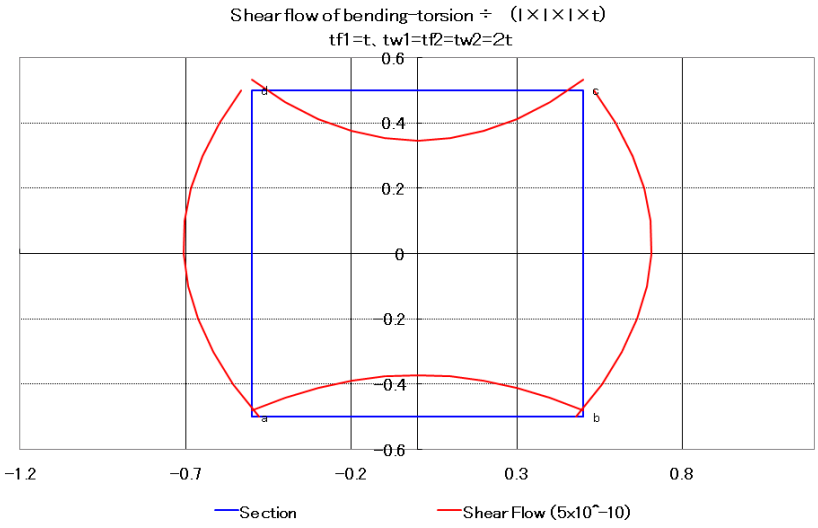

Fig．3．1－111

Appendix 3．1－6　Strength experiment of torsion type gate

Preceding to construct the first torsion type gate in Japan, a big scaled model experiment was carried out at the fabrication factory. Purpose of the experiment is to verify analysis method of structure, vibration and buckling strength and to confirm operation function of the gate. This appendix presents a brief explanation of it[*1].

（1）Measurement items

(1) Strain and displacement

(2) Natural frequency

(3) Operating load

(4) Shear buckling load

Principal items of tested gate		
Items	Prototype gate	Model gate
Scale ratio	2	1
Length （m）	68 （Two blocks）	34(1/2 fabricated)
Height （m）	2.000	1.000
D. head （m）	2.300	——
Max. tq.(t･m)	112.00	14.00
Skin p.t.(mm)	9.0	4.5
Weight （t）	30.000	2.500
Drive method	Shaft drive	Shaft drive

Table 3．1－106

（2）Experimental model

Table 3．1－106 shows the principal items of assumed prototype and experimental model. The model gate is 1.000m height and 17.000m long and Fig. 3．1－112 is a sketch of the model being installed on the concrete foundation blocks for a measurement of strain and deformation and its one end is supported by a drive shaft detail of which is shown on Fig．3．1－113．A beam fitted on other end of the model is used for loading of a buckling test. The gate bottom is supported by hinge brackets on the concrete blocks. Fig. 3．1－6 of the body text shows the inside of model gate body where web frames are arranged at a constant interval and the skin plate between the frames is stiffened by an angle against shear buckling.

[*1] Bibliography (3)。

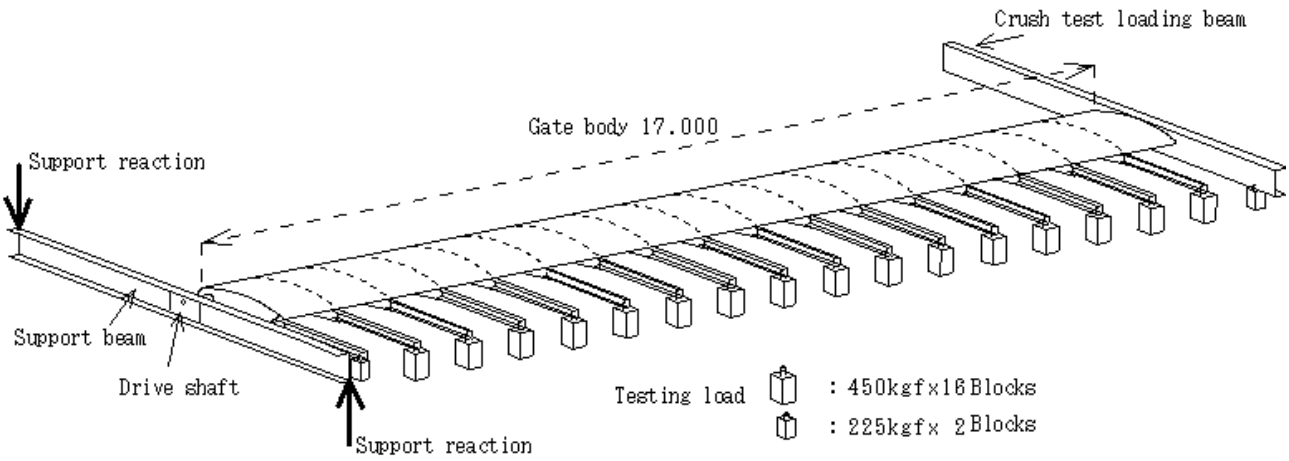

Fig. 3. 1－112

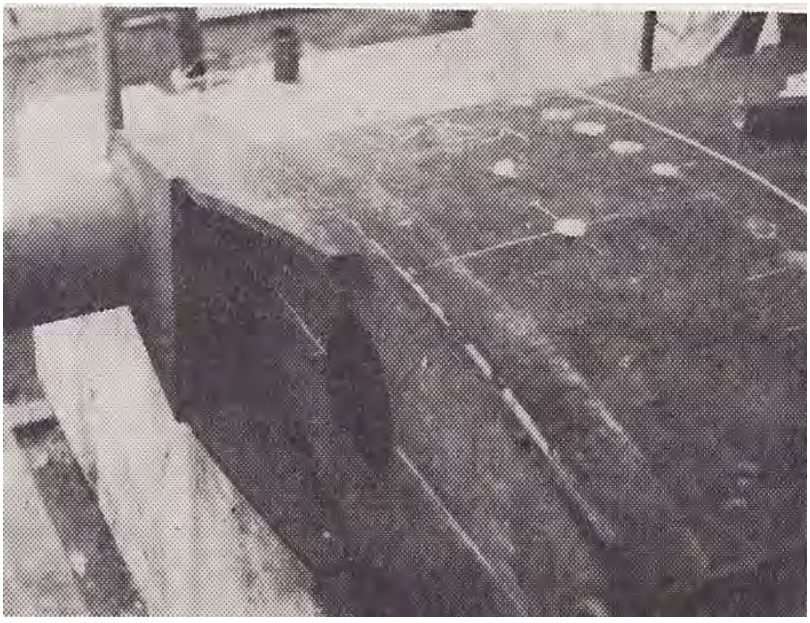

Fig. 3. 1－113

（3）Test method

(1) Measurement of strain and deformation

Fig. 3. 1－112 shows loading method by concrete block weights hanged on cantilever beams fitted on the model sections including hinge brackets. Ordinary loading and extreme loading conditions can be realized by adjusting weight hanging

position on the beam. The block weight distribution was chosen so that statically determinate torsion moment which is described at the item (2) of the body text clause 3.1.3.2 may be realized. Strain measurement was made by a wire resistance strain gauge and deformation was measured by reading a scale on the gate through a transit.

(2) Natural frequency measurement

After natural vibration was given to the gate body by an impact power application, a gate strain variation was recorded automatically.

(3) Operating load measurement

Suppose a torsion type flap gate is installed on long span main gate, the measurement of operation load on the flap gate and observation of the gate movement were made during the gate operations with the gate hinge removes which corresponds to the main gate deflection and with the hinges in a straight line. Gate operation was made in such a way that the gate end support beam was lifted up by a crane when the gate stood up and the gate moved down by its own weight when the gate laid down. The load measurement was made by a load cell provided to the crane suspension wire.

(4) Shear buckling load measurement

Load of buckling was applied by hydraulic oil cylinders provided to the beam of gate body non-drive end in addition to the ordinary concrete loading blocks and twist couple was increased in a step-by-step manner until buckling occurred on the gate body shell. The measurement was made by strain gages and oil pressure gages. The buckling portions were cut off and their patterns were identified by measurements.

(4) View of experiment

Fig. 3.1－114 and 115 show the views of experiment. The Fig. 114

is a full view of strain and deformation test and the Fig. 1 1 5 shows status at the maximum loading condition.

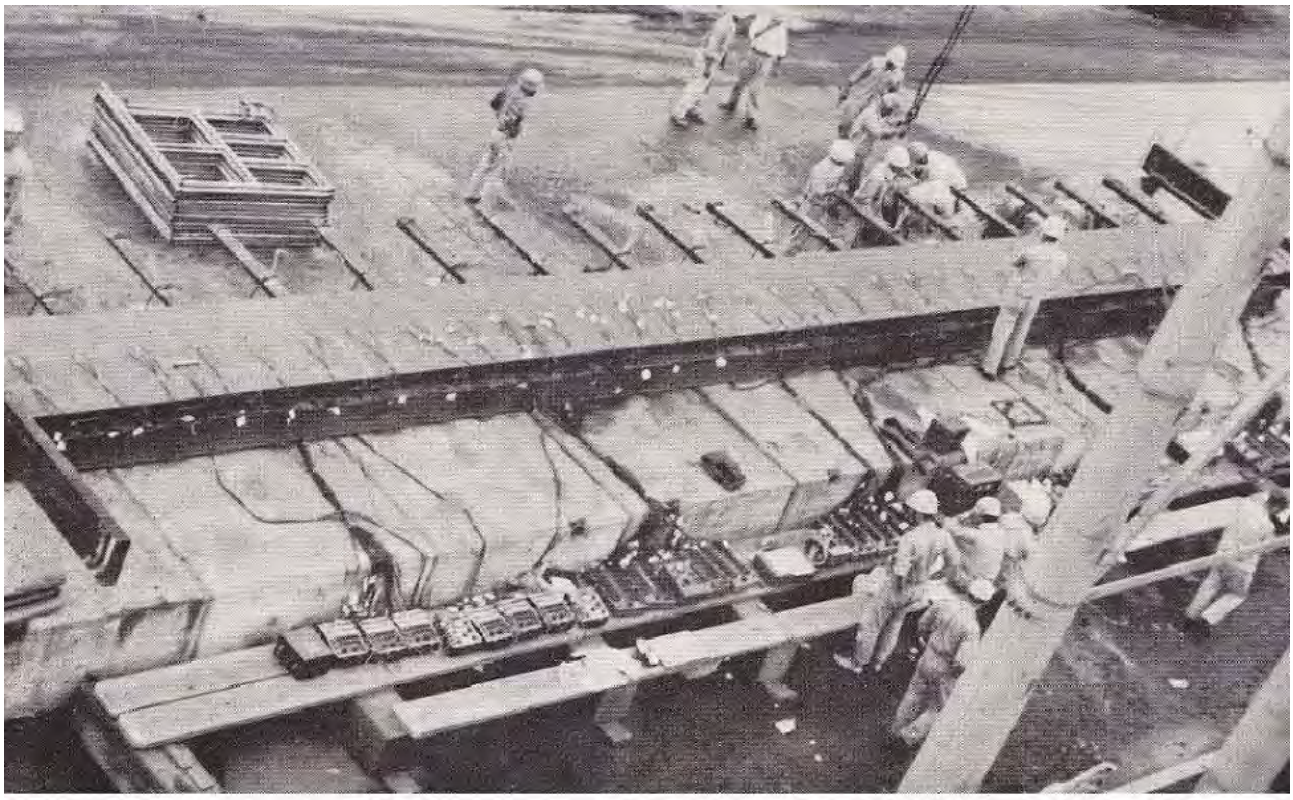

Full view of torsion type gate strength test (Yokohama ship yard)

Fig. 3. 1－1 1 4

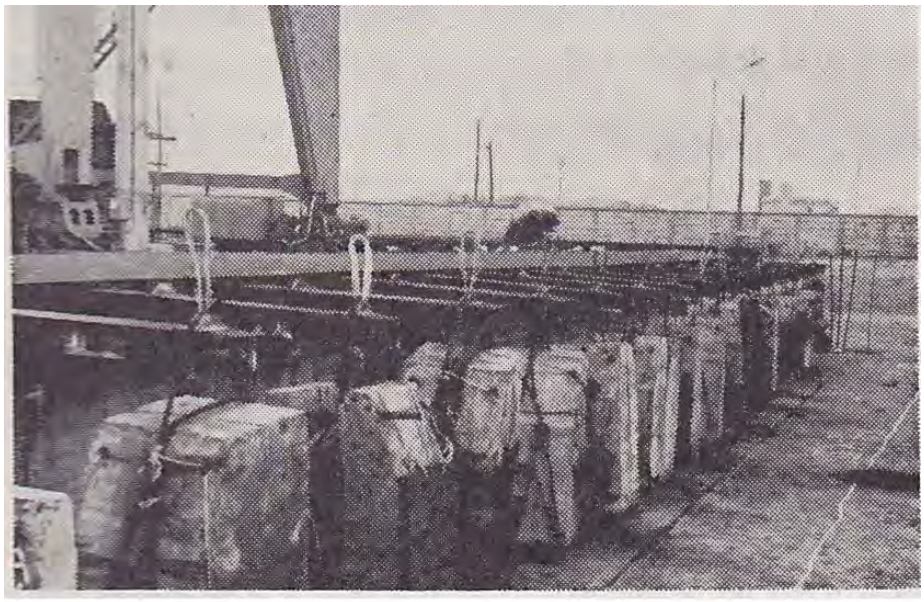

Max. loading test (concrete weight:450Kg /block)

Fig 3. 1－1 1 5

Appendix 3．1－7　Bibliography for structural analysis of torsion type gate

(1) Hiroshi Terata, Strength of fish belly flap gate, Conference at Kyoto branch of Japanese Society of Irrigation, Drainage and Reclamation Engineering, 1965

(2) Mitsubishi Heavy Ind. Ltd. (Hiroshi Terata), Fllap gate (Number 1), Earth and concrete, 1965

(3) Hiroshi Terata, Mitsubishi fish belly gate, Mitsubishi Heavy Ind., Ltd. TECHNICAL REVIEW Vol. 2 No. 2, 1965

(4) Hiroshi Terata, Stress Analysis of Flared Tubular Joint Stiffened with Diaphragms, Master Thesis prepared for Prof. J. G. Bouwkamp of U. of California at Berkeley, 1969

(5) J. G. Bouwkamp、A. K. Vaish and Hiroshi Terata、A Study of Defferent Flared Joint Configurations (PAPER NUMBER OTC 1229), OFFSHORE TECHNOLORY CONFERENCE 6200 North Central Expressway, Dallas, Texas, 1970

(6) Hiroshi Terata, Noriaki Shigenaga, Torsion type flap gate for docks, Mitsubishi Heavy Industries, Ltd. TECHNICAL REVIEW Vol. 16 No. 6, 1979

(7) Hiroshi Terata, Noriaki Shigenaga, Torsion type flap gate for docks, Hydraulic Gate & Penstock Association, No. 128, 1980

(8) YACHIYO ENGINEERING CO., LTD.、FINAL REPORT OF PRELIMINARY ENGINEERING AND COST ESTIMATES (PHASE 1) FOR THE STUDY OF ALTERNATIVES TO THE PANAMA CANAL, COMMISSION FOR THE STUDY OF ALTERNATIVES TO THE PANAMA CANAL, 1992

(9) YACHIYO ENGINEERING CO., LTD.、FINAL REPORT OF PRELIMINARY ENGINEERING AND COST ESTIMATES (PHASE 2) FOR THE STUDY OF ALTERNATIVES TO THE PANAMA CANAL, COMMISSION FOR THE STUDY OF ALTERNATIVES TO THE PANAMA CANAL, 1993

(10) M.A.N., M.A.N KLAPPENWEHRE LIEFERVERZEICHNIS

(11) Von o. Professor Dr. Paul Cicin, Die Fischbauchklappe und verwandte

Wehrsysteme, DER BAUINGENIEUR, 1958 Heft 10、1958

(12) Von o. Professor Dr. Paul Cicin, Die Fischbauchklappe und verwandte Wehrsysteme (Fortsetzung und Schlu β aus Heft 10)、DER BAUINGENIEUR, 1958 Heft 11, 1958

(13) Von Dipl.- Ing. I Borocz, Eine Methode zur Berechnung der Fischbauchklappe, DER BAUINGENIEUR, 1966 Heft 1, 1966

(14) Masateru Hayashi, Yukihiko Ueda, Statical analysis of shell type flap gate and calculation method of its natural frequency, Ishikawajima- Harima Technical Review Vol. 9 No. 3, 1969

(15) Sadaharu Takagi, Kaisekigairon, Iwanamishoten, 1942

(16) Tetsuo Inui, Partial Differential Equation and its Application, Koronasha, 1957

(17) Masatsugu Kuranishi, Elasticity, Kokusairikoukenkyusha, 1949

(18) Masatsugu Kuranishi, Applied Elasticity, Kyoritsuzennsho, 1957

(19) S. Timoshenko (Translation：Akimasa Kitabatake, Kenjirou Katayama), Strength of Material, Number 2, Koronasha, 1955

(20) Timoshenko and Goodier, Theory of Elasticity, Mc Graw- hill Koogakusha, 1959

(21) Arthru P. Boresi, Elasticity in Engineering Material, Prentice Hall, 1965

(22) J. S. Przemieniecki, THEORY OF MATRIX STRUCTURAL ANALYSIS, McGraw- Hill, 1968

(23) Mem. savants, vol. 14, 1855

(24) H.Wagner, Verdrehung und Knickung von offenen Profilen, Festschrift. 25 Jahre T.H. Danzig, S.329, 1929

(25) H.Wagner, W. Pretscher, Verdrehung und Knickung von offenen Profilen, Lufo., Bd 11. Nr.6, 1934

(26) Seal H. and Seal G., Die Berechnung von Stutzen in schwach gekrummten Schalen, Der Stahlbau 5/ 1974, 1974

(27) Ichirou Konishi, Sadao Komatsu, Akimitsu Ohashi, Stress analysis and method of design calculation of a composite box girder bridge, Japan

Society of Civil Engineers Collection of Papers No. 25, 1955

(28) Д. В. ВЫЧКОВ, СТРОИТЁЛЬНАЯ МЁХАНИКА, СТЕРЖНЁВЫХ ТОНКОСТЁННЫХ КОНСТРУКЦИЙ, (open thin shell cross section)

(29) Д. В. ВЫЧКОВ (Partial translation: Masahiro Manaabe, Mitsutoki Hisamatsu), Theory of open section thin shell structure (bending-torsion theory) (Statically determinate version Ⅰ～Ⅲ) ・・Original name: "On open section thin shell structure", Kogakushuppankabushikikaisha Vol.147 ～ September version, 1965

(30) Д. В. ВЫЧКОВ (Partial translation: Masahiro Manaabe, Fumihiko Saka), Theory of open section thin shell structure (bending-torsion theory) (Statically indeterminate version Ⅰ～Ⅳ) ・・Original name: "On open section thin shell structure", Kogakushuppankabushikikaisha Vol.15 ～ November and December versions and Vol. 16 ～ January and February versions, 1967

(31) V Z Urasohf (Translation: Toshie Okumure & others), Theory of thin shell elastic beam, ,

(32) Toshie Okumura, Characteristics of bending-torsion in thin shell section, Recent subjects in structural engineering, 1967

(33) Shyunzo Okamoto(Editor), Study on steel structure, Toshie Okumura's 60 years old memorial group, 1977

(34) Bridge handbook editing committees (Chairman; Toshie Okumura), Bridge Handbook, Investigation Committees of Construction Industry, 1976

(35) Kansai Shipbuilding Association, Shipbuilding Design Handbook (No. 4 edition), Kaibundo, 1983

(36) Japan Society of Mechanical Engineers, Mechanical Engineering Handbook (1987 version), Japan Society of Mechanical Engineers, 1987

(37) Japanese Society of Steel Construction, Fatigue design guide (draft), JSSC, 1989

(38) Japanese Society of Irrigation, Drainage and Reclamation Engineering,

Handbook for irrigation, drainage and reclamation engineering, JSIDRE

(39) Column Research Committee of Japan (Edited by), Handbook of structural stability, Corona Publishing Co. Ltd, 1987

(40) Ikuo Higasa, Movable dam, Kogyozougeisha